ELSEVIER

Contents lists available at ScienceDirect

# **Earth-Science Reviews**

journal homepage: www.elsevier.com/locate/earscirev



# Tsunami versus storms: Diagnostic sedimentary criteria in coastal lakes, lagoons and sinkhole deposits

Patrick D. Sharrocks\*, Jeffrey Peakall, David M. Hodgson, Natasha L.M. Barlow<sup>1</sup>

School of Earth and Environment, University of Leeds, LS2 9JT, UK

#### ARTICLE INFO

#### Keywords: Storm Tsunami Sediment deposit Density Process Lakes Lagoons

#### ABSTRACT

Sedimentary deposits of coastal flooding by tsunamis and storms extend archives of these events across millennia. However, the utility of these records remains clouded by an inability to unequivocally differentiate between a deposit of storm or tsunami origin. This review takes a novel approach by compiling a large integrated dataset of modern and palaeo tsunami and storm deposits in coastal lakes and lagoons to infer the processes that occur during these events. We find that storm and tsunami deposits each comprise three differing groups. Using these groups, we infer the processes involved in tsunamis, including the formation of a sediment gravity flow as the tsunami flows into the lake; the progression of a dense, cohesionless flow head, or the displacement of the shallow lake water by the tsunami wave. In contrast, storm deposits are inferred to be formed by bedload under an overwash regime or in a dilute flow under full inundation of the coastal lake or lagoon. From these processes, we show that the composition of tsunami deposits is dependent on the environmental setting of the lake or lagoon whereas, for storms, the event size is a greater factor. Our findings show that in most cases, storm events are inherently unable to generate the tsunami deposits found in coastal lakes and lagoons. This insight enables the establishment of recognition criteria and a framework that can be applied to candidate deposits to differentiate unequivocally between the two event types. Nonetheless, for some deposits, a differentiation on sedimentology alone is impossible.

#### Contents

1.	Intro		
	1.1.	Storms v	78 Tsunamis: An overview of the debate
	1.2.	An alteri	native approach: Process sedimentology
	1.3.		akes and lagoons
2.	Tsuna	amis and s	torm deposit synthesis
	2.1.	Methodo	ology 3
		2.1.1.	Confidence in event attribution
3.	Tsuna		entation in coastal lakes and lagoons
	3.1.		characteristics
	3.2.		deposits in coastal lakes and lagoons
			Norway – Storegga tsunami
			Chile – 1960 and older tsunami
			British Virgin Islands – 1755 Lisbon tsunami
			Oman – 1945 Makran tsunami
			Sri Lanka – 2004 tsunami
			Doubled 1755 lishon temponi

E-mail addresses: eepsha@leeds.ac.uk (P.D. Sharrocks), J.Peakall@leeds.ac.uk (J. Peakall), d.hodgson@leeds.ac.uk (D.M. Hodgson), natasha.barlow@haskoning.com (N.L.M. Barlow).

<sup>\*</sup> Corresponding author.

<sup>&</sup>lt;sup>1</sup> Current Address: Haskoning, 1 Aire Street, Leeds, LS1 4PR.

		3.2.7.	Summary of known examples	. 5
	3.3.	Tsunami	facies	. 5
	3.4.	Tsunami	deposit groups	. 6
		3.4.1.	Confidence and uncertainty across the dataset	. 6
		3.4.2.	Group A deposit trends	. 7
			Group B deposit trends	
			Group C deposit trends	
	3.5.		process and mechanisms	
	0.0.	3.5.1.	State of the science: Depositional processes and mechanisms during a tsunami	
			Group A processes	
			Group B processes	
			Group C processes	
	0.6		1 1	
	3.6.	-	ions for tsunami sedimentation	
		3.6.1.	Controls on deposit type	
			Implications for tsunami events	
4.	Storm	-		
	4.1.		n characteristics	
	4.2.	Storm de	eposits in coastal lakes and lagoons	18
		4.2.1.	Lesser Antilles - Hurricanes Irma and San Felipe	18
		4.2.2.	Mainland USA – Historical and palaeo hurricanes	18
		4.2.3.	Caicos Islands – Blue hole deposits	19
	4.3.	Storm de	eposit facies	19
	4.4.	Storm de	eposit groups	19
		4.4.1.	Confidence and uncertainty within the dataset	
		4.4.2.	Group X deposit trends	
			Group Y deposit trends	
			Group Z deposit trends	
	4.5.		s of storm sedimentation in coastal lakes, lagoons and sinkholes	
			Processes of storm deposition in back-barrier settings	
			Group X processes	
			Group Y processes	
			Group Z processes	
	4.6.		ions for storm sedimentation	
5.			imi	
э.				
	5.1.		s on deposit type	
	5.2.		nent-specific diagnostic criteria	
		5.2.1.	Blue holes	
			Coastal lakes and lagoons	
	5.3.		ork for event attribution	
	5.4.		ns where event attribution is not possible	
	5.5.	-	nents for successful differentiation	
	5.6.		ion to other records	
6.	Case s		olying the framework to re-evaluate existing deposits	
	6.1.	Case 1: 1	Puerto Rico	31
	6.2.	Case 2: J	Jamaica	31
	6.3.	Implicati	ions for Caribbean tsunami hazard	31
7.	Concl	usions		31
	Declar	ration of c	competing interest	32
			ents	
			data	
		•	у	

# 1. Introduction

Around 650 million people live in coastal areas less than 10 m above sea level, with this number projected to hit 1 billion by 2050 (Oppenheimer et al., 2019). In such context, the population are highly vulnerable to coastal hazards (tsunamis and coastal storms) coupled to rising sea levels (IPCC, 2019). To understand these threats, there is a need to understand the recurrence intervals and severity of past events, to better comprehend future ones. However, the instrumental record is too short for tsunamis (e.g. since 1850 in California; Satake et al., 2020) and coastal storm flooding (e.g. Atlantic hurricane record extends to 1851; Wallace et al., 2021a). Sedimentary deposits extend the archive of past events back for several millennia in many locations for past tsunamis (Costa and Andrade, 2020) and storms (Donnelly et al., 2015;

Bregy et al., 2018), making them vitally important for accurate hazard and risk assessments. Pre-Holocene deposits, such as those linked to the K-Pg impact event (Smit et al., 1996), can further extend this record onto geological timescales; however, accurately dating these older deposits and identifying the events that triggered them becomes increasingly challenging. The deposit (often coarse-grained material found out-of-situ in a coastal setting) is used to provide an inundation distance(s) and/or run-up height(s) for the tsunami (e.g. Costa and Andrade, 2020) or storm flooding. This provides an estimate of the relative magnitude of past inundation events which can be used in hazard and risk assessments (Woodruff et al., 2008; Engel et al., 2016). However, one of the main challenges in using the geological record is distinguishing between palaeo-tsunami and palaeo-storm deposits, the debate around which is still ongoing (e.g. Prizomwala et al., 2018; Brill et al., 2020; Biguenet

et al., 2021).

#### 1.1. Storms vs Tsunamis: An overview of the debate

Tsunamis and storms have been argued to leave similar sedimentary deposits in coastal settings (Kortekaas and Dawson, 2007; Brill et al., 2020). The debate over how to differentiate between the events in the sedimentary record remains unresolved as no unambiguous criteria have been established (Morton et al., 2007; Kortekaas and Dawson, 2007; Costa and Andrade, 2020). This is despite the events' different wave dynamics and generation mechanisms (Table 1), which show that a tsunami has a greater height, longer period and faster velocity than coastal storm flooding. The wave period is especially important as typically tsunami events travel inland as 5-15 min waves but storms inundate as repeated 10-25 s waves. These factors suggest a tsunami wave would have a greater force and energy than a comparable storm wave thus altering how the flow erodes, transports and deposits sediment. However, comparative studies have not identified any silver bullets to distinguish between the two event types, but rather the combined evidence from contextual, sedimentological and other proxies is usually required to attribute a specific deposit to a generation mechanism (Goff et al., 2004; Morton et al., 2007; Kortekaas and Dawson, 2007; Brill et al., 2020).

Contextual information is considered the most effective proxy to distinguish between tsunami and storm deposits due to their different characteristics including their generation, size and duration (Table 1). The landward extent is a common approach to differentiate between event types, with tsunami deposits typically extending greater distances and elevations inland than coastal storm flooding events (Tuttle et al., 2004; Morton et al., 2007; Watanabe et al., 2017). Furthermore, in seismically active regions, such as Chile (León et al., 2023), a tsunami origin is often preferred as tsunamis are predominantly caused by earthquakes (78 %) (NCEI, 2024). However, this ignores the premise that tsunamis can also be triggered by submarine or subaerial landslides, volcanic eruptions and impact events. Similarly, a storm origin is often favoured where their main trigger, tropical cyclones, are present (e.g. western North Atlantic and Caribbean) or in regions where an extratropical storm and high spring tide combine (e.g. Eastern Atlantic). However, there are many areas where both events occur relatively frequently, for example in the Eastern Caribbean (Biguenet et al., 2021), Japan and southeast Asia (Brill et al., 2020). It is in these locations that a correlation and comparison to known, modern events may be possible, but in many areas, there may be no historical record of the event (e.g. Biguenet et al., 2021; Fabbri et al., 2024). Else, other deposit criteria need to be considered, which differ depending on the depositional location.

The differing flow velocity, period and depth of tsunamis and storms alters the type and volume of sediment the wave can transport (Table 1). Tsunamis typically entrain a wide assemblage of sediments from dunes, beaches and alluvial plains (Richmond et al., 2012; Costa et al., 2018), whereas storms only transport sandy beach or dune sediments (La Selle et al., 2017). Therefore, in open coast settings, the inclusion of mud either as rip-up clasts or a mud cap can be a criterion for recognition of a tsunami deposit, as storm deposits often contain little mud (Morton et al., 2007; Biguenet et al., 2021). Furthermore, a more chaotic nature and poorer sorting in a deposit generally imply a tsunami rather than storm origin due to the mixed sediment assemblage and shorter inundation time that restricts sorting of the deposit (Kortekaas and Dawson, 2007; Switzer and Jones, 2008; Prizomwala et al., 2018). Tsunami deposits also generally lack the planar laminations and foreset cross stratification commonly found in storm deposits (Tuttle et al., 2004). Finally, the distribution of the deposit over the landscape can be indicative of the event type, with storms filling in the macrotopography to create a uniform surface whereas tsunami deposits drape the land surface, conforming to the antecedent topography as they thin inland (Morton et al., 2007). The occurrence within deposits of marine microorganisms (foraminifera and diatoms) from habitats below the storm wave base is another criterion for interpreting a tsunami origin (Pilarczyk et al., 2014, 2020). However, the generally relatively low numbers of microfossils in most storm or tsunami deposits (Kortekaas and Dawson, 2007) reduce the utility of this criterion. Together, these criteria may differentiate between event types but often fail to remove uncertainty as they are equivocal. Therefore, an alternative approach founded on process sedimentological criteria is required.

#### 1.2. An alternative approach: Process sedimentology

Previous attempts at establishing criteria for storms and tsunami deposits have focused on identifying differences between a limited number of deposits (2 or 3) and extrapolating this to determine criteria for all events (e.g. Tuttle et al., 2004; Morton et al., 2007; Brill et al., 2020). However, this approach is flawed due to the high variability of tsunami deposits even on a local scale as topography and sediment availability have strong influences on the deposit composition (Abe et al., 2012; Costa and Andrade, 2020). Therefore, an alternative approach is required. To reduce potential bias, criteria should be developed based on the synthesis of a large dataset of deposits that comprise a range of different environments and events. To date, synthesis or database studies have focused on either tsunamis or storms, evaluating deposits from a specific region (e.g. Oliva et al., 2018b; Costa et al., 2021; León et al., 2023) or in global databases (Ramírez-Herrera and Coca, 2024). Other studies have considered the general

Table 1
Characteristics of tsunamis compared to coastal storm flooding; these characteristics determine the composition of the resultant deposits from each event type.

Flow Characteristic	Tsunami	Coastal storms
Length of coastline impacted	10-10,000 km	100-600 km
Deepwater wave height	<0.5 m	>5 m
Nearshore wave height, wave period	10-20 m, 100-2000 s	<10 m, 10-25 s
Potential run-up heights	Most 10s of m, can be 100 s of m.	A few metres
Number of overland waves	<10	>1000
Inundation depth	0-20 m	<5 m
Active flow duration	Minutes to hours	Hours to days
Overland floodwater velocity	<20 m/s	<5 m/s
Flow directions	Mostly shore normal	
Flow-direction change	Alternating run-up and backwash	Return flow only at the end
Boundary layer structure	Entire water column	Current boundary layer
Influence of wind stress	Not a factor	Increases water velocities and surge heights
Sediment transport mechanism	Mostly suspension, some traction	Mostly traction, some suspension
Phases of flooding	Repeated rise and fall	Gradual initial rise, rapid intermediate rise, gradual fall
Event frequency	Infrequent locally, moderately frequent globally	Frequent locally and globally

Reproduced after Morton et al. (2007).

characteristics of both storms and tsunami deposits together in broader event overviews (e.g. Sabatier et al., 2022); however, no study has satisfactorily considered the reasons or factors that govern variation between deposits. To fully understand where and why the deposits differ, their processes need to be determined using established principles of process sedimentology.

The processes of sediment deposition in tsunamis and storms are poorly described compared to other fields within sedimentology (e.g., Talling et al., 2012; Peakall et al., 2020). The process description is often limited to an assumption of suspension and traction transport under a turbulent and relatively clear water wave for tsunamis (Moore et al., 2011; Richmond et al., 2012; Jaffe et al., 2016), with traction transport more important in storms (Morton et al., 2007). Whilst this can explain the deposition of some deposits, namely the widely reported clean sand deposits attributed to tsunamis and storms (e.g. Cisternas et al., 2005; Goslin and Clemmensen, 2017), it lacks the complexity and flexibility to explain how other deposit types, such as layers with muddy inclusions, are formed (Richmond et al., 2012; Kempf et al., 2015). Clues to the depositional processes may lie in other fields of sedimentology where in recent years increasingly mud-rich deposits have been used to infer differing processes of sedimentation within new depositional models (Mulder and Alexander, 2001; Talling et al., 2012; Peakall et al., 2020). This product to process approach has recently been utilised in offshore tsunami deposits to elucidate processes that were otherwise poorly described (Feist et al., 2023). However, aside from one recent study (Majumdar and Bhattacharya, 2025), this approach is severely lacking in onshore tsunami sedimentology (Costa and Andrade, 2020) and thus prevents an accurate reconstruction of past events. Determining the processes during tsunamis and storms from their deposits would enable an understanding of which features and trends in the deposits are unique to one event and/or environmental conditions (Majumdar and Bhattacharya, 2025). This could then be used to establish diagnostic criteria that unequivocally differentiate between the events. Therefore, we aim to use a large dataset of deposits to infer the processes involved in tsunami and storm sedimentation using the principles of process sedimentology.

# 1.3. Coastal lakes and lagoons

This synthesis work focuses on a subset of deposits produced by marine inundation from tsunamis or coastal storms; those found in coastal lakes and lagoons. Hereafter, "lakes" refers to coastal lakes located within a few kilometres of the shoreline and thus this work does not consider lacustrine tsunamis generated internally in large inland lakes, such as Lake Geneva (Kremer et al., 2015), which have different depositional mechanisms (Mountjoy et al., 2019; Kremer et al., 2021). Whilst considering all coastal depositional settings (such as marshes and coastal plains) would have yielded a larger dataset, the variability in the different settings would present a dataset too complex to identify specific features and trends in deposits that differ between the events. Coastal lakes and lagoons offer the best preservation potential with records often stretching across millennia (Lane et al., 2011; Sullivan et al., 2013; Kempf et al., 2015) and have the most distinct deposits of any depositional setting on land (e.g. Kelsey et al., 2005; Kempf et al., 2015). This is likely due to the unique interaction of the tsunami or storm waves with the standing water of the lake which results in different processes than those proposed on the dry, relatively flat land of a coastal marsh or plain (Jaffe and Gelfenbuam, 2007; Moore et al., 2011). However, these differing processes are not readily acknowledged in the established literature (e.g. Bondevik et al., 1997b) but are likely to relate at least in part to sediment gravity flows that are widely recorded for floods, lahars and mass movement events in coastal and terrestrial lake environments (e.g., Sabatier et al., 2022). This focus on coastal lakes enables utilisation of recent advances in the sediment gravity flow literature where the product to process approach is well established (Talling et al., 2012; Peakall et al., 2020). Overall, coastal lakes and lagoons represent the ideal environment to undertake this novel product to process approach to differentiate between storms and tsunamis.

In this synthesis, we aim to evaluate the literature for tsunami and storm deposits globally in coastal lakes and lagoons to determine how and why the deposits differ. First, a global literature synthesis of these deposits is conducted and the trends within the deposits evaluated to describe a series of typical depositional sequences for the two event types. These sequences are then interpreted to elucidate the depositional processes and mechanisms under which they form. In turn, these processes are evaluated to consider why and how certain deposits are unique to a single event, enabling diagnostic criteria to be established. Finally, a framework for using these criteria on a candidate deposit will be presented and tested using two storm and tsunami deposits in the Caribbean whose origin is presently uncertain.

#### 2. Tsunamis and storm deposit synthesis

#### 2.1. Methodology

A synthesis of the existing literature describing tsunami and storm deposits in coastal lakes and lagoons was conducted using key word search criteria including "coastal storm", "storm surge", "tsunami", "deposits", "sediment", "lakes", "lagoons" and any combination thereof. Subsequent literature was incorporated from databases of deposits, including the palaeotempestology database of Oliva et al. (2018b) for the North Atlantic region, the database of palaeotsunami deposits of Ramírez-Herrera and Coca (2024) and through searching citations within other identified literature. Only studies where the depositional sequence contained a fresh/brackish water sediment layer below the event layer were considered. This includes restricting the dataset to studies which sampled the lagoon/lakebed rather than the surrounding shoreline or where the lake/lagoon was not present when the tsunami/storm occurred.

This search generated an initial list of 152 articles (77 tsunamis, 71 storms, and 4 both) which were reviewed in this study. The quality of the grain size data and the detail in which the deposit composition was described within a study determined how useful the data presented could be in determining an accurate deposition sequence, including the identification of sublayers within a deposit. Therefore, studies were split into three categories: 1: High quality grain size data, usually laser granulometry or dynamic image analysis; 2: Some grain size data: typically sieving or sand fractions and/or detailed stratigraphic description; 3: No grain size data. The latter were excluded from any subsequent analysis of deposit composition, reducing the number of articles to 135.

A table (Supplementary Datasets 1, 2) containing key attributes from deposits in each coastal lake or lagoon was compiled and an entry was inserted for each study. The information in this table provided the basis for the discussion of this synthesis study.

# 2.1.1. Confidence in event attribution

Most commonly storm and tsunami deposits are differentiated using contextual evidence (Morton et al., 2007; Palmer et al., 2020). This means that in a region where tsunamis or storms are considered more likely, that event will be attributed to the deposit. This leads to circular reasoning where all or many events for a given region are attributed to one or the other event despite both events being feasible for a given location. In this study, we aim to separate our diagnostic criteria from these biases by focusing interpretation on deposits where the event origin is known. These events are either modern events (e.g., 1960 (Chile), 2004 (Indian Ocean) and 2011 (Japan) tsunamis) or historical/palaeo events where the events are widespread, and dating is constrained (1755 Lisbon and Storegga tsunamis). Modern and historical events were also identified for storms. Two lower confidence intervals are also utilised: 'likely', where the dating and other evidence ties the deposit to a specific event that is known in other records, and

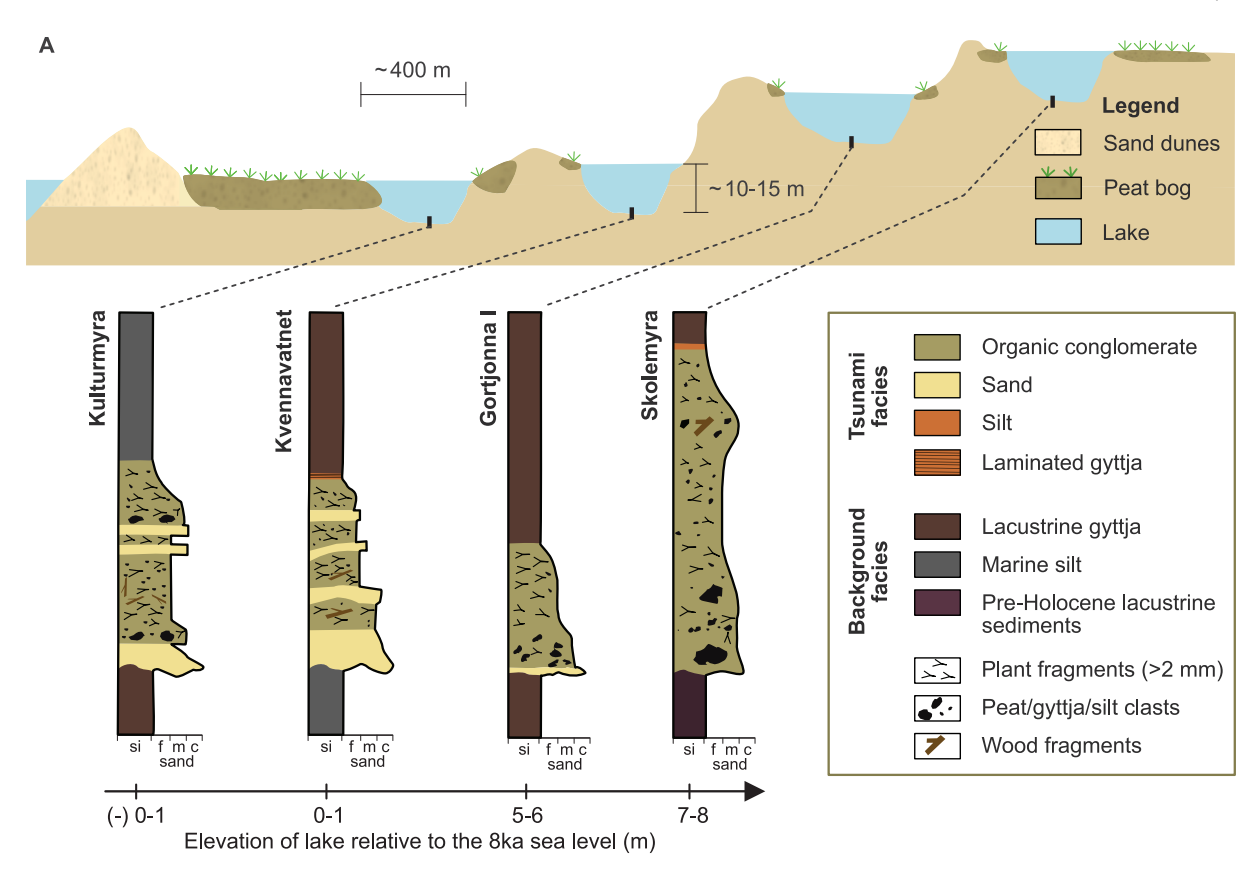


Fig. 1. Schematic of the landscape showing lake basins of increasing elevations relative to the sea level at the time of the Storegga tsunami (8150 BP). Logs for each lake show the tsunami deposits and background sedimentation as composite examples of 10 cores taken within each basin (Bondevik et al., 1997b).

"uncertain" where the deposits could not be tied to a specific event and/ or there was a contemporary storm/tsunami event. For each study, the authors' interpretation of the event type was used to place uncertain studies in either the storm or tsunami datasets. Events assigned to these lower confidence intervals were used to complement the deposits of the known events in the interpretation of the depositional groups and processes of the deposits. This ensured that the deposits of known events were representative of the wider dataset. Furthermore, this approach enabled each deposit group to be tied to known events and coastal geomorphologies that could be used to assess where and under which circumstances each deposit type may form.

In the remainder of this study, we aim to:

- 1) Describe the deposits of six key studies of known tsunamis in lakes and lagoons.
- 2) Describe the typical depositional groups and present the wider database of deposits for tsunami events.
- 3) Identify trends within each depositional group and use these to infer the depositional processes under which the deposits are formed.
- 4) Repeat steps 1-3 for storms.
- 5) Evaluate and discuss how storm and tsunami deposits can be distinguished within coastal lakes and lagoons.

# 3. Tsunami sedimentation in coastal lakes and lagoons

#### 3.1. Location characteristics

Across the 102 sites, the locations and the parameters of the lakes and lagoons containing the deposits varied. Deposits in lakes have been found in 21 countries from tsunamis generated predominantly by large subduction zone earthquakes (e.g. Chile 1960: Kempf et al., 2015), but also smaller events with more localised impacts (e.g. Virgin Islands,

1867: Fuentes et al., 2017) and 30 from the Storegga submarine landslide (Bondevik et al., 1997b; Grauert et al., 2001). The size of the lakes and lagoons varied greatly from small ponds less than 0.01 km² to large lagoons >20 km² in area, with a depth of generally <10 m, although 27 lagoons had a depth of less than 1 m. The lakes were typically separated from the ocean by a barrier (or sill) whose elevation above sea level varied between 3 and 10 m, with lagoons generally separated from the sea by barriers that are a few hundred metres wide and only 2-4 m in height. Both lakes and lagoons were located at varying distances from the contemporary coastline, ranging from 50 m to 3 km, with the majority between 100 and 500 m inland.

#### 3.2. Tsunami deposits in coastal lakes and lagoons

Tsunami deposits in lacustrine environments are found as anomalous layers within an otherwise fine-grained succession of lacustrine organic mud deposits. Their composition is highly variable. Here, six examples from known tsunami events are described that encompass the range of deposit types seen in the wider database.

#### 3.2.1. Norway - Storegga tsunami

In Norway, 18 coastal lake basins record sedimentary evidence for the Holocene Storegga tsunami, a widely recorded event (Smith et al., 2004; Bondevik et al., 2005) of 8150 BP (Rydgren and Bondevik, 2015) generated by a large submarine landslide in western Norway (Haflidason et al., 2005). These lakes are typically 100-400 m long, 50-100 m wide, and 10-15 m deep (e.g. Fig. 1; Bondevik et al., 1997a, 1997b) and were situated 1-10 m above contemporary sea level but today have been uplifted by 15-20 m due to glacial-isostatic uplift. Each lake had at least 10 cores taken in which tsunami deposits were found (Bondevik et al., 1997b). The tsunami deposits consist of a 4-6 cm thick basal medium to coarse sand (massive or normally graded) containing

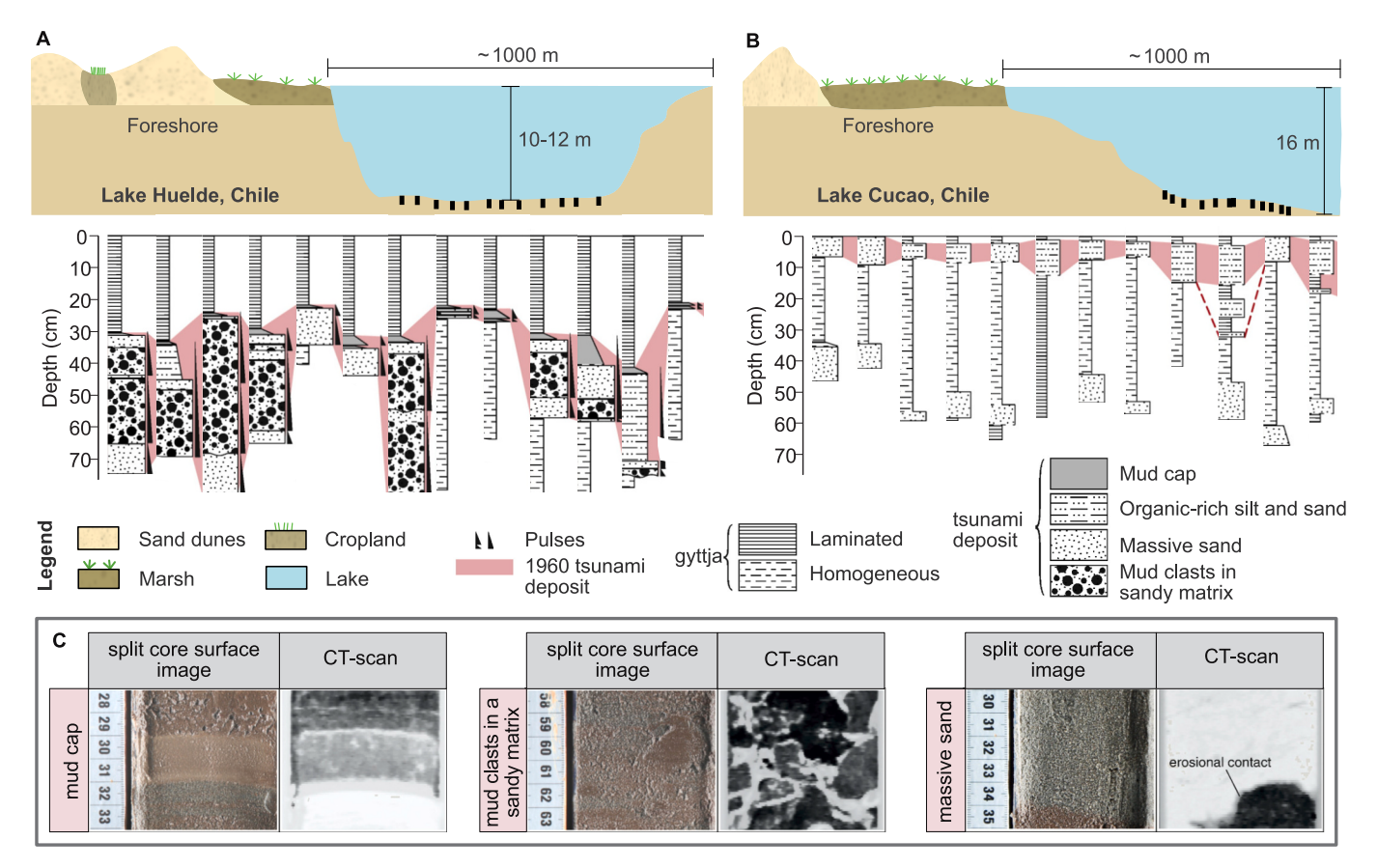


Fig. 2. A: Distribution of tsunami deposits through Lake Huelde (A) and Lake Cucao (B) shown within a schematic of the lake with the position of the cores indicated by vertical black lines. A legend is given below. C: Images from sediment cores and CT scans of typical examples of the three tsunami facies observed in Lake Huelde. Modified from Kempf et al. (2015) and reprinted with permission from Elsevier.

fine shell fragments overlain by what the authors termed an organic conglomerate layer (Fig. 1). This layer, locally up to 50 cm thick, consists of a poorly sorted matrix of gyttja (lake mud) with sand and silt incorporating organic detritus (twigs, wood, shell fragments) and often with irregular peat, gyttja and silt clasts (Fig. 1). A thin layer of silt or laminated gyttja sometimes overlies the deposit with the latter inferred to form after an anoxic bottom layer developed in the lake after the tsunami (Bondevik et al., 1997b). The lake basins show evidence of extensive erosion by the removal of around 2000 years of sediment from the lakebed underlying the tsunami deposits. The tsunami deposit varies inland with the basal sandy layer thinning landwards both within and between lakes. Whereas the organic conglomerate layer thickens at depth within a lake and is thicker in basins at higher elevations (Fig. 1). In lakes less than 5 m above the contemporary sea level this layer often lacks clasts and repeats of the sands and organic conglomerate/debris layers are often observed (Fig. 1; Bondevik et al., 1997b). These deposits are found in what is today a cold but wet environment (Beck et al., 2023) with the lakes inferred to have originally been within a boggy environment similar to present.

#### 3.2.2. Chile - 1960 and older tsunami

In Chile, two large coastal lakes record tsunami deposits from the 1960 tsunami as well as older events from the last 4500 years (Kempf et al., 2015, 2017, 2020). In Lake Huelde, tsunami deposits consist of a massive sand with a sharp, often erosional lower contact with the underlying lacustrine gyttja (Kempf et al., 2015; Fig. 2). This is usually overlain by poorly sorted sandy matrix, rich in 0.5-6 cm diameter mud clasts, interpreted as rip-ups from the underlying lake gyttja and terrestrial peats (Fig. 2a). Often the deposit is topped by a thin mud cap (Fig. 2). This depositional sequence is found at depths of 9-12 m in 8 out

of 14 cores taken in the lake basin. A repeat of the basal sands and mudclast layers was recorded in some cores close to the lake outlet, interpreted as being deposited under successive waves of the tsunami. Lower in the stratigraphic profile, deposits from palaeo deposits over the last 4500 years record deposits of similar composition (Kempf et al., 2017). In Lake Cucao, a larger lake which extends several kilometres inland, 1960 tsunami deposits consist of thin layers (<10 cm thick) of organicrich silt and sand within the background lagoonal sedimentation (Fig. 2b; Kempf et al., 2015). However, deposits from palaeo events are like those in Lake Huelde, with massive basal sands and an overlying layer of mud clasts within a silty sand matrix (Kempf et al., 2020). This deposit sequence was most prominent where the lake depth was greater than 10 m.

# 3.2.3. British Virgin Islands - 1755 Lisbon tsunami

Other locations record rather different deposits. Shallow marine coastal ponds (< 1 m depth) in the British Virgin Islands record tsunami deposits in over 20 cores related to the far field wave of the Lisbon 1755 tsunami (Atwater et al., 2012, 2017). These ponds on Anegada (tropical climate) are situated behind 2.25 m high sandy coastal barriers (Fig. 3a). The Lisbon tsunami, modelled to over 2 m within the eastern Caribbean (Roger et al., 2011), is thought to have overtopped these barriers and inundated the shallow ponds. In the proximal pond (Fig. 3a), deposits consist of a  $\sim 10$  cm thick pink sand, transported from the sandy barrier (Atwater et al., 2012). In a second pond further inland beyond limestone pavements tsunami deposits comprise sand and shell sheets. Thus, these sheets transition inland from sand-dominated layers capped by a thin densely-packed shell layer to a single clast-supported shell-rich layer 10-20 cm thick, over a distance of 1 and 1.5 km. The shell assemblage consists of 27 % bivalves and 73 % cerithiid (sea snail) shells consistent

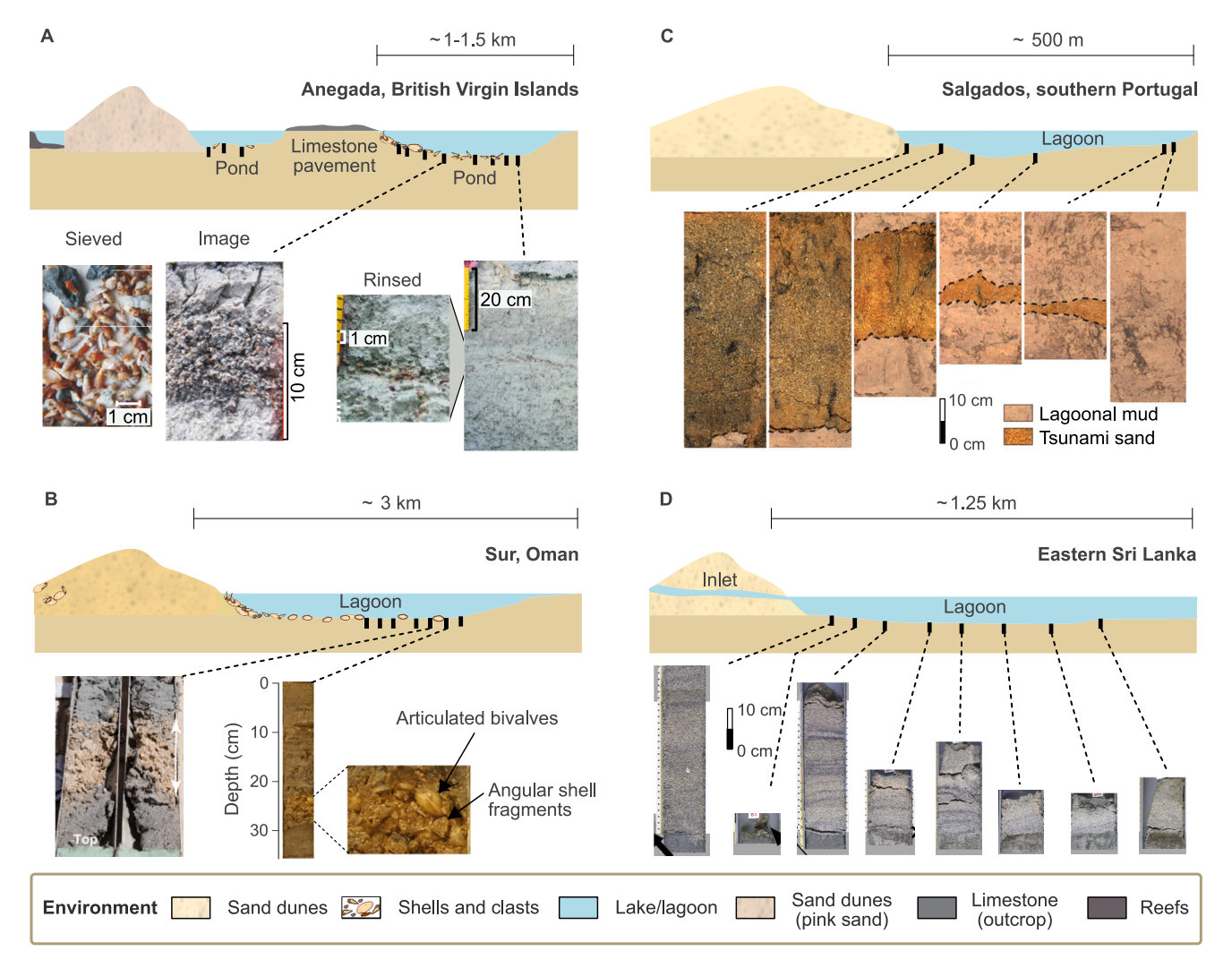


Fig. 3. Schematics depicting a simplified cross-sectional view of four coastal lakes and lagoons containing tsunami deposits, with core positions indicated by vertical black lines. Core photos are shown in each panel corresponding to the position from where they were taken. A: Anegada, British Virgin Islands (Atwater et al., 2012, images are reproduced with permission from Springer Nature); B: Sur Lagoon, Oman (Donato et al., 2009; Pilarczyk and Reinhardt, 2012, images are reprinted with permission from Elsevier); C: Salgados Lagoon, Portugal (Moreira et al., 2017, images reprinted with permission from Elsevier); D: Periya Kalapuwa Lagoon, Sri Lanka (Matsumoto et al., 2010, images reprinted with permission from Elsevier).

with the ecology of the ponds (Reinhardt et al., 2012). However, highly preserved shallow marine foraminifera were also abundant within the deposit. Most of the shells were either whole or large angular fragments (Fig. 3a; 6 bioclasts per cm³), with any fragmentation more consistent with pre-tsunami crab predation rather than during tsunami transport (Reinhardt et al., 2012). Limestone grains and pebbles are also common within these layers (Fig. 3a). The sand and shell sheets are locally overlain by a mud cap which thickens landwards to 10-15 cm thick (Fig. 3a).

#### 3.2.4. Oman - 1945 Makran tsunami

In Oman, a large  $12~{\rm km}^2$  coastal lagoon records deposits from the  $8.1~{\rm M}_{\rm W}$   $1945~{\rm Makran}$  Earthquake and tsunami, which produced  $3~{\rm m}$  high waves (Donato et al., 2009). The lagoon, in a very arid environment, has a shallow depth (max of  $2~{\rm m}$ ) and is separated from the ocean by a  $2.5~{\rm m}$  high sandy coastal barrier that has a single inlet to the ocean. Eight cores (Fig. 3b) record  $5-25~{\rm cm}$  thick clast-supported shell layers deposited by the Makran tsunami. These layers contain whole and angular shell fragments ( $5.6~{\rm to} > 70~{\rm mm}$  in diameter) that comprise  $16-65~{\rm w}$  of the deposits, with the spaces between filled with very fine to fine sand. The shell assemblage is mixed, with shells from the lagoon and the shallow marine environments,  $36~{\rm w}$  of bivalves in the deposit are whole

fragments and 7 % are articulated (e.g. Fig. 3b; Pilarczyk and Reinhardt, 2012). Spatially, the deposits thin and fine inland and become better sorted. Throughout many of the cores, a fine mud drape caps the deposit. This deposit was proposed to have been deposited through suspension and traction mechanisms during tsunami run-up with finer sediment settling out from the suspension during the quiescent phase (Donato et al., 2009).

# 3.2.5. Sri Lanka – 2004 tsunami

A different deposit type is evidenced by an extensive dataset of deposits from the 2004 tsunami in a 13 km² lagoon in Sri Lanka (Matsumoto et al., 2010). The Periya Kalapuwa lagoon was separated from the Indian Ocean by a narrow sandy coastal barrier (Fig. 3d) which locally reached 9 m in height and prevented direct inundation by the 4-6 m high tsunami waves through much of the lagoon. However, the lower height of the barrier adjacent to the two inlets of the lagoon (both transversed by a road bridge) allowed inundation of the tsunami into the lagoon (Matsumoto et al., 2010). Near these inlets, 27 sediment cores contain massive well-sorted fine to coarse sand layers deposited by the 2004 tsunami that overlie muddy lagoonal sediments at a sharp boundary. The deposits contain little internal structure except within muddy laminations in a few cores within 500 m of the two inlets

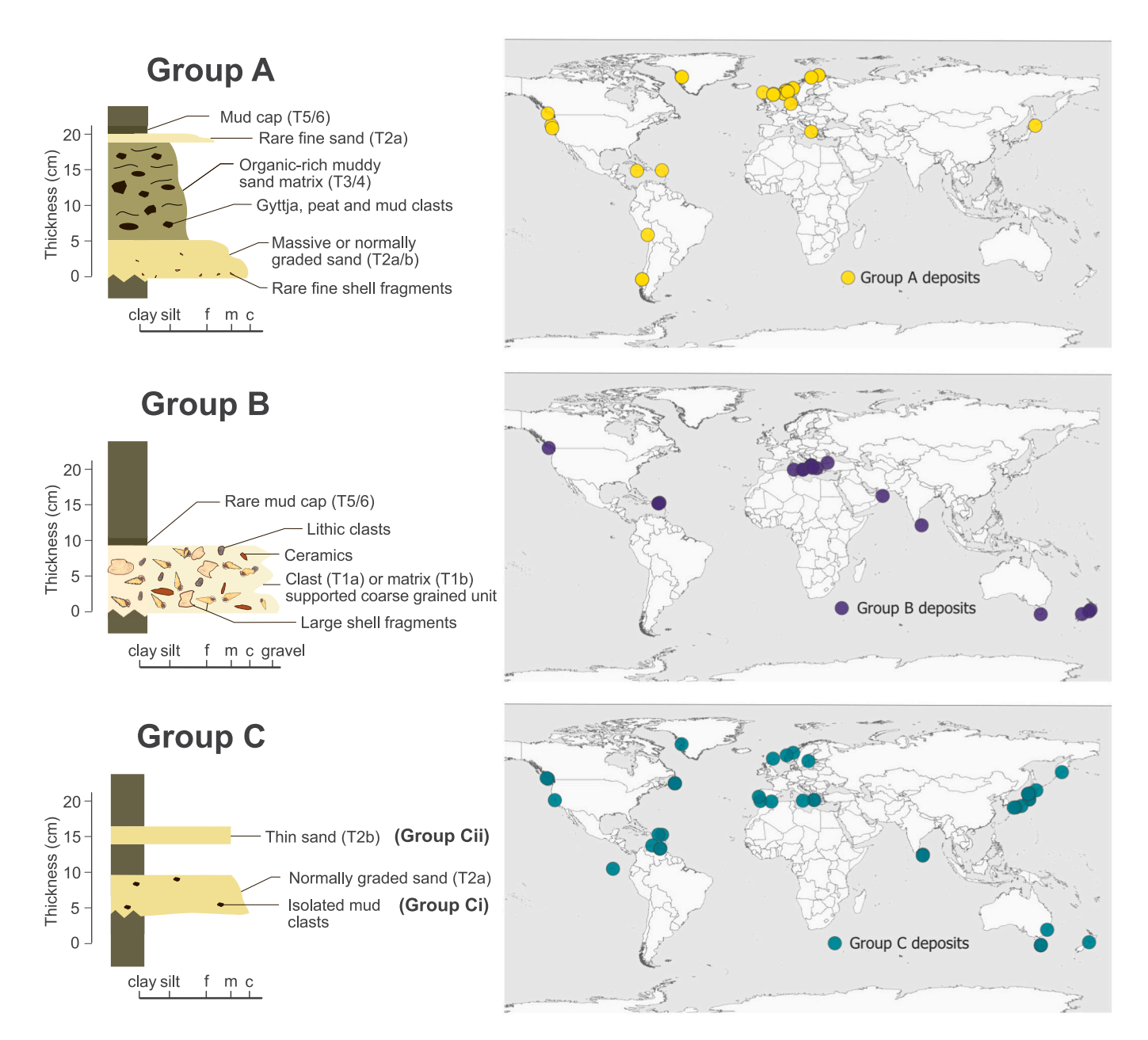


Fig. 4. Standard depositional diagrams showing the typical tsunami deposit composition, with each layer's respective facies code (T1-6), of each deposit group (A-C) (left) and their geographical distribution (right). Variations from these "typical" deposits are discussed in the text.

(Fig. 3d). These deposits are on average 9 cm thick but thin and fine inland from up to 35 cm thick near the lagoon inlet to 1 cm thick up to 1 km inland and consist of a low mud content (0.61 vol% on average). The source of these sediments was the sandy coastal barrier, where scour marks showing the erosion by the tsunami are evident (Matsumoto et al., 2010). The climate of the area is tropical, but the lake is situated on the more arid side of Sri Lanka (Punyawardena, 2009).

# 3.2.6. Portugal – 1755 Lisbon tsunami

Other sandy deposits recorded within a coastal lagoon in southern Portugal have been associated with the 1755 Lisbon tsunami event (Costa et al., 2012; Moreira et al., 2017). Here, the climate is temperate with hot and dry summers. The studied lagoon was around 1 m in depth, behind a sandy sparsely vegetated 3-10 m high dune which extended to the lagoon edge (Fig. 3c). The beach and dunes were the source of the sediment in the tsunami deposits (Costa et al., 2012). These deposits, of

medium sand with fine shell fragments, thin rapidly from 50 cm thick at the lagoon edge to a few mm thick up to 450 m further inland (Fig. 3c). At least 2 fining upwards sequences are identified, and potentially a coarsening upwards sequence in the lower few centimetres of the thicker deposits (Costa et al., 2012). Isolated centimetre-sized mud rip-up clasts from the underlying lagoonal sediment were found in some deposits. These deposits share the same characteristics as most tsunami deposits from marshes and coastal plains (e.g. Szczuciński et al., 2012; Costa et al., 2021).

# 3.2.7. Summary of known examples

These six studies represent deposits in lakes and lagoons from known tsunami deposits where the geomorphology of the coastline and the characteristics of the tsunami event are well known. Together they cover the breadth of deposits found in coastal lacustrine environments. These deposits were complemented with the wider database for lakes and

**Table 2**Summary of the key characteristics of the group A deposits within the literature.

Paper	Lake depth (m)	Barrier height (m)	Thickness of T2a/b	Thickness of T3/4	Is T5/6 present	Clast composition	T2 grain size	T3/4 grain size	Confidence
Fabbri et al., 2024	0.5	2	Thick-Thin	Thin-Mid	Some	Organic-rich clasts	f-vc sand isolated mud clasts	Sandy + organic- rich clasts (lagoonal)	Yes
Bondevik et al., 1997a,b	10 to 15	1.5	Mid	Mid	Yes	Organics $+$ rare gyttja	F gravel - f sand $+$ shell frag.	Gyttja, silt + little sand, fine plant frag, graded	Yes
Bondevik et al., 1997a,b	10 to 15	5.5	Thin	Thick	No	Peat, gyttja + silt	F gravel - f sand + shell frag.	Gyttja, silt and sand + clasts + organics	Yes
Bondevik et al., 1997a,b	10 to 15	1.5	Mid	Mid	Yes	Peat, gyttja + silt	F gravel - f sand + shell frag.	Gyttja, silt and sand + clasts + organics	Yes
Bondevik et al., 1997a,b	10 to 15	5.5	Thin	Very Thick	Yes	Peat, gyttja + silt	F gravel - f sand + shell frag.	Gyttja, silt and sand + clasts + organics	Yes
Bondevik et al., 1997a,b	10 to 15	5.5	Mid	Thick	No	Peat, gyttja + silt	F gravel - f sand + shell frag.	Gyttja, silt and sand + clasts + organics	Yes
Bondevik et al., 1997a,b	10 to 15	9.5	Thin	Thick	Yes at depth	$\begin{array}{l} \text{Organics} + \text{rare} \\ \text{gyttja} \end{array}$	F gravel - f sand + shell frag.	Gyttja, silt + little sand, fine plant frag, graded	Yes
Bondevik et al., 1997a,b	10 to 15	9.5	Thin	Very Thick	Yes at depth	Organics + rare gyttja	F gravel - f sand + shell frag.	Gyttja, silt + little sand, fine plant frag, graded	Yes
Bondevik et al., 1997a,b	10 to 15	10.5	Thin	Mid	No	Organics + rare gyttja	F gravel - f sand + shell frag.	Gyttja, silt + little sand, fine plant frag, graded	Yes
Bondevik et al., 1997a,b	10 to 15	0	Mid	Mid	No	Peat, gyttja + silt	F gravel - f sand + shell frag.	Gyttja, silt and sand + clasts + organics	Yes
Bondevik et al., 1997a,b	10 to 15	1.5	Mid	Mid	No	Peat, gyttja + silt	F gravel - f sand + shell frag.	Gyttja, silt and sand + clasts + organics	Yes
Bondevik et al., 1997a,b	10 to 15	6.5	Thin	Thick	No	Peat, gyttja + silt	F gravel - f sand + shell frag.	Gyttja, silt and sand + clasts + organics	Yes
Bondevik et al., 1997a,b	10 to 15	8.5	Very Thin	Very Thick	Yes Distal	Peat, gyttja + silt	F gravel - f sand + shell frag.	Gyttja, silt and sand + clasts + organics	Yes
Bondevik et al., 1997a	10 to 15	0.5	Thin	Mid	No	Organics + rare gyttja	F gravel - f sand + shell frag.	Gyttja, silt + little sand, fine plant frag, graded	Yes
Bondevik et al., 1997a,b	10 to 15	1.5	Thin	Thick	No	Organics + rare gyttja	F gravel - f sand $+$ shell frag.	Gyttja, silt + little sand, fine plant frag, graded	Yes
Bondevik et al., 1997a,b	10 to 15	2.5	Thin	Mid	No	Organics + rare gyttja	F gravel - f sand + shell frag.	Gyttja, silt + little sand, fine plant frag., graded	Yes
Bondevik et al., 1997a,b	10 to 15	3.5	Very Thin	Very Thick	Yes	Organics + rare gyttja	F gravel - f sand + shell frag.	Gyttja, silt + little sand, fine plant frag., graded	Yes
Romundset and Bondevik, 2011	-	0.4	Mid	Mid	Yes	Peat and gyttja	Very coarse sand	Silt and organic detritus	Yes
Romundset and Bondevik, 2011	-	1	Thin	Mid	No	Peat and gyttja	Very coarse sand	Sand and mud matrix, gyttja + peat clasts	Yes
Romundset and Bondevik, 2011	-	3	None	Thick	No	Peat and gyttja	None	Sandy silt matrix, gyttja and peat clasts	Yes
Vasskog et al., 2013	20	3	Thick	Thin	Yes	Olive-coloured mud clasts	Massive silt + shell frag.	Sandy silt to clayey silt with clasts	Yes
Vasskog et al., 2013	15	3	Thick	Mid	Yes	Olive-coloured mud clasts	Massive silt + shell frag.	Sandy silt to clayey silt with clasts	Yes
Kelsey et al., 2005	10	5.5	Mid-Thick	Mid	Yes	Silt	Medium sand	Silt, fine sand and silty clasts	Yes
Kempf et al., 2015, 2017	15	5.5	Thin-Mid	Thick	Sometimes	Peat and gyttja	Fine sand	Poorly sorted sand	Yes
Kempf et al., 2015, 2020	20+	5.5	Mid	Mid-Thin	Yes distal/at depth	Peat and gyttja	Silty sand	Poorly sorted silty sand	Yes
Fruergaard et al., 2015	4	3.5	Thin	Very Thick	No	Gyttja and peat	Coarse sand + pebbles	Poorly sorted medium sand with clasts	Yes
Rasmussen et al., 2018	6	2.55	Mid	Thick	Yes	Peat and gyttja	Medium-fine sand	Sand, silt, peat + gyttja clasts + detritus	Yes
Rasmussen et al., 2018	5	6.75	Thin	Thin	No	Gyttja	Fine to coarse sand	Muddy sand matrix, gyttja clasts	Yes

(continued on next page)

Table 2 (continued)

Paper	Lake depth (m)	Barrier height (m)	Thickness of T2a/b	Thickness of T3/4	Is T5/6 present	Clast composition	T2 grain size	T3/4 grain size	Confidence	
Korsgaard et al., 2024	10	41	Thin	Mid	Yes	Gyttja and silt	Coarse to very coarse sand	Silty sand with gyttja and silt clasts + plant	Yes	
Korsgaard et al., 2024	5	21	Thin	Mid	Yes	Gyttja	Coarse sand	Fine-medium sand- gyttja clasts + plant frag.	Yes	
Grauert et al., 2001	5	10	Mid	Thick	Sometimes	Gyttja clasts	Coarse to medium sand	Sand, gyttja and silt	Yes	
Bondevik et al., 2005	10	17.5	None	Thick	Maybe	Silt and gyttja	Coarse sand	Silt and sandy gyttja	Yes	
Bondevik et al., 2005	6	17.5	Thin	Thick	No	Silt and gyttja	Medium-fine sand	Silt and sandy gyttja	Yes	
Bondevik et al., 2005	6	17.5	Thin	Thick	No	Silt and gyttja	Coarse sand	Silt and sandy gyttja	Yes	
Hutchinson et al., 2000	20	5	Thin-Mid	Mid-Thick	No	None (plant fragments)	Coarse sand to gravel	Sandy mud with plant frag.	Yes	
Nanayama et al., 2000	6	5	Mid	Mid	Yes	Mud	Medium to coarse sand with shells.	Medium sand matrix (+ fine s to silt in 7)	Likely	
Cuven et al., 2024	-	-	Thin	Mid-Thick	None	Mud or soil	Fine-medium sand	Silty sand with freq. Clasts	Likely	
Palmer et al., 2020	-	low?	None	Mid	None	Lagoonal mud + Bioclasts	None	Silty sand of bioclasts and organic clasts	Likely	
Garrison-Laney, 1998	5	5	None	Thin-Mid	Probably	Peat and mud	Medium sand	Sand with organic debris + clasts	Likely	
Finkler et al., 2018	-	?	None	Mid-Thick	Maybe	Lagoonal mud	None	Poorly sorted fine sand + silty clay.	Uncertain	
Footnotes:	Thickness:	Thin: < 5 cm; N	Mid: 5-15 cm; Thio	c <b>k</b> : 15+ cm		Abbreviations: fr	Abbreviations: frag. = fragment; freq. = frequent; $f$ = fine			

**Table 3**Summary of the key characteristics of the Group B deposits within the literature.

Paper	Lake depth (m)	Thickness of T1a/b	Is T5/6 present	Clast or matrix	Matrix composition	Shells: Frag. or whole	Gravels	Confidence	
Jackson et al., 2014	0 to 1.52	Thin-Mid	No	Matrix	F-c muddy sand	Frag.	No	Yes	
Atwater et al., 2012	<1	Mid	Yes-thick	Clast	F-vf sandy mud	Whole $+$ large frag.	Limestone	Yes	
Donato et al., 2009; Pilarczyk and Reinhardt, 2012	up to 2	Mid	Yes	Clast	Vf-f sand	eq:whole of the whole	No	Yes	
De Martini et al., 2010	N/A	Thin-Mid	No	Matrix	Gravelly sand	Frag. $+$ rare whole gastropods	Carbonates	Likely	
May et al., 2012a	<1	Thick/Thin	Yes	Clast	Sand	Frag.	At top	Likely	
Finkler et al., 2018	?	Mid-Thick	No	Matrix	Sandy silt	Frag. shell $+$ ceramics	Yes	Likely	
Bony et al., 2012	?	Thick	None	Clast	Silty sands	Frag. (large $+$ angular)	Marble	Likely	
Kohila et al., 2021	0.8	Mid	None	Matrix	Sand	Frag.	No	Likely	
Goff et al., 2000	0.5	Mid	Yes	Matrix	Silty sand	Frag. $+$ articulated	At base	Likely	
Pizer et al., 2021	<1	Mid	None	Matrix	Silty f sand	Whole, large $+$ small frag.	No	Likely	
López, 2012	3	Thin	Yes	Matrix	Gravelly sand	Well preserved large frag.	Yes	Likely	
De Martini et al., 2010	<1	Thin-Mid	No	Matrix	Silty sand	Frag. $+$ whole gastro	No	Likely	
May et al., 2012b	<1	Mid	No	Clast	M-f sand	Whole $+$ frag. Molluscs	At top	Likely	
Nichol et al., 2007; Goff et al., 2004	-	Mid	Yes	Clast	M sand	$\label{eq:whole of the frag.} Whole + frag.$	At base	Likely	
Fuentes et al., 2017	1	Thin-Mid	Yes	Clast	Sandy mud	Frag.	Coral/ lithics	Uncertain	
Fuentes et al., 2017	1	Thin-Mid	None	Clast	Sandy mud	Frag. + whole	At top	Uncertain	
Finkler et al., 2018	?	Mid-Thick	No	Matrix	C-m sand $+$ silt	Frag. shell + ceramics	Yes	Uncertain	
Fischer et al., 2016	1	Mid-Thick	No	Matrix	Sandy silt	No indication	No	Uncertain	
Fischer et al., 2016	1.5	Thick	Probably	Matrix	M sand	No indication	Some	Uncertain	
Hadler et al., 2013	?	Mid-Thick	None	Matrix	F sandy silt	Frag. large/whole	Yes-Rubble	Uncertain	
Vött et al., 2014	<1	Mid-Thick	None	Matrix	C sand - sandy silt	Frag., rare whole $+$ ceramics	Yes	Uncertain	
Clark et al., 2011	0.15	Mid	None	Matrix	M sand	Frag. (Oyster)	No	Uncertain	
Footnotes:	Thickness: Tl	nin: < 5 cm; Mid: 5	5-15 cm; <b>Thick</b> : 1	15+ cm		Abbreviations: frag. = fragment; $\mathbf{vf}$ = very fine $\mathbf{f}$ = fine; $\mathbf{m}$ = medium; $\mathbf{c}$ = coarse			

lagoons (see Supplementary Dataset 1) to define the key facies in tsunami deposits and their typical depositional groups, as described next.

# 3.3. Tsunami facies

The layers within the tsunami deposits can be grouped into several different facies (numbered 1-6) based on their grain size characteristics and inclusions of other materials:

T1a: Clast-supported shells: Dense mixture of whole shells, large

shell fragments and other coarse debris including ceramics, lithics and coral fragments within a sandy matrix. Poorly sorted. Often has a sharp basal contact.

**T1b: Matrix-supported shelly, silty sand:** Silty sand matrix with shell fragments, occasional whole shells and other coarse clasts that are less numerous than in F1a. Layer is massive and usually poorly sorted. Often has a sharp basal contact.

**T2a: Normally graded sand:** Coarse to medium sand with limited inclusions of shells and/or mud clasts. Normally graded. Typically has a sharp and erosional basal contact.

**Table 4**Summary of the key characteristics of the Group C deposits within the literature.

Paper	Lake depth (m)	Cores: distance from inlet (m)	Thickness of T2a/b	Is T5/6 present	Clast or mud inclusions	T2a/b grain size	Confidence
Matsumoto et al., 2010	1	0-1000	Mid-Thick	No	Rare (some mud clasts on shore)	Medium sand	Yes
Moreira et al., 2017	1	400-850	Mid	None	Isolated mud balls	Medium sand $+$ shell frag.	Yes
Shinozaki et al., 2015	2	50	Thin-Mid	Thick	None	Fine-medium sand	Yes
Bondevik et al., 1997b	10	_	Thick	Yes	None	Fine-medium sand	Yes
Bondevik et al., 1997b		_	Mid	No	None	Fine-medium sand	Yes
Pleskot et al., 2023	0.5	50	Thin	None	Peat clasts	Coarse sand	Yes
Pleskot et al., 2023	3.1	200	Thin	None	None	Coarse sand	Yes
Pleskot et al., 2023	1.5	25	Thin	None	None	Coarse sand	Yes
Pleskot et al., 2023	2.1	150	Thin	None	None	Coarse sand	Yes
Arcos et al., 2013	Shallow	50	Thin	None	None	Coarse sands with very rare shell frag.	Yes
Pinegina et al., 2018	_	800	Thin-Mid	None	None	Medium-c sands with some gravels	Yes
Sawai et al., 2008	2	50	Thin-Mid	Maybe	Plant detritus	Coarse sand to sandy mud	Yes
Biguenet et al., 2021, 2022	0.8	10-200	Mid	None	Single rip-up clast, rare mud laminae	Coarse to medium sand	Likely
Minoura et al., 1994	3.5	1000	Thin	No	None	Medium sand + some pebbles	Likely
King et al., 2023		300	Mid	None	Fine shell hash $+$ charcoal	M-c sand, fines up, very poorly sorted	Likely
Costa et al., 2012	2	1250-2750	Mid	None	None	Medium sand to sandy mud	Likely
Engel et al., 2023	2.8	75	Mid	No	Isolated small mud clasts (upper)	Medium sand	Likely
Obrocki et al., 2020	_	~2000	Thick	None	Clay (lagoon), small shell frag.	Coarse-m sand to sandy silt	Likely
Shimada et al., 2023	2.3	250	Thin-Mid	None	Rare mud clasts (terrestrial)	Fine-coarse sand	Likely
<b>Tuttle and Fuentes, 2021</b>	0.5	10\40	Mid	None	Clay clasts, Halimeda segments	Poorly sorted carbonate silty sand	Likely
Reicherter and Becker- Heidmann, 2009	2.5	100-200	Mid-Thick	Yes	Isolated clay clasts	Medium sand	Likely
Koster et al., 2015	2	1000-1500	Mid-Thick	Maybe	None	Medium to c sand	Likely
Lawrence, 2016	6	50	Very Thin	Very Thin	None	Medium sand	Likely
Mörner et al., 2020	-	-	Thin	Maybe	None	Sands or silty sands	Likely
Shinozaki et al., 2020	1.5	100	Thin	None	None	Fine sands	Likely
Wilson et al., 2013	<1	300-400	Thin	None	Isolated mud balls	Medium sand	Likely
Switzer and Jones, 2008	1	50 to 450	Very Thick	Yes	Rare org. Clasts + debris (nearshore)	Massive sand	Uncertain
Tanigawa et al., 2018	-	100-900	Thin-Mid	None	None	Medium-c sand	Uncertain
De Martini et al., 2010	N/A	up to 460	Thin-Mid	No	None	Clayey sand	Uncertain
Minoura and Nakaya, 1991	2	-	Thin	No	None	Fine to medium sand.	Uncertain
Minoura and Nakaya, 1991 Clark et al., 2011	2 0.15	- 250-500	Thin Mid	No None	None Oyster shells	Fine to medium sand. Medium sand + shells/	Uncertain Uncertain
					•	plant frag.	
Clark et al., 2011	0.25	40-120	Mid-Thick	None	Rare silt clasts	Medium-f sand, fines up	Uncertain
Engel et al., 2012	< 0.75	25	Thin	None	Shell frag base	Fining up sands	Uncertain
Leal et al., 2014	1	250	V Thin	None	None	Very fine sands	Uncertain
Oropeza et al., 2015	-	100	Thin	None	None	Fine sands	Uncertain
Ranasinghage et al., 2010	Shallow	100	V Thin	None	None	Coarse sands with rare shell frag.	Uncertain
Baranes et al., 2016	2	50	Thin-Mid	No	None	Medium sands	Uncertain
Hutchinson and Clague, 2017	2	-	Thin	Yes	Plant fragments	Sandy with plant frag.	Uncertain
Hutchinson and Clague, 2017	1	-	Thin	Yes	Organic fragments	Coarse sand to gravel	Uncertain
Minoura and Nakaya, 1991	_	_	Mid	No	None	Fine to medium sand.	Uncertain
Footnotes:	Thickness: Th	nin: < 5 cm; Mid: 5-15	cm; <b>Thick</b> : 15+ cm		Abbreviations: frag = fra	$\mathbf{r}_{\mathbf{f}}$ agment; $\mathbf{c} = \text{coarse},  \mathbf{f} = \text{fine};$	org = organic

**T2b:** Massive sand: Coarse to medium sand with limited inclusions of shells and/or mud clasts, moderate to poor sorting, typically thinner than T2a when present. Massive. Typically has a sharp and erosional basal contact.

**T3: Organic conglomerate:** Muddy sand or silty matrix containing clasts of peat, gyttja, silt and organic fragments. Poorly sorted layer. Typically occurs above T2a or T2b. Often has a sharp basal contact.

**T4: Organic debris layer:** Sandy mud or silty matrix, similar to T3 but with no clasts, finer organics and fewer sand inclusions. Typically, poorly sorted but sometimes normally graded. Typically overlies T2a or 2b. Often has a sharp basal contact.

T5/6: Silt/Gyttja laminae: Thin laminae or layers of silt or gyttja, typically overlie a sequence of the other facies.

These facies are in addition to the background lagoonal sediment of gyttja or organic silts which are present below and above the deposit at most locations.

#### 3.4. Tsunami deposit groups

The variability within the composition of the tsunami deposits can be encapsulated within three main arrangements of the facies in deposit groups. These are split into groups A-C (see also Fig. 4):

**Group A:** Consists of a thin (typically <5 cm thick) basal layer of T2a or b (massive or graded sand) which has a sharp erosional basal contact, overlain by a thicker (c. 10-15 cm thick) T3 or T4 layer, that is an organic conglomerate or organic debris layer. This is sometimes topped by a T5 or 6 deposit and occasionally by another T2a or b layer. The whole sequence is sometimes repeated within a single deposit to form couplets in basins close to sea level.

**Group B:** Consists of a poorly sorted 5-15 cm thick basal layer of T1a or b which is consistent with all the deposits in this group and is predominant. T2a/b or T5 occasionally cap this layer. Repeated sequences rarely occur.

**Group C: Split into two subgroups: Ci:** T2a/b sand layer that is 5-15 cm thick with limited mud laminae and clasts near the lake edge and the deposit is often poorly sorted. Sand layer occasionally capped by T5/6. **Cii:** thin (<5 cm thick) and structureless T2a/b sand layer.

In the following, the variation within these groups from the deposit database is described including how the deposits vary spatially with distance inland and lake depth. The environment surrounding the lake and the event types for each group are also summarised. Tables present the key information on the deposits of each group type, for full information on each deposit the reader can refer to the supplementary information (Table S1).

# 3.4.1. Confidence and uncertainty across the dataset

Across the dataset, 23 % of the deposits are recorded as uncertain events, 50 % as known events and 26 % as "likely" in their event attribution. Of the uncertain events, only one is attributed to a group A deposit, whereas 15 events have an uncertain origin for Group C deposits, with the majority (10) comprising the thinner Group Cii subtype. Outside of the Storegga tsunami deposits that are well known, the proportion of uncertain events rises to 50 % for deposits outside the historical record (earlier than  $\sim$ 1500). There appears to be no immediate correlation between the certainty of an event and the thickness of the deposit. However, there was a correlation between the detail of grain size data and the certainty of the event attribution. Across all deposit groups 68 % of "known" events were described with detailed grain size data (laser granulometry /dynamic image analysis techniques) compared to just 38 % for "likely" events and 17 % for "uncertain" events.

# 3.4.2. Group A deposit trends

Group A deposits are the most prominent group for tsunamis in coastal lakes/lagoons with deposits in 40 lakes/lagoons across the dataset, with a consistent structure across these deposits. The basal

sands (T2a/b) are relatively clean typically coarse to fine sands (Table 2). This contrasts sharply with the overlying organic conglomerate/debris layer (T3/4), which is a very poorly sorted mixture of gyttja (lake mud), silts and sands with plant fragments and clasts (Table 2). A mud cap (T5/6) overlies the sand-organic conglomerate couplet in many lakes, being most prominent in lakes with a greater depth (Table 2). In some lakes, this cap is laminated and is inferred to form post-event (Bondevik et al., 1997b; Kempf et al., 2015). In lakes of higher elevations there is a trend towards thicker T3/4 layers (and thinner T2a/b layers) that are more clast-rich (Table 1). Within the lakes, the basal sandy layer thins landwards (Bondevik et al., 1997b; Kempf et al., 2015) like deposits on land (e.g. Szczuciński et al., 2012). However, the thickness of the upper organic-rich layer is controlled by depth rather than distance inland, with thicker deposits at greater depths in the lake environments (Bondevik et al., 1997b; Grauert et al., 2001; Kelsey et al., 2005).

The environment of these Group A deposits shows trends across the dataset, for most lakes at least 5 m in depth. Furthermore, severe erosion from the tsunami is common in the proximal part of these lakes along the central axis (Korsgaard et al., 2024), where erosion can incise through thousands of years of accumulated sediment (Romundset and Bondevik, 2011; Fabbri et al., 2024). This erosion is recorded in the deposits by ripup clasts of cohesive gyttja from the lake floor (Table 2) and by peaty, silt and mud clasts from the surrounding mud-rich environments including marshes, peat bogs, farmland and estuarine muds (Table 2; Grauert et al., 2001; Kelsey et al., 2005; Kempf et al., 2015). These environments have been inferred at the time of the event, rather than the present day. Overall, these similar deposits were formed in a common environment and suggest these deposits were formed by the same processes.

#### 3.4.3. Group B deposit trends

Group B comprises 22 deposits across the dataset, consisting of sand to silty sand matrices, which contain abundant shell inclusions (whole and fragmented) and other coarse clasts within 5-15 cm thick deposits (Table 3; Atwater et al., 2012; Finkler et al., 2018; Pizer et al., 2021). The dataset shows a continuum of deposits from clast-supported layers with whole shells and large shells fragments (Atwater et al., 2012; Bony et al., 2012) through to sandy silt layers with finer shell fragment inclusions (Table 3; Jackson et al., 2014). In between, layers can be matrix-supported but still contain densely packed large shell inclusions (Fischer et al., 2016; Pizer et al., 2021). Shells are ubiquitous within deposits of this group, likely due to the nature of the sites in low-lying coastal environments where readily transportable shells are abundant (Atwater et al., 2012; May et al., 2012b). However, the shell assemblage comprises differing components (Table 3) from gastropods (often found whole) to molluscs (both articulated and disarticulated). These shells are primarily from the marine environment (Table 3), but in several deposits, shells were present from a brackish environment (i.e. a lagoon). Other inclusions vary depending on the material available within and around the coastal barrier and include marine corals, lithics, ceramics and other anthropogenic debris (Table 3). These different clast materials and shells are found mixed within the same layers (e.g. Atwater et al., 2012), suggesting their transport within the tsunami occurred simultaneously. In a quarter of Group B deposits, a mud cap was present, in common with the other deposit types (Group A and C).

The Group B deposits are found almost exclusively in lagoons where water depths are below 3 m (Table 3) and which have narrow (<500 m) and coarse-grained (often gravelly) coastal barriers (Bony et al., 2012; Hadler et al., 2013; Kohila et al., 2021). These barriers can also be anthropogenic such as harbour jetties that provide the source of gravels and clasts within the tsunami deposits (Finkler et al., 2018). The environments of these lagoons are generally quite arid (Mediterranean, Oman), but also occur in more temperate settings (New Zealand) (Beck et al., 2023). Overall, within these shallow lagoons, tsunami deposits consist of a dense mixture of clasts, whole shells and large shell

fragments derived from within and outside the lagoon.

#### 3.4.4. Group C deposit trends

Group C consists of 37 deposits across the dataset. These can be divided into two subsets, termed Ci and Cii. In Group Ci, deposits are 5-15 cm thick, massive or graded, coarse to medium sand layers that sometimes contain isolated mud or peat clasts from the underlying sediment, with limited coarse sand-sized shell fragments in the basal sections of some deposits (Table 4; Clark et al., 2011; Engel et al., 2012). These deposits often thin and fine inland. In 20 % of these lakes, a mud cap overlies this layer (Table 4). In contrast, Group Cii deposits are thinner (< 5 cm thick) and lack the internal structure or spatial trends observed in the thicker sand deposits. They are linked to smaller localised events or from the effects of waves from a distal tsunami (e.g. Arcos et al., 2013), suggesting these thinner layers may be associated with smaller waves. However, many of these studies containing thinner deposits were based on a single core taken from the coastal lake (Baranes et al., 2016; Pleskot et al., 2023) or had an uncertain tsunami or storm origin (Table 4). Across all Group C deposits, the lakes and lagoons have a shallow depth of less than 3.5 m, except for one lake in Greenland, where tsunami wave heights are often greater than the norm (Lawrence, 2016). The lakes and lagoons sit within a generally shallow gradient coastline backed by sandy beaches and barrier dune systems that are sparsely vegetated. These sandy beaches and dunes provide the main sediment source for the Group C deposits and show evidence of extensive erosion in the modern examples (Minoura and Nakaya, 1991; Matsumoto et al., 2010). However, some of the Group Cii coastlines have less erodible substrates of pebbles or vegetated ground (Table 4). Overall, these trends show that Group C deposits consist of predominantly sandy deposits that may vary depending on the event and surrounding environment.

# 3.5. Tsunami process and mechanisms

The database of tsunami deposits has enabled three key groups to be identified in coastal lakes and lagoons. The following discussion uses these groups to infer the different depositional processes based on the product to process approach. This approach is rarely taken in tsunami research, but in a recent review of tsunami sedimentology, Costa and Andrade (2020) state that a "better understanding [of] the univocal relationship between products and patterns of flow" is still required. Therefore, the processes involved in the deposition of each deposit group will be established by integrating knowledge of tsunamis with the processes of other environmental flows.

# 3.5.1. State of the science: Depositional processes and mechanisms during a tsunami

The current understanding of sediment transport and deposition during tsunamis is limited. However, one of the most obvious signs of a recent event is the marked erosion of underlying material as it inundates coastal land, especially adjacent to the coastline (Richmond et al., 2012; Szczuciński et al., 2012). This eroded sediment is interpreted to be transported inland by the tsunami flow through a combination of bedload traction (Moore et al., 2011; Koiwa et al., 2014) and suspension (Jaffe and Gelfenbuam, 2007; Morton et al., 2007). Traction transport of coarse-grained sediment at the base of the flow is thought to dominate initially as the tsunami wave inundates the land (Moore et al., 2011). However, further inland, sediment is lifted into the flow and carried in suspension incorporating finer grains before depositing gradually as the flow energy wanes (Jaffe and Gelfenbuam, 2007; Moore et al., 2011). This process is often known as differential settling and is assumed to occur within relatively clear-water turbulent waves in experimental (Yoshii et al., 2018), numerical modelling (Marras and Mandli, 2020), and sedimentological (Goto et al., 2011; Takashimizu et al., 2012) studies. However, one recent study (Majumdar and Bhattacharya, 2025) has utilised the process sedimentological approach to infer different

flow conditions during the Indian Ocean 2004 tsunami, including debris flows and turbidity currents. Aside from this study, little consideration has been given to the tsunami flow rheology, density and concentration, which are important determinants of the processes of deposition during a flow event (Peakall et al., 2020; Baas et al., 2021). This means that the current tsunami sedimentation models lack the complexity necessary to reconstruct how sediment is transported and deposited during past events.

#### 3.5.2. Group A processes

The standard tsunami sedimentation models have been used to explain deposits in (deep) coastal lakes, represented by the Group A deposits in this study. For these deposits, the model of Bondevik et al., 1997b is still applied, based on Storegga tsunami deposits in 18 lakes in Norway (see Fig. 1). In the study areas, the shoreline before the tsunami consisted of gyttja sediments in the lake basin, peat on the lake rim, sand and gravel on the beach and marine silt and fine sand below sea level. The tsunami is hypothesised to have flowed into the lakes as debris-rich water, with turbulence generated on the lee-side of the lake barrier due to the increased velocity as the wave overtopped the barrier. Sediments on the basin floor were "stirred into suspension" by the tsunami flow and sometimes ripped up as clasts (Bondevik et al., 1997b). The tractiontransported sand was then deposited in a normally graded sand layer above the erosion surface. As the wave slowed, rip-up clasts, sand, wood and other organic fragments settled out from suspension in T3/4 layers. The subsequent withdrawal of the waves following backwash allowed the fines to settle out from suspension as a mud cap. This model applies the same ideas as the standard tsunami sedimentation models (e.g., Jaffe and Gelfenbuam, 2007; Moore et al., 2011) and similarly lacks the complexity to explain how these deposits are formed. This model fails to adequately explain its key feature, the T3/4 layers (organic conglomerate/detritus). These layers are a poorly sorted mixture of inclusions of differing densities that could not settle preferentially through suspension as suggested into such a poorly sorted layer, despite some grading in the upper portion. In offshore tsunami deposits, similar mud-rich poorly sorted layers are inferred to be deposited via en-masse deposition (Riou et al., 2020; Feist et al., 2023). The rapid deposition under this mechanism would enable the components of differing densities observed in T3/4 layers to be deposited in a single poorly sorted layer. However, such deposition would occur under laminar rather than (the assumed) turbulent flow conditions (e.g., Talling et al., 2012). The existing theories also fail to acknowledge the different processes that occur when a tsunami reaches a lake. The interaction between the ambient lake water and the incoming tsunami wave will alter the wave's depositional processes, as is observed for other event deposits within lakes.

Flows of other extreme events (e.g., floods, earthquakes, lahars, landslides) entrain and transport large amounts of sediment into lake environments (Sabatier et al., 2022). These sediment-laden flows create a strong density contrast with the clear water of lakes that causes the flow to travel along the lake floor as a subaqueous gravity flow (Girardclos et al., 2007). These flows typically take the form of highly turbulent turbidity currents that deposit characteristic sand beds on the lake floor (Girardclos et al., 2007; Van Daele et al., 2020; Sabatier et al., 2022) and are common in other environmental settings (Mulder and Alexander, 2001; Talling et al., 2012; Peakall et al., 2020). During tsunamis, sediment gravity flows as they are collectively known (Middleton and Hampton, 1973) have been proposed to occur in offshore settings, including turbidity currents (Arai et al., 2013; Riou et al., 2020; Bondevik et al., 2024) and debris flows (Feist et al., 2023; Earland et al., 2024), that transport sediment to the deep sea. However, in coastal lakes, gravity flows have only received a single brief mention during tsunamis, for a deposit in Norway of the Storegga tsunami (Vasskog et al., 2013). The authors suggested that the entrainment of fine-grained sediment by the tsunami wave would create a "strong contrast in density... [and] may have caused the initial inflow of the tsunami to travel along the lake floor in the form of a highly concentrated subaqueous

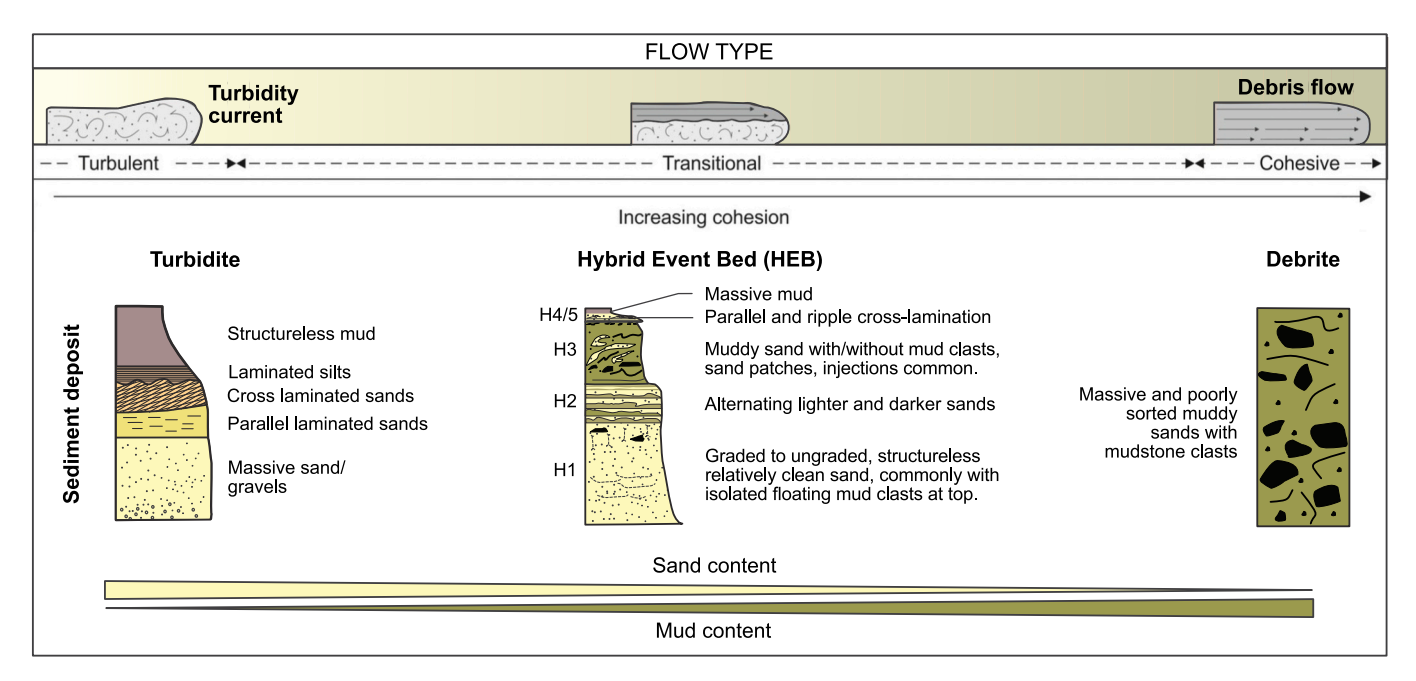


Fig. 5. Schematic of the continuum of flow types and their deposits from fully turbulent turbidity currents to fully cohesive debris flows. Deposit diagrams are based on the proposed models from the literature, namely the Bouma sequence (turbidite) (Bouma, 1962; Peakall et al., 2020), hybrid event beds (HEBs) (Haughton et al., 2009) where H1-5 indicate the layers in the deposit noting that H3 can be with or without the inclusion of mud clasts, and debrites (Talling et al., 2012). Top of the figure modified from Peakall et al. (2020), and reprinted with permission from John Wiley and Sons.

density flow (cf. Mulder and Alexander, 2001)." The authors convey that this scenario is unique to the setting at the head of a long (>100 km) fjord comprising copious amounts of readily erodible fine-grained sediment. However, as we discuss in the next section, there is

evidence to suggest that a similar density contrast with freshwater coastal lakes and lagoons is present during many tsunami events.

The current theory of tsunami flow dynamics suggests that they are relatively clear water waves (Jaffe and Gelfenbuam, 2007; Yoshii et al.,

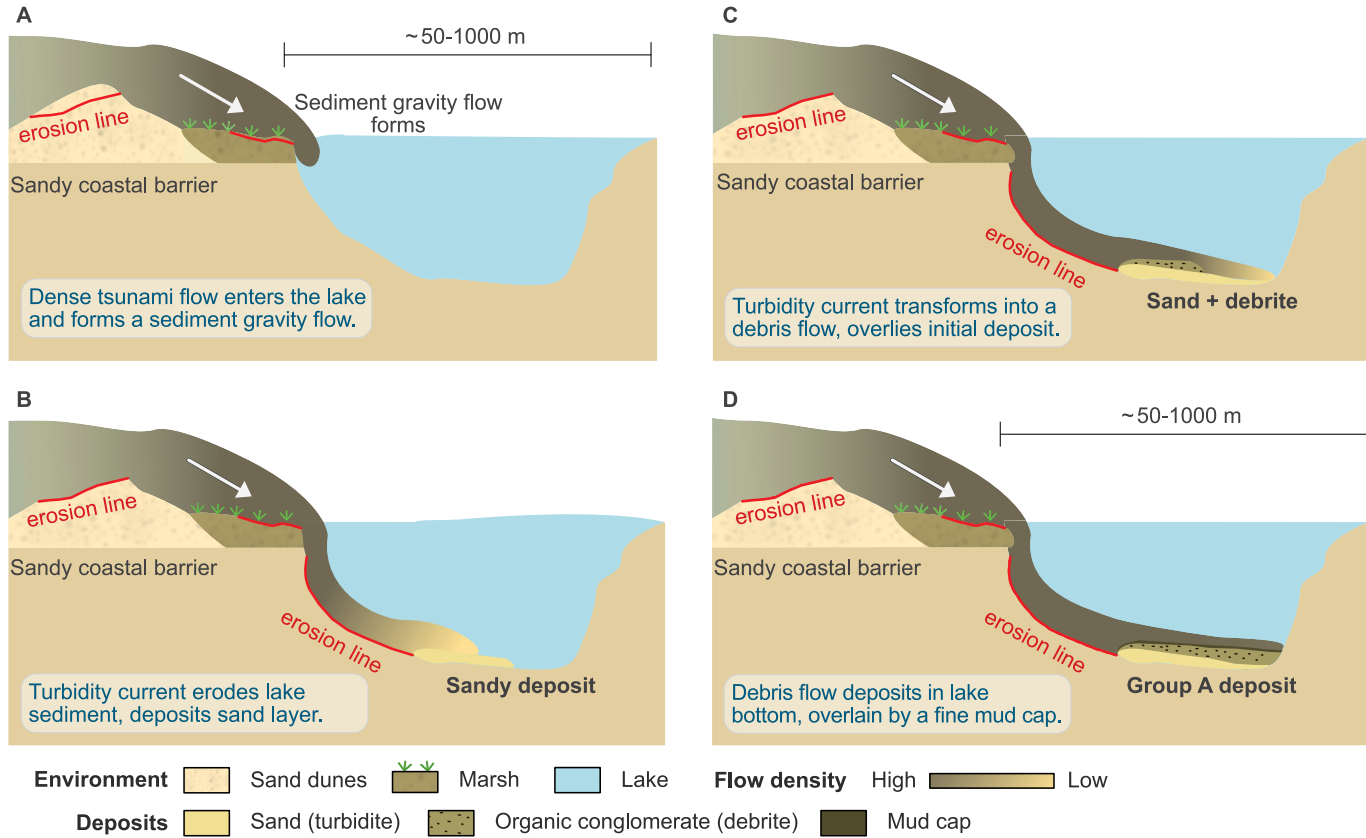


Fig. 6. Schematic showing the formation of a sediment gravity flow as a tsunami enters a coastal lake and the subsequent deposition of a Group A (hybrid event bed) tsunami deposit. The arrow indicates the direction of tsunami travel. The legend shows the environment, deposits and flow densities depicted.

2018; Marras and Mandli, 2020), however, even under such conditions a density contrast is present between the seawater of the tsunami wave ( $\sim$ 1025 kg m<sup>-3</sup>) and the freshwater ( $\sim$ 1000 kg m<sup>-3</sup>) or brackish water  $(>1000 - <1025 \text{ kg m}^{-3})$  of the coastal lake or lagoon. This equates to an up to 2.5 % density difference, in the case of seawater entering a freshwater lake, a density difference more than sufficient to generate a subaqueous gravity flow (e.g. Best et al., 2005; Felix et al., 2006). In fact, such a density difference is an order of magnitude greater than those typically seen in marine sediment gravity flows (Konsoer et al., 2013; Simmons et al., 2020). Although not previously acknowledged, even clear water tsunamis would therefore be expected to plunge as a gravity flow as they entered a coastal lake or lagoon given sufficient depth. However, the evidence suggests that tsunami waves are not clear water as they will entrain virtually all sediments they pass over (Peters and Jaffe, 2010; Shanmugam, 2011; Richmond et al., 2012) and transport this sediment over 10s to 100 s of kilometres of coastline and up to several kilometres inland (Abe et al., 2012). This suggests that in many scenarios, the sediment concentration and thus the density of the tsunami will be greater. Indeed, for areas during the Indian Ocean tsunami a dense debritic flow regime has recently been inferred to develop through analysis of sedimentary and video evidence (Majumdar and Bhattacharya, 2025). More broadly, eyewitness accounts for the event across Thailand, Indonesia and Sri Lanka describe the tsunami changing to a dark brown or black colour, depicting a flow with a high sediment concentration (Spence et al., 2007). Therefore, in many coastlines, tsunami flows may be sediment-laden, and in combination with their predominantly seawater composition, are sufficiently dense to be able to generate a subaqueous gravity flow in the manner of other event types that transport sediment into lakes (e.g. Sabatier et al., 2022). We suggest that given the predominantly readily erodible mud-rich substrates present on Group A coastlines, this process of subaqueous gravity flow formation occurred during those tsunamis. This process would explain why the Group A tsunami deposits in lakes differ from the usual sandy deposits observed in other terrestrial environments such as coastal plains and marshes (Smith et al., 2004; Peters and Jaffe, 2010). The Group A deposit composition needs to be compared to the deposits of subaqueous gravity flows to consider the type of subaqueous gravity flow that forms.

Deposits from subaqueous gravity flows are governed by the flow deceleration rate and the balance of turbulence to cohesive forces (e.g., Stevenson et al., 2020). The latter is represented by the flow rheology (type) (Fig. 5; e.g., Baas et al., 2009; Peakall et al., 2020). At one extreme, deposits consist of a series of normally graded or massive sand deposits, termed Bouma sequences, that form from suspension under a fully turbulent turbidity current (Fig. 5; Bouma, 1962). At the other extreme, mud- and debris-rich deposits that are poorly sorted form via en-masse deposition under a fully cohesive debris flow. In between these end-members, deposits from transitional flows that involve mud-rich sediments are increasingly being recognised in the geological record (Fig. 5; e.g., Haughton et al., 2003, 2009; Talling et al., 2004; Baas et al., 2009, 2011, 2021; Peakall et al., 2020). If we consider the layers of the Group A deposits, the basal sand (T2a/b) closely resembles the deposits formed under a turbidity current. Whereas the organic conglomerate layer (T3) contains mud clasts that "float" within a chaotic poorly matrix of sands and silts. This suggests that these layers are formed under a fully cohesive debris flow in en-masse deposition. Under this flow regime, the cohesivity generates buoyancy forces and matrix strength sufficient to support the clasts within the flow (Peakall et al., 2020). Overall, the two main layers of the Group A deposits are likely deposited under different flow rheologies, but during the same event. In subaqueous gravity flows, this situation is referred to as a hybrid flow where turbidity currents, at a given point in space, transform over time into more cohesive states depositing a series of linked layers termed hybrid event beds (HEBs) (Fig. 5; e.g., Haughton et al., 2009; Peakall et al., 2020; Baas et al., 2021; Łapcik and Baas, 2024). HEBs are now widely reported in the literature (e.g., Talling et al., 2004; Haughton et al., 2009; Fonnesu et al., 2015;

Baas et al., 2021; Siwek et al., 2023) and closely resemble those of Group A deposits formed during tsunamis. Therefore, the evidence suggests that Group A deposits are a form of HEB that is generated under a transforming gravity flow initiated by the tsunami wave. However, the exact processes and mechanisms by which HEBs form are still debated (Haughton et al., 2009; Fonnesu et al., 2015; Baas et al., 2021; Łapcik and Baas, 2024).

Flow transformations forming HEBs can be driven by the incorporation of cohesive fine-grained material within the flow (Talling et al., 2004; Baas et al., 2021). The front of turbidity currents preferentially erodes and concentrates the most mobile sediment in a system (Baas et al., 2021). Therefore, where these flows pass over mud-rich cohesive substrates and the erosion is sustained, the cohesivity and density in the head can increase due to the incorporation of fine cohesive sediment (mud) (Baas et al., 2021; Peakall et al., 2024). If erosion is continuous and the system is mud-rich the head can transform into a fully debritic flow (Kane et al., 2017; Baas et al., 2021; Peakall et al., 2024), else a more transitional flow front may form instead (Lapcik and Baas, 2024). Thus, the availability of mud and the ability of the flow to continuously erode sediment are crucial factors in the formation of HEBs. The Group A deposits share these features. First, both the lake-bed and often the surrounding mud-rich substrate (Table 2) provide readily erodible and mud-rich cohesive substrates over which the tsunami passed. Furthermore, the erosion both within these lakes and between the lake and the ocean is shown to be severe and sustained through to the bottom of the lakes. The resultant deposit has a consistent structure but varies in its mud content, clast size and thickness (Table 2), comparable to the high variability in HEB deposits (Fonnesu et al., 2015, 2018; Privat et al., 2024). Finally, the thinning landward of the basal sandy layer and the thickening of the more cohesive upper layer (interpreted as the debrite) is also observed for HEBs (e.g., Talling et al., 2007, 2012) consistent with the downdip progression of a turbulent flow into a more dominant debritic regime further from the source (Fonnesu et al., 2015), although over shorter spatial scales. Overall, the Group A deposits resemble HEBs and share the characteristics and conditions under which a HEB forms. Therefore, we conclude that Group A deposits are essentially HEBs that form under a tsunami-induced, rapidly transforming subaqueous gravity flow within the coastal lakes. The following provides the depositional model for Group A deposits.

We propose that the tsunami wave becomes dense and sedimentladen through erosion of beach and muddy substrates (marsh, peat, farmland) in the nearshore region. Depending on the morphology of the waves and distance inland, the densest part of the flow may be at the flow front where erosion is concentrated or behind a more dilute front where entrainment has been less intense. In either case, the density difference between the sediment-laden seawater-dominated tsunami and the freshwater in the coastal lake, produces a sediment gravity flow as the tsunami enters the coastal lake, initially taking the form of a turbidity current (Fig. 6a). This current erodes the cohesive lake sediment on the slope as it travels, further increasing the density of the flow (Fig. 6b). Subsequently, this would, like similar situations in the deep sea (Baas et al., 2021), increase the cohesivity of the flow, causing transformation to more transitional and debritic flow types further into the lake as the flow decelerates. The degree to which the transformation occurs is dependent on the lake depth, length and mud content of the flow. Deceleration of the flow leads to initial deposition of sand (Fig. 6b), followed by flow transformation to a debris flow (Fig. 6c,d). The flow therefore deposits a turbidite-debrite couplet as seen in HEBs that closely resemble those of Group A for tsunami deposits in coastal lakes and lagoons (Fig. 6c). A mud cap would settle through the suspension of fine sediment within the water column after the flow has receded (Fig. 6d). The influx of saline water from the tsunami can aid the formation of a stratified water column with a saline, anoxic bottom layer that may subsequently facilitate the formation of laminated varves (Minoura and Nakaya, 1991; Kelsey et al., 2005; Kempf et al., 2017).

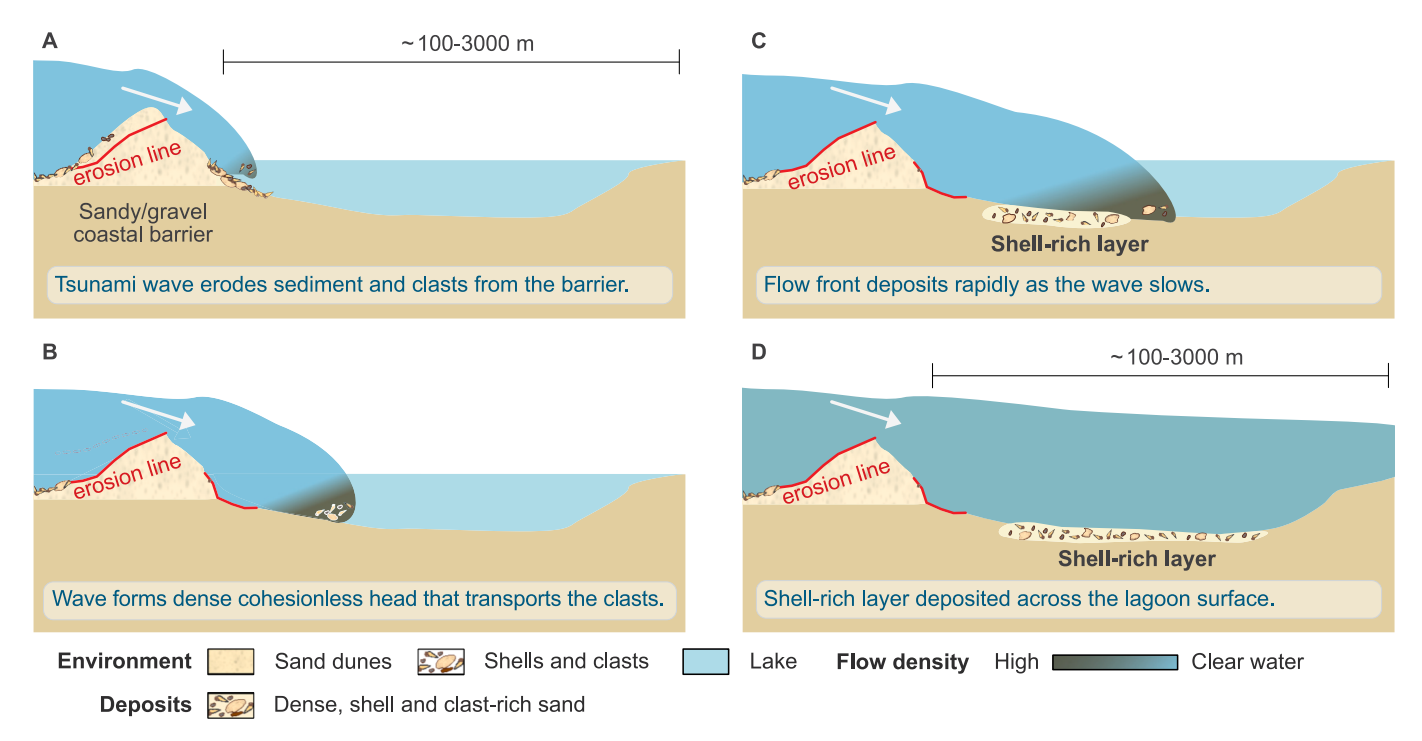


Fig. 7. Schematic showing the processes involved in the formation of Group B (shell-rich) tsunami deposits in shallow coastal lagoons. The arrow indicates the direction of tsunami travel. The legend indicates the environments, deposits and flow densities depicted.

#### 3.5.3. Group B processes

Group B deposits typically occur in shallow coastal lakes and lagoons, many less than 1 m in depth, in sharp contrast to the typically >5 m depth of Group A coastal lakes. Therefore, there is an insufficient depth for a subaqueous gravity flow to plunge based on the density difference between fresh and saline water. Furthermore, the Group B deposits consist of single shell-rich layers that are visually distinct from those of Group A. This suggests that a different depositional mechanism occurs in these lagoons under a flow with a single rheology.

The key component of Group B deposits is their chaotic nature, comprising a poorly sorted and often clast-supported mixture of shells, lithics and ceramics within sandy matrixes. In other depositional settings, the size and quantity of such coarse components would suggest a flow would only have sufficient energy to transport and deposit via traction rather than in suspension (Chiodi et al., 2014). Under traction conditions, deposition occurs incrementally grain-by-grain permitting longitudinal segregation and sorting of the components of the flow as the energy wanes (Steidtmann, 1982). This results in well sorted deposits that fine inland, in sharp contrast to the Group B deposits which often have very poor sorting. Furthermore, the abrupt and inconsistent landward fining of the Group B deposits suggests limited longitudinal segregation is occurring in the tsunami flow. Instead, the chaotic distribution of non-hydrodynamically equivalent components from large and whole shell fragments to lithics and ceramics points to transport in a high-concentration flow that restricts segregation, and deposition under capacity-driven sedimentation (Hiscott, 1994). In capacity-driven sedimentation, as the flow decelerates, there becomes insufficient energy for the flow to carry the total sediment load, thus driving sedimentation of all grain-sizes simultaneously. This occurs even though velocity is sufficient (competent) to transport all grain-sizes (Hiscott, 1994). Consequently, segregation of different grain sizes is restricted, and sedimentation at the base of the flow occurs rapidly (Hiscott, 1994). Prior to sedimentation the flow must have an appreciable density to restrict movement and thus sorting and segregation (Peakall et al., 2020). This high-density component of the flow may explain the considerable thickness (often 10-20 cm) of the Group B deposits, which are far thicker than could be generated by the small quantities of bedload-sediment transported by traction over the short timescale of the flow. Overall, we suggest that the deposits cannot have formed under simple traction transport, but instead under a flow of high-density that deposits rapidly via capacity-driven sedimentation. Such deposition has recently been suggested for a tsunami deposit in Scotland where sediments of a wide range of grain sizes remained unsegregated within the deposit (Hill et al., 2023). However, this process is otherwise not referred to in the existing tsunami literature, restricting our understanding of how this process develops. Recent developments in the study of subaqueous gravity flows may provide an answer.

A cohesive flow state such as that proposed for the process of deposition during tsunamis in Group A would have a high density and deposit *en-masse* as the wave slows. However, the deposits of cohesive flows (debritic and transitional flows) are mud-rich and generally characterised by the inclusion of cohesive clasts (mud and organics). Group B deposits lack indication of sufficient cohesive clays or organic sediments required to produce a cohesive flow. Therefore, unlike during Group A tsunamis, a cohesive flow state is unlikely to develop.

An alternative is that the tsunami flow developed a dense but cohesionless flow head as recently observed in turbidity currents (Gwiazda et al., 2022; Pope et al., 2022). Turbidity currents much like tsunamis have suffered from a lack of direct measurements of the flow of actual events (e.g. Dorrell et al., 2019). However, recent observations have shown that in high-velocity flows (those >1.5 m/s), a dense and cohesionless flow head can develop where substrates are sand-rich (Clarke, 2016; Paull, 2018; Pope et al., 2022). This head has a high sediment concentration (estimates are 10-38 % volume) resulting in a region of dampened turbulence and a flow which is strongly stratified between the dense basal layer and the dilute upper layer (Gwiazda et al., 2022; Pope et al., 2022). The flow head is estimated to transport 1000 times more sediment than the dilute flow body and is dominated by grain-to-grain interactions (Pope et al., 2022). Therefore, clasts entrained by the flow are either encased within the dense head or rafted on its surface, resulting in objects of different shapes, densities and size moving synchronously together (Paull, 2018). Although this high concentration cohesionless head has been observed through measurements of modern flows, no association has been made to the resultant deposits

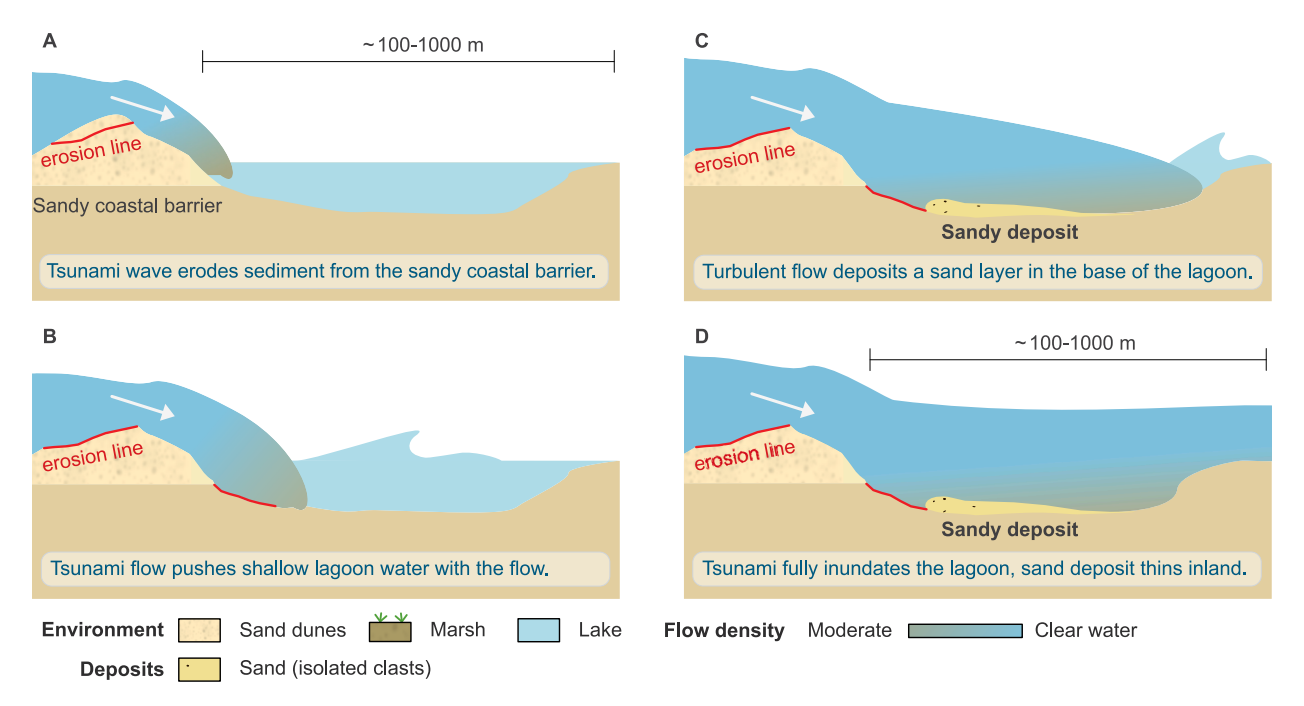


Fig. 8. Schematic showing the processes involved (from A-D) in the formation of Group C (sandy) tsunami deposits in shallow coastal lakes. The arrow indicates the direction of tsunami travel. The legend shows the different environments, deposits and flow densities depicted.

in the geological record (Pope et al., 2022). However, if we consider the likely mechanism of deposition, the high density of the head and the grain-to-grain interactions within the flow will result in deposition as grain-supported layers. Overall, a flow with a cohesionless flow head can form during an event and can deposit rapidly in clast-supported layers.

This flow condition can explain how the Group B deposits formed. First, the cohesionless head fits with the lack of cohesive material in the Group B deposits, but the high density enables the shells, lithics, ceramics and other clasts to be held in a relatively fixed position within the flow head. This restricts the sorting and segregation of these differing components during transport. Furthermore, the dominance of grain-tograin interactions in the flow head (Pope et al., 2022) and high sediment concentration could explain the presence of clast supported and high-density layers in Group B deposits. Therefore, we suggest a similar process and mechanism occurs during tsunamis in shallow lakes and lagoons that lack cohesive substrates. First, the turbulent tsunami entrains sandy sediments, shells and other clasts from the shallow marine, beach and coastal barriers (Fig. 7a). As the tsunami overtops the coastal barrier into the shallow lagoon, the sediment concentration within the flow rapidly increases, forming a dense flow head akin to that formed in rapid turbidity currents (Fig. 7b; Pope et al., 2022). This dense flow head transports the sands, shells and other clasts through the lagoon and erodes further non-cohesive sands and silts from the lagoon bed as well as further clasts. As the tsunami slows, the wave no longer has the capacity to support the sediment and clasts within the flow, causing rapid capacity-driven deposition (Hiscott, 1994) as proposed for a tsunami event by Hill et al. (2023) (Fig. 7d). This produces deposits in grainsupported, poorly sorted layers of sands, shells and clasts (Fig. 7c, d). A dense flow head is hypothesised to develop in all Group B deposits, however, the relative ratio of sands to shells and other clasts within the flow largely determines whether the layer is clast- or matrix-supported. In the latter, the deposits are massive, poorly sorted sands with frequent clast inclusions rather than clast-supported layers. This continuum of deposits reflects the variability in the source sediments in the immediate coastal environment.

#### 3.5.4. Group C processes

Group C deposits are differentiated from Group B by finer grain sizes and the absence of shells and other clasts. The thinner, Group Cii deposits are correlated with the waves of distal tsunamis (Arcos et al., 2013; Wilson et al., 2013) or are present in coastal lakes at high elevations near the inundation limit. These events are likely to have a lower inundation depth. Furthermore, a positive relationship between tsunami depth and deposit thickness is often recorded and used within inverse tsunami modelling (Jaffe et al., 2016; Naruse and Abe, 2017). Overall, this suggests that many of these thin deposits record events of a low inundation depth that more closely resembles that of storm events (Chaumillon et al., 2017). Alternatively, some of the deposits are found in rocky or vegetated coastlines where the substrate is not readily erodible (Hutchinson and Clague, 2017; Pleskot et al., 2023). This limited sediment supply would reduce the amount of sediment a tsunami could transport, resulting in a dilute flow. However, there is major uncertainty in the processes involved due to reliance on single or dual cores in many of these studies (Minoura and Nakaya, 1991; Pleskot et al., 2023). Overall, Group Cii deposits represent deposition under a more dilute, and likely lower depth, flow compared to the events represented by other deposit groups.

The thicker, Group Ci subset shows distinctive similarities with deposits of modern and palaeo tsunamis in many different environments (Peters and Jaffe, 2010; Moore et al., 2011; Hocking et al., 2021). First, they thin and fine inland within the lakes and lagoons. This process occurs as the tsunami slows and becomes shallower further inland, resulting in a flow that can only transport smaller amounts of finer sediment (Naruse and Abe, 2017). Furthermore, isolated mud clasts are found within these thicker Group C deposits as seen in other predominantly sandy deposits for tsunami deposits in marshes (e.g. Hocking et al., 2021); tidal flats (e.g. Cisternas et al., 2005) and coastal plains (e. g. Morton et al., 2007). A highly erosive, high-velocity flow is required to erode and entrain these cohesive clasts (Peters and Jaffe, 2010), therefore, where the flow is turbulent these clasts are often limited to the immediate coastal areas where the flow velocity is greatest (Fritz et al., 2006; Hayashi and Koshimura, 2013). This is also reflected in the Group Ci deposits where clasts if present are only found near the lake outlets (Matsumoto et al., 2010). However, these Group Ci deposits lack the

major inclusions of muddy components seen elsewhere (e.g. Richmond et al., 2012; Dura et al., 2015) due to the dominance of sandy substrates in the Group C deposit coastlines. Overall, these deposits share the characteristics of deposits identified in other depositional environments as being from a turbulent high-velocity tsunami wave.

Group Ci deposits exhibit a similar composition to those on land suggesting that similar depositional processes occurred, this can be explained by their lake's shallow depth. Of all the coastal lakes and lagoons that contain Group Ci deposits only one has a depth greater than  $\sim$ 3 m. These lakes lie behind very narrow coastal barriers (<300 m wide) meaning the tsunami height will be near its maximum nearshore value which is variable but typically more than 5-10 m for large earthquake generated tsunami (Röbke and Vött, 2017). This depth is far greater than that of the lake, making a sediment gravity flow akin to those proposed to form for the other deposit groups harder to envisage as the lakes do not have the vertical space to allow their formation. Instead, the tsunami would likely incorporate the lake water within the tsunami flow. By removing the ambient water of the lake or lagoon the tsunami would act in the same manner as one passing over other terrestrial environments, such as a coastal marsh. The exception to the shallow lake depth is a lake from Greenland (Korsgaard et al., 2024), hypothesised to be associated with a localised subaerial landslide tsunami, which can reach heights well above the typical tsunami heights (Svennevig et al., 2024). Therefore, even in this case, the tsunami depth would dwarf that of the lake or lagoon, and a similar process would occur. Overall, in Group Ci deposits, we can return to the notion of a tsunami with a high-velocity turbulent wave that transports the sediment via bedload and suspension (Jaffe and Gelfenbuam, 2007).

The following model is proposed for Group C deposits. The initial tsunami wave erodes sediment from the nearshore of sandy beaches and dunes and transports this sediment into the coastal lake or lagoon (Fig. 8a). As the wave reaches the water of the lake or lagoon, it pushes the water with the flow and in tsunamis of high-velocity limited mud clasts are ripped up from the lagoon surface and incorporated into the flow (Fig. 8b). Transport of sediments from the coastal barrier dominates the flow. As the wave slows through the lake, it deposits sediment through suspension and bedload mechanisms (Fig. 8c, d). Which mechanism dominates is related to the wave size, with theory dictating that a higher energy wave is required to transport sediment via suspension rather than traction (bedload) (Chiodi et al., 2014). Therefore, in larger events with a readily erodible sandy substrate (typically Group Ci events), suspension transport will be more dominant. Whereas in small events (Group Cii), bedload transport will be dominant, resulting in thinner deposits. In the quiescent phase of the wave, any fines will settle in a fine mud cap.

In summary, across the three deposit groups a continuum of flow processes is thought to occur. These include the formation of fully cohesive sediment gravity flows that transform rapidly within the lake environment to produce hybrid event beds; cohesionless flow fronts that transport sediment and fragile clasts together before undergoing capacity-driven deposition in grain- or matrix-supported layers. Finally, the deposition of sandy deposits under a turbulent tsunami flow. This shows the range of possible processes that occur during tsunami inundation of coastal lakes and lagoons.

# 3.6. Implications for tsunami sedimentation

#### 3.6.1. Controls on deposit type

The interpreted processes from Groups A-C suggest a major control of the surrounding environment on the deposit type. This reflects a wider trend in tsunami deposits that are often highly dependent on the locally available sediment and antecedent topography (Peters and Jaffe, 2010; Richmond et al., 2012). The environment of Group A deposits is clearly distinct from the other two deposit groups, with a deeper lake and often with mud-rich sediments from marshes and bogs between the lake and the sea. These characteristics facilitate the conditions necessary for the

formation of a sediment gravity flow. Superficially, the environment of Group B and C deposits is similar, with a coastline typically consisting of a relatively short sandy beach barrier separating a shallow ( $<5\,\mathrm{m}$  depth) lagoon from the ocean. However, the key difference in these environments is the availability of shells (in their growth positions) together with other pebble- to cobble-sized clasts. In this respect, Group B deposits occur when there are more shells, rocky outcrops or ceramics from anthropogenic debris available to be transported from the marine and/or brackish (lagoonal) environment by the tsunami wave. This difference in sediment supply results in the differing nature of these deposits and the processes that occur during their formation.

The dataset shows that the same tsunami event can record different deposits in varying environments. The Lisbon 1755 tsunami is recorded across the three deposit groups. The deposits local to the tsunami in Portugal are in shallow lagoons on sandy but shell-deficient coastlines (Costa et al., 2012) and thus form sandy Group C deposits that thin and fine inland. In contrast, deposits in the Caribbean show the far-field effects of the tsunami, with Group A deposits in a narrow coastal lagoon (Fabbri et al., 2024), sandy Group C deposits on a sandy tropical island (Biguenet et al., 2021) and clast-supported shell layers (Group B) on a low-lying reef atoll rich in shells (Atwater et al., 2012). This variability highlights the greater influence of the local environment on the resultant deposit, rather than the tsunami size which might be expected to produce a common deposit for a single event over a wide geographical area. However, a common deposit is observed where a preservation or search bias results in the deposits of a single event being recorded in very similar environments. This is observed for the Storegga tsunami where deposits in Norway (Bondevik et al., 1997a), Shetlands (Bondevik et al., 2005), Faroes (Grauert et al., 2001) and Denmark (Fruergaard et al., 2015) all record Group A deposits dominated by cohesive clast inclusions eroded from the surrounding peat and gyttja eroded from the lakebed. Therefore, a single event may either record similar or different deposits dependent on the variety of environments where they are found.

#### 3.6.2. Implications for tsunami events

The product-to-process approach used in this study has proposed new and more detailed ideas about the processes and dynamics of a tsunami flow.

The processes interpreted for tsunamis in this study contradict the widely held notion of a relatively low sediment concentration and turbulent flow during inundation (Moore et al., 2011; Yoshii et al., 2018). The inferred processes for Group A and B deposits show that in both these environments a high-density flow (head) must develop. This suggests that a flow of high density can develop on coastlines with mud-rich substrates (Group A), but even over cohesionless substrates (Group B) the flow front can attain a high density. This phenomenon of tsunami waves is not surprising given their widely cited erosive capacity (Takashimizu et al., 2012) and the spatially extensive distribution of their deposits (Peters and Jaffe, 2010; Abe et al., 2012). Furthermore, a sediment-laden tsunami flow is visually evident, if not directly acknowledged, on the muddy plains of the Sendai plain during the Tôhoku-oki tsunami (Hayashi and Koshimura, 2013). However, a consideration of the density of a tsunami wave has been conspicuously absent in modelling studies (Marras and Mandli, 2020) and tsunami hazard assessments (Macabuag et al., 2018; Behrens et al., 2021). There is an urgent need to address this deficiency as the increased hazard from a denser flow is evident when comparing to extreme examples such as mud-rich lahars and huaycos, which cause such widespread destruction (Vallance and Iverson, 2015; Thouret et al., 2020). Therefore, further research is required to improve understanding of the density of tsunami flows, particularly through analysis of mud- and organic-rich deposits using a product to process approach.

The results of this study may be used as a guide to the likely deposits in different environments. An issue in recognising past events is that researchers will look for a "typical" deposit and hence may not consider

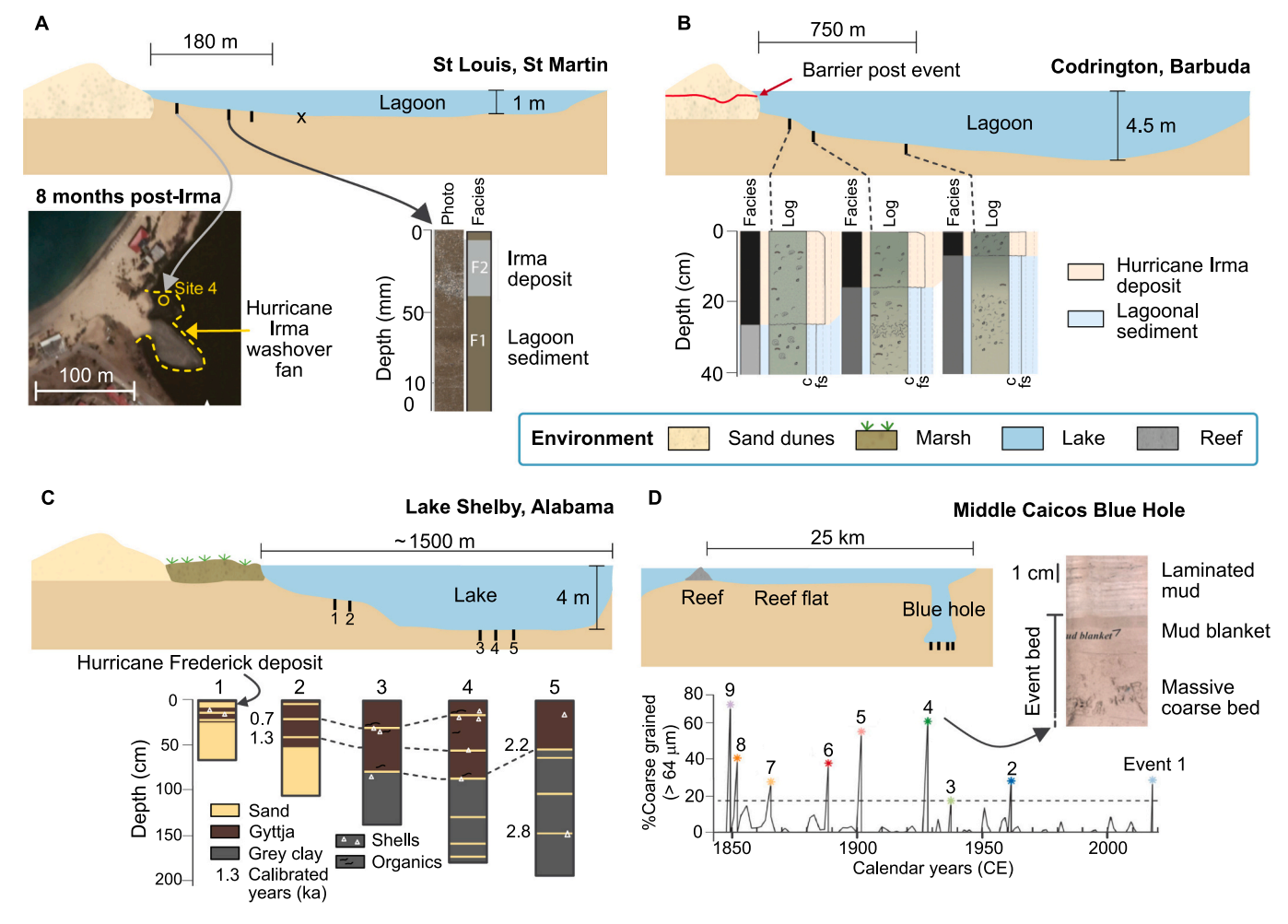


Fig. 9. Schematic diagrams of the coastal lakes and lagoons for four examples described in the text. Core photos, logs and/or post-event satellite imagery are shown for each (A-D) (Images adapted and reproduced respectivley from: Fabbri et al. (2024) with permission from Elsevier; Biguenet et al. (2023) with permission from Copernicus Publications on behalf of the European Geosciences Union; Liu and Fearn (1993) and Wallace et al. (2021a) with permission from Elsevier. D additionally shows the mean grain size of a core from the blue hole over the historical period (1850-present) (Wallace et al., 2021a).

alternative deposit types. This has led to reinterpretation of previously investigated sites when new information on a deposit appearance is discovered, for example for the Storegga tsunami in Scotland (Smith et al., 2004; Woodroffe et al., 2023). Here, we show that using the known characteristics of an environment and the tsunami event, a deposit type could be predicted. Therefore, this study could allow the recognition of new sites that differ from those already studied (for example more mud- or organic-rich layers) and potentially enable a more complete view of a past event.

This study also marks the first postulation of both sediment gravity flows (Group A) and a dense, cohesionless head (Group B) in tsunamis on land (in lakes). The flow front of both event types is inferred to generate major erosion of the lake substrate with erosion in some Group A examples eroding over 1 m from the lakebed, equivalent to sediment deposited over 2000 years (Romundset and Bondevik, 2011). This sediment is lost as a potential archive of past events, and palae-oenvironmental and climatic changes, for which lake sediments are widely used to reconstruct (Misra et al., 2019; Sabatier et al., 2022). This notion needs to be identified to ensure the record is not misinterpreted, especially in the construction of age-depth models for past archives that would require adjustment to account for erosion by the tsunami (e.g. Fabbri et al., 2024). Indeed, sediments used to constrain the 8.2 ka climatic event in the North Sea have recently been reinterpreted as originating from tsunami-induced sediment gravity flows (Bondevik et al.,

2024; Earland et al., 2024), prompting a re-evaluation of this climate history.

# 4. Storm deposits

#### 4.1. Location characteristics

Across the 66 sites, the locations and the parameters of the coastal lakes and lagoons containing the deposits varied. Deposits associated with coastal storm inundation have been found within 20 countries from predominantly hurricanes in the Atlantic region (e.g. Hurricanes Irma -2017; Ike - 2008; Katrina - 2005); Typhoons and Cyclones in the Pacific and Indian Oceans (e.g. Typhoon Rammasun - 2014; Isewan - 1959). However, other deposits in higher latitudes are formed by coastal inundation by extratropical storms (e.g. on Mediterranean coastlines). The size of the lakes and lagoons varied greatly from large lagoons that cover >10 km<sup>2</sup> to small ponds less than 0.1 km<sup>2</sup> in area, with a depth often in the range of a few metres (1-6 m), although 10 lakes or lagoons had a depth of less than 1 m. Several sinkholes in karst regions are also considered in this review. The lakes were typically separated from the ocean by a barrier (or sill) whose elevation above sea level varied from just 1 m to 4-5 m above sea level and were only a few hundred metres wide. Both lakes and lagoons were located between several hundred metres to a few kilometres from the contemporary coastline.

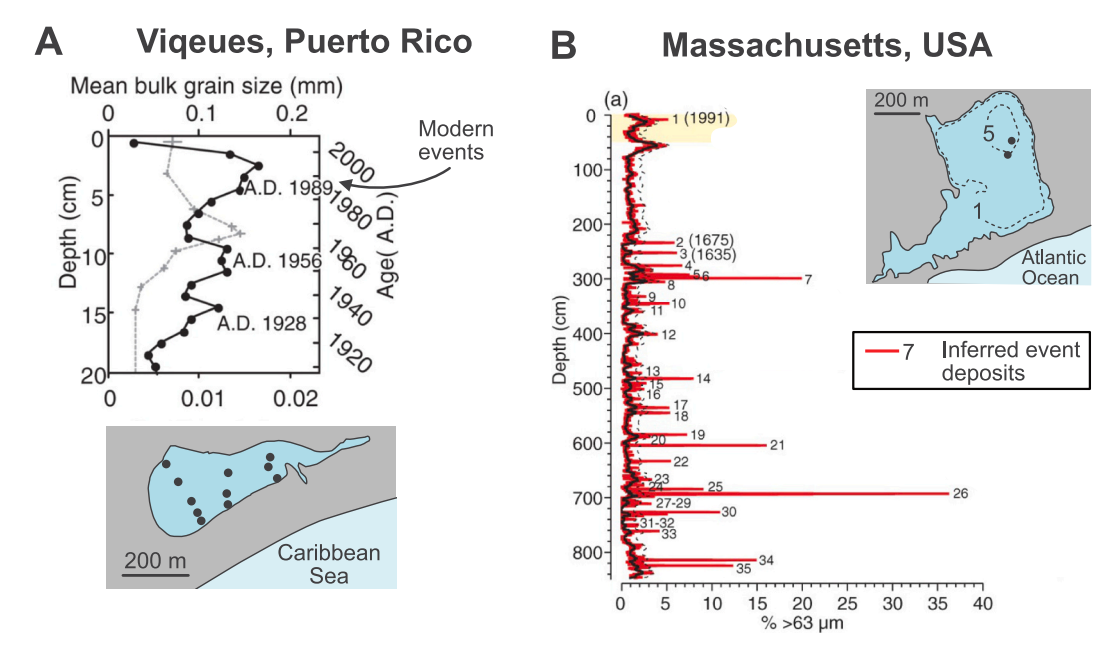


Fig. 10. Plan view diagrams of the coastal lakes with the core locations containing storm deposits indicated by filled circles. The bulk mean grain size (A) and percentage coarse-grained fraction (% > 63 m) (B) respectively of one core in each coastal lake are shown. A spike in these values indicates when a storm event transported coarse-grained sediment into the lake, with numbers and/or dates delineating each separate storm event in the record (Adapted and reprinted respectively from: Donnelly et al. (2015) with permission from Jon Wiley and Sons; Woodruff et al. (2008) with permission from the Geological Society of America).

#### 4.2. Storm deposits in coastal lakes and lagoons

Storm deposits in lacustrine environments are found as anomalous coarse-grained layers within an otherwise mud-rich and fine-grained succession of lacustrine organic mud deposits. Their composition is highly variable. Here, six examples from known storm events are described that encompass the range of deposit types seen in the wider database.

#### 4.2.1. Lesser Antilles - Hurricanes Irma and San Felipe

In Saint Martin, Lesser Antilles, deposits are recorded in a shallow lagoon from the recent, 2017, category 5 Hurricane Irma, the largest storm to hit the region in the historical record (1851-present; Fabbri et al., 2024). The lagoon is around 300 m wide and is fully enclosed from the ocean by a 2 m high sand dune (Fig. 9a). The lagoon sits within a sheltered bay away from the typical paths of storm events so only records the largest events such as Hurricane Irma and tsunami deposits from Lisbon 1755 and older events (Table 2). The sheltered location meant that wave heights were likely only around 2-3 m during Hurricane Irma (Fabbri et al., 2024), similar to the height of the coastal barrier. Aerial imagery before and after the event shows the formation of a sandy washover lobe landward of the coastal barrier that extends into the lagoon (Fig. 9a). The sediment cores show this deposit from Irma extended 180 m into the lagoon and comprised a visually distinct 1-2 cm thick poorly sorted fine sand that was absent in the 4th core taken 230 m inland within the lagoon (Fig. 9a).

Another storm deposit from Hurricane Irma was found within Codrington lagoon, Barbuda, where the hurricane caused barrier-breaching in the lagoon (Biguenet et al., 2023). The exceptionally large lagoon covers 22.5 km² and has a variable depth (maximum 4.5 m deep; Fig. 9b), and a narrow 1-3 m high sandy (carbonate) barrier separated the lagoon from the ocean before the hurricane event, which recorded a surge of 2.4 m. Satellite imagery shows that Hurricane Irma caused two breaches in the barrier 1.2 and 0.5 km wide, the larger of which persists at the time of writing. Behind these breaches, sediment cores record massive fine sand layers which thin inland from 27 to 7 cm (Fig. 9b). Locally, shell fragments are present on the top of these deposits, fine shell segments are also interspersed within the main sand

layers (Biguenet et al., 2023). No other historical event has recorded a barrier breaching for this lagoon, showing the exceptional nature of Hurricane Irma. However, similar deposits were found from palaeo events from the last 3700 years (Biguenet et al., 2023).

In Puerto Rico, deposits with a different morphology were observed within a 0.75 km<sup>2</sup> lagoon from Hurricane San Felipe [1928], Hugo [1989] and numerous palaeo events (Donnelly and Woodruff, 2007; Woodruff et al., 2008). The lagoon sits behind a 2 m high narrow (~80 m wide) vegetated sandy barrier with a single outlet to the ocean. The deposits were identified within 11 cores distributed across three transects perpendicular to the coast in the lagoon's west, centre and east (Fig. 10a). The San Felipe [1928] hurricane deposits consist of 2-3 cm thick coarse to medium sand with small shell fragments (Fig. 10a) and stretch across the entire lagoon from 20 to 400 m inland, with a distinct landward fining in the deposits. These layers contain the same material as the barrier beach. The consistent identification of the deposit across the lagoon suggested complete overtopping of the entire barrier rather than a spatially restricted barrier breach or overwash (Donnelly and Woodruff, 2007). Using an advective settling model, Woodruff et al. (2008) estimated the wave height as being  $2.6\,\mathrm{m}$  greater than the barrier height, permitting full inundation of the lagoon environment. Another event recorded as occurring ~1350 BP was observed to have similar trends, however, several other deposits were only recorded as thin (1-3 cm) layers in cores close to the coastal barrier (Fig. 10a).

#### 4.2.2. Mainland USA - Historical and palaeo hurricanes

Coastal lake deposits in Alabama represent one of the first studies looking at storm deposit records (Liu and Fearn, 1993). Lake Shelby is located by a sandy beach with dunes  $\sim$ 2-4 m high. This large lake (Fig. 9c) has a depth of 3-4 m and is connected to two further lakes, Middle Lake, and Little Lake, located further inland where hurricane deposits have also been found (Liu et al., 2008). Hurricane Frederick, 1979, produced a 4.8 m high wave in the surrounding area, causing inundation of the back-barrier environment, including Lake Shelby. However, only the nearshore region of the lake records sediment deposits from this event which thins from a 9 cm thick white sand layer within 100 m of the lake edge to <0.1 cm thick 325 m inland (Fig. 9c). In the centre of the lake (cores 3-5 in Fig. 9c), deposits from this event were

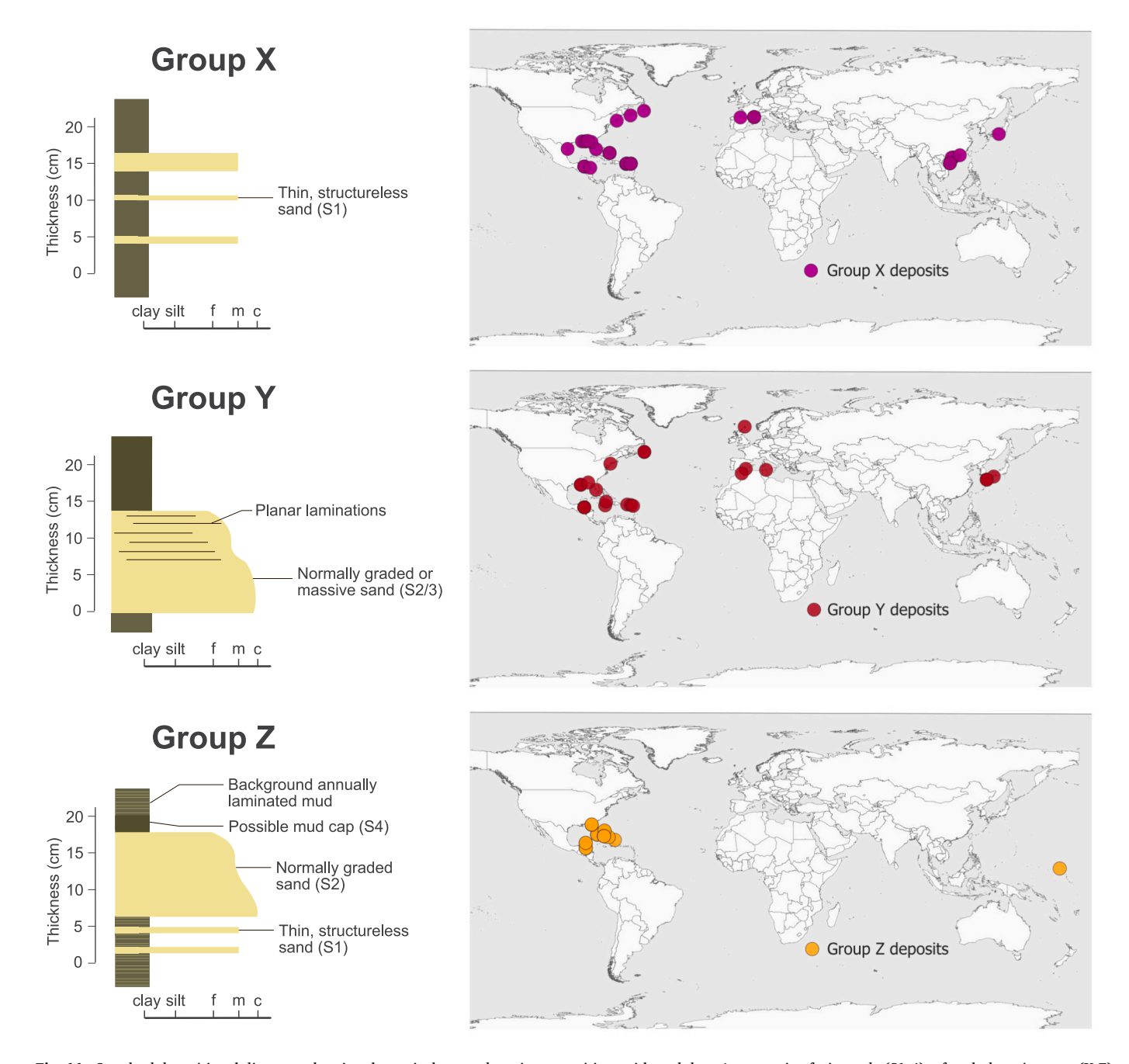


Fig. 11. Standard depositional diagrams showing the typical storm deposit composition, with each layer's respective facies code (S1-4), of each deposit group (X-Z) (Left) and their geographical distribution (Right). Variations from these typical deposits are discussed in the text.

absent, suggesting the storm event did not inundate the entire lake. Older events (0.7-3.4 calibrated yr ka) were recorded in the cores taken in the centre of the lake, where layers were found comprising 0.1-1 cm thick coarse sand grains with a sharp upper and lower contact at a recurrence interval of roughly 600 years (Fig. 9c). These layers are suggested to have been caused by category 4 or 5 hurricanes of greater intensity than Hurricane Fredrick (Cat 3 event) as they caused full inundation and sediment transport into the centre (distal) of the lake (Liu and Fearn, 1993).

In Massachusetts, a brackish coastal pond, Salt Pond, recorded evidence for past storms and hurricanes in the NE USA (Donnelly et al., 2015). The pond was separated from the ocean by a 1.3-1.8 m sandy barrier with a small tidal inlet in a microtidal region. Two cores were taken in the deepest part of the pond basin where depth reaches 5 m  $\,$ 

(Fig. 10b). The deposits consist of quartz sand event beds within annual laminated organic-rich sediments. Events are categorised as having a coarse fraction in the grain size distribution greater than 99 % of the background (red numbered spikes in Fig. 10b; Donnelly et al., 2015). These layers are often not identifiable to the naked eye and are typically c. 0.1 cm thick (Fig. 10b). The most recent deposit was formed by Hurricane Bob [1991], which produced a thin sand layer in the upper portion of both cores within the lake. A total of 35 beds were observed within the record, including attribution to two other historically recorded events in 1675 and 1635 CE (Fig. 10b). Overall, this example shows that event deposits in some lakes can produce very thin deposits that represent the small sedimentary load of past storm events.

**Table 5**Summary of the key characteristics of the Group X deposits within the literature.

Paper	Lake Depth (m)	Barrier height (m)	Cores distance from barrier (m)	Thickness of S1/2/3 (cm)	S1/2/3 Grain Size	Confidence
Biguenet et al., 2021	_	3.5	10-200	2\3	Medium-coarse sand	Yes
Bregy et al., 2018	1	1	200	3\4	Muddy fine sands	Yes
Donnelly and Woodruff, 2007	-	2.5	10-200	2\5	Coarse-m sand $+$ shell frag.	Yes
Woodruff et al., 2008	-	2.5	10-200	2\5	Coarse-m sand + shell frag.	Yes
Donnelly et al., 2015	5	1.55	300-350	<1	Fine silty sands. 1 clast	Yes
Oliva et al., 2018a	2	1	50-100	0.5-2	Fine sand	Yes
Sabatier et al., 2008	0.6	3	200-500	5\10	Fine sands	Yes
Qi et al., 2021	1.5	1	50	12\26	Medium sands	Yes
Qi et al., 2024	3	_	100-300	25\40	Medium sand to silty sand	Yes
Xian et al., 2022	1.5	<5	2000-3000	1\3	Coarse sand	Yes
Blanco et al., 2024	14.7	<1	200	1	Medium sand	Yes
Blanco et al., 2024	15	<1	300	1	Medium sand	Yes
Liu and Fearn, 1993	3.5	3	1000	0.1-1	Coarse Sand	Likely
Liu et al., 2008	1.2	1.5	100	2	Coarse sand (vf sand)	Likely
Ercolani et al., 2015	<1	1.5	60	1\5	Coarse sand + shell hash	Likely
Cochran et al., 2009	_	_	200	2\5	Sand	Likely
Donnelly, 2005	0.3	_	100	1\2	Coarse sand (rare shells)	Likely
Lane et al., 2011	2.3	2.5	360-450	0.1-1	Medium sands	Likely
Mattheus and Fowler, 2015	2.5	2.5	50	1\2	Fine-m (muddy) sand	Likely
Mattheus and Fowler, 2015	2.5	2.5	50	1\2	Fine (muddy) sand	Likely
Mattheus and Fowler, 2015	2.5	2.5	10	1\2	Fine sand (some shells)	Likely
Rodysill et al., 2020	1.5	1.8	100-1250	1\5	Fine sand	Likely
Sabatier et al., 2012	0.6	3	350	3\5	Fine sands	Likely
Dezileau et al., 2011	1	2.5	500	5\10	Fine sands (some shells)	Likely
Degeai et al., 2015	<1	_	500-1000	1\10	Fine sands (some shells)	Likely
Zhou et al., 2021	4.2	Low	1000-5000	1\5	Coarse sands (some shells)	Likely
Zhou et al., 2017	4.2	Low	2000	1\3	Coarse sands	Likely
Zhou et al., 2017	5.5	8	1000	1\2	Coarse sands $Medium sand + parallel$	Likely
Shimada et al., 2023	2.3	5	250	5\25	laminae	Likely
Pleskot et al., 2023	3.1	few metres	200	2\3	Coarse Sand	Uncertain
Bertran et al., 2004	1.5	_	250-600	2\3	Coarse sands	Uncertain
Malaizé, 2012	1.5	_	250-600	1\3	Coarse sands	Uncertain
Toomey et al., 2013	35	0	1000-1500	1\3	Coarse sands	Uncertain
Abbreviations:	frag = fragment	$\mathbf{vf} = \text{very fine}; \mathbf{f} = \mathbf{f}$	ine; $\mathbf{m} = \text{medium}, \mathbf{c} = \text{coarse}$			

**Table 6**Summary of the key characteristics of the Group Y deposits within the literature.

Paper	Lake Depth (m)	Barrier height (m)	Cores: distance from barrier (m)	Thickness of S1/2/3 (cm)	S1/2/3 Grain Size	Confidence
Wallace and Anderson, 2010	0.5	2	500-1500	2\5	Fine sand	Yes
Brandon et al., 2014	1.2	1.5	50-150	2\20	Very fine-fine sand	Yes
Liu et al., 2011	2.5	<1	300	10	Coarse sands	Yes
Dietz et al., 2021	2.5	<1	300	10	Coarse sands	Yes
Palmer et al., 2020	-	~5	50-100	3\10	Silty sand Fine-medium sand (rare	Yes
Martin and Muller, 2021	-	0.83-0.88	25	2-9.5	shell)	Yes
Tuttle and Fuentes, 2021	1	2	80	1\5	Well sorted fine sand	Yes
Fabbri et al., 2024	-	2	40-180	1\2	Fine sand	Yes
Das et al., 2013; Liu and Fearn,						
2000	3.3	6.2	up to 300	0.2-3	Coarse Sand	Likely
Peros et al., 2015	_	few m	100	few cm	Fine-medium sand	Likely
Adomat and Gischler, 2016	1.5	1.5	70	10\20	Coarse sands	Likely
McCloskey and Liu, 2013	1.5	1.5	10-140	2\5	Medium sand to silty clay	Likely
Adomat and Gischler, 2016	1	-	140	30	Coarse sands + corals	Likely
Hess et al., 2024	2.4	2	100	0.1\3	Fine sands Medium sands (some	Likely
Dezileau et al., 2016	3.6	3	800	5\10	shells)	Likely
Pleskot et al., 2023	1.5	few m	25	2\3	Coarse Sand	Uncertain
Pleskot et al., 2023	2.1	few m	150	2\3	Coarse Sand	Uncertain
Kohila et al., 2021	0.8	-	50	6\10	Sand + shells	Uncertain
Tanigawa et al., 2018	_	12	100-900	1\15	Medium-coarse sand	Uncertain
Biguenet et al., 2023*	4.5	2.5	250-750	10\25	Fine sands	Yes
Woodruff et al., 2009*	21	-	250	1\3	Coarse sands	Likely
Woodruff et al., 2009*	10.7	-	150	1\3	Coarse sands	Likely
Raji et al., 2015*	4.8	_	1500	2\5	Silty sands (some shells)	Uncertain
Footnotes:	* Barrier breach	ing event Abbreviatio	ns: sh = shells			

#### 4.2.3. Caicos Islands - Blue hole deposits

A different type of environment is also widely used to record storminduced flooding which are sinkholes located in coastal environments. One example from the Turks and Caicos Islands is from a blue hole located on a reef platform adjacent to tidal flats of the Caicos islands (Fig. 9d; Wallace et al., 2021a). Storms impacting the site must cross sand banks and patch reefs and then across the 25-30 km of shallow (<5 m depth) marine carbonate platform. The blue hole itself is around 600 m diameter and up to 61 m deep, with steep, sub-vertical sides (Wallace et al., 2021a). Cores were taken at the marine side, centre and land side of the blue hole. Deposits consisted of a combination of 2-10 cm thick beds of massive carbonate sands and thicker >30 cm thick beds that locally reach 100 cm thick, consisting of normally graded coarse-grained beds often capped with mud blankets (Fig. 9d). Across a 1500-year period, approximately 70 events were recorded with an average thickness of 7.7 cm. Spatially, the deposits remained relatively consistent in composition with little thinning or fining inland over 350 m of the blue hole surface. However, only 70 % of the deposits in the seaward core were present in the inner two cores, suggesting not all events reach the centre of the blue hole.

# 4.3. Storm deposit facies

Four facies are recognised for storm beds.

**S1:** Thin structureless sands: well sorted sands less than 5 cm in thickness. Fine to coarse sands, usually ungraded. Present in single layers with a sharp but not erosional basal contact.

**S2: Graded sand beds:** graded coarse to fine sands with occasional fine shell fragments. Often laminated or contain multiple layers. Sharp and sometimes erosional basal contact.

S3: Massive sand beds: massive coarse to fine sands with occasional shell fragments. Can contain laminations or multiple layers. Sharp basal contact.

S4: Mud cap: thin (1-3 cm) silt layer located on the top of S2, rare.

#### 4.4. Storm deposit groups

These four storm facies form three distinct deposit groups (Fig. 11). Group X: consists of a thin S1 layer, <5 cm in thickness. Not found in conjunction with any other storm layer, overlies background lagoonal/lake sedimentation. Frequent deposits within a single record.

**Group Y:** consists of a S2 or S3 layer typically 5-15 cm in thickness but locally up to 50 cm thick near to coastal barriers. Typically graded

and often have planar lamination or contain repeated sequences. Rarely overlain by a mud cap. Sharp but usually non-erosional base. Commonly termed "washover fans" in the literature.

**Group Z:** consists of a series of event layers within annually laminated mud sedimentation. Event layers are present as a combination of thin S1 layers (which in isolation resemble group X deposits) or thicker (20-30 cm) S2 layers which have a distinct normal grading and sometimes contain a mud cap (S4). The basal surface of the thicker layers is often sharp and erosional.

#### 4.4.1. Confidence and uncertainty within the dataset

Across Groups X and Y, 43 % of event deposits are from known events, 38 % from events classified as 'likely' confidence and just 16 % as uncertain events. These proportions are similar for both group types individually. Across Group Z deposits, 40 % were from known events with the remaining deposit sequences containing at least one event classified as 'likely'. There is little correlation between the deposit's thickness and the confidence attributed to the deposit with very thin deposits linked both to unknown palaeo events and known modern events. Uncertain deposits comprise those from events outside of the instrumental and historical record, with many known events comprising deposits from the 21st century.

#### 4.4.2. Group X deposit trends

Across the dataset, 34 coastal lakes contain Group X deposits, comprising thin sand (< 5 cm thick) deposits that cover the entire or greater extent of the lake or lagoon from 100 s to around 1000 m inland (Table 5). These deposits differ from those of Group Y in that they reach the middle/deepest parts of the lagoon and are not limited to just the immediate edge or margin (e.g. Donnelly and Woodruff, 2007; Rodysill et al., 2020). Throughout these areas of up to several square kilometres across the coastline, the deposits appear relatively homogenous with little thinning inland but often with a slight fining trend towards the landward edge (e.g. Donnelly and Woodruff, 2007). Many of the deposits are not visible as identifiable layers within the core (Donnelly et al., 2015; Mattheus and Fowler, 2015) but are instead marked by peaks in the coarse-grained or sand fractions within the generally fine background sediment of the lake floor. This shows that little sediment is transported into the lake/lagoon environment. The deposits are repeated in multiple layers (usually >5) within the background sediment in a single core sequence (Sabatier et al., 2008; Ercolani et al., 2015; Xian et al., 2022). These lakes and lagoons are all separated from the ocean by a sandy or gravel coastal barrier which sometimes has a

**Table 7**Summary of the key characteristics of the Group Z deposits in the literature.

Paper	Sinkhole depth (m)	Sinkhole width (m)	Thickness of S1/2/3 (cm)	S1/2/3 Grain Size	Confidence			
Brown et al., 2014	80	~65	25-30	Sandy mud to m sand	Yes			
Wang et al., 2021	>1	~50	7	Coarse sands + gravels	Yes			
Wang et al., 2021	>1	~10	4	Coarse sands	Yes			
Wang et al., 2021	>1	~15	4	Coarse sands	Yes			
Wang et al., 2021	>1	~20	2	Coarse muddy sands	Yes			
Wallace et al., 2021a	60	500	7.7	Coarse sands (some shells)	Yes			
Winkler et al., 2020	70	50	1\3	Coarse sands	Yes			
Wallace et al., 2021b	12	150	1\3	Fine-coarse sands	Yes			
Rodysill et al., 2020	5	~125	2\11	Fine sand	Likely			
Brandon et al., 2013	15	~120	2\3	Fine-medium sand	Likely			
Van Hengstum et al., 2016	40	~30	0.5\2	Fine sand	Likely			
Wallace et al., 2019	17	150	1\4	Fine sand (sh $+$ m leaf)	Likely			
Wallace et al., 2019	18	95	1\4	Fine sand (sh $+$ m leaf)	Likely			
Wallace et al., 2019	95	80	1\8	Fine sand (sh $+$ m leaf)	Likely			
Gischler et al., 2008	125	~320	1\10	Coarse sands to silts	Likely			
Schmitt et al., 2020	125	~320	0.3-2	Fine sands	Likely			
Gischler et al., 2025; Schmitt et al., 2025	125	~320	0.25-37.6	Carbonate sands	Likely			
Bramante et al., 2020	30	500	1\2	Fine-medium sands	Likely			
Brown et al., 2014	15	_	3\4	Very fine sand	Yes/Likely			
Footnotes:		Thickness indicates the range in the identified event layers. <b>Abbreviation:</b> $m$ leaf = mangrove leaf; $sh$ = shells; $m$ = medium						

marsh environment between the barrier and the lake/lagoon. The basins have a variable depth but are usually a few metres (1-6 m) deep (Table 5) and extend over an area of 1-4 km². A few lagoons have large tidal channels (> 100 m wide), and deposits linked to storm flooding are thicker (5-20 cm) but still laterally extensive across the lagoon (Qi et al., 2021; Zhou et al., 2021). Furthermore, in these lagoons with a large tidal influence, a mud cap was present but was absent from all other lakes and lagoons. Some large lakes and lagoons record both Group X and Y deposits for differing events within the record (Liu and Fearn, 1993; Wallace and Anderson, 2010).

# 4.4.3. Group Y deposit trends

There are 23 coastal lakes containing Group Y deposits across the dataset, with these deposits consisting of a lobate thick sand layer that is laterally restricted (Table 6). The sand layers comprise fine to coarse sands that are often graded and locally can contain planar laminations or multiple layers within the deposit (Table 6). The deposits contain no mud inclusions and very rare shell fragments (e.g. Biguenet et al., 2023). Furthermore, the sand layers thin abruptly inland from 10 to 20 cm close (<50 m) to the coastal barrier to a few centimetres further from the barrier up to <100 m, but in some cases up to 150 m inland (Brandon et al., 2014; Table 6). They are also usually confined to a small lateral extent being restricted to less than a few hundred metres across the width of the lake or lagoon (Liu et al., 2011; Palmer et al., 2020). The size of the lagoon or lake varies between very large lagoons several kilometres across, to smaller lakes only a few hundred metres wide. The barrier is typically sandy with occasional mangroves or marsh environments between this barrier and the lake or lagoon. A few of the deposits are located behind a breach in the barrier caused by the storm event (Table 6; Woodruff et al., 2009; Raji et al., 2015; Biguenet et al., 2023); these deposits can extend further inland (750-1000 m) than the other Group Y deposits but with a similar restricted lateral extent. Overall, Group Y deposits have a limited extent both laterally across the lagoon and extend only a limited distance inland.

#### 4.4.4. Group Z deposit trends

Group Z deposits, with 18 sinkholes in the dataset, are characterised by their distinct depositional location, within the karst regions of the Caribbean. These sinkholes (or blue holes) are located within a low energy environment such as a reef flat/atoll where water depth is typically 2-3 m and is separated from the open ocean by reefs, sand

banks or tidal flats (Schmitt et al., 2020; Winkler et al., 2020; Wallace et al., 2021a). Hence, these blue holes are mainly saline rather than freshwater environments. The blue holes are typically only small with a diameter of less than 100 m, but a few are several hundred metres in diameter (Table 7; Bramante et al., 2020; Wallace et al., 2021a; Schmitt et al., 2025). Depths are typically 10s of metres but at one site the hole reaches 125 m depth (Table 7) with sub-vertical sides in an hourglass structure in many cases (e.g. Brown et al., 2014). The deposits consist of two types, firstly relatively laterally continuous thin (<5 cm) coarse to fine carbonate sand layers with little structure (e.g. Schmitt et al., 2020, 2025). These layers share a similar appearance and composition to Group X deposits but differ through a more dominant carbonate signature and being enclosed within annually laminated carbonate mud (e.g. Winkler et al., 2020; Wallace et al., 2021a). These layers were typically repeated tens of times within the record of a blue hole creating a detailed record of past events (Winkler et al., 2020; Wallace et al., 2021a). The second thicker (30-100 cm) deposit type comprised coarse, often normally graded sands and rarely with a mud cap (Wallace et al., 2021a). They also showed evidence of a sharp and sometimes erosional base (Brown et al., 2014; Wallace et al., 2019) compared to the gradual contact observed for the thinner deposits in the sequence. Both deposit types contained sediment originating from the reef edge/barrier and the shallow marine platform (Wallace et al., 2019, 2021a).

# 4.5. Processes of storm sedimentation in coastal lakes, lagoons and sinkholes

The presented database of storm deposits in coastal lakes, lagoons and sinkholes has enabled three different groups to be identified. The following discussion undertakes a process sedimentology approach to infer the depositional processes, an approach so far underutilised within the literature (Chaumillon et al., 2017). However, the greater availability of modern observations has meant that processes are far better understood in storms than in tsunamis and show deposition occurs under a highly turbulent flow which lasts for several hours to days (Morton et al., 2007; Ghionis et al., 2015). This is interpreted for all back-barrier environments (Schwartz, 1982; Morton and Sallenger, 2003; Chaumillon et al., 2017), rather than specifically for lakes and lagoons. Therefore, these processes will be refined to lakes, lagoons and sinkholes by integrating existing process arguments with basic principles of process sedimentology.

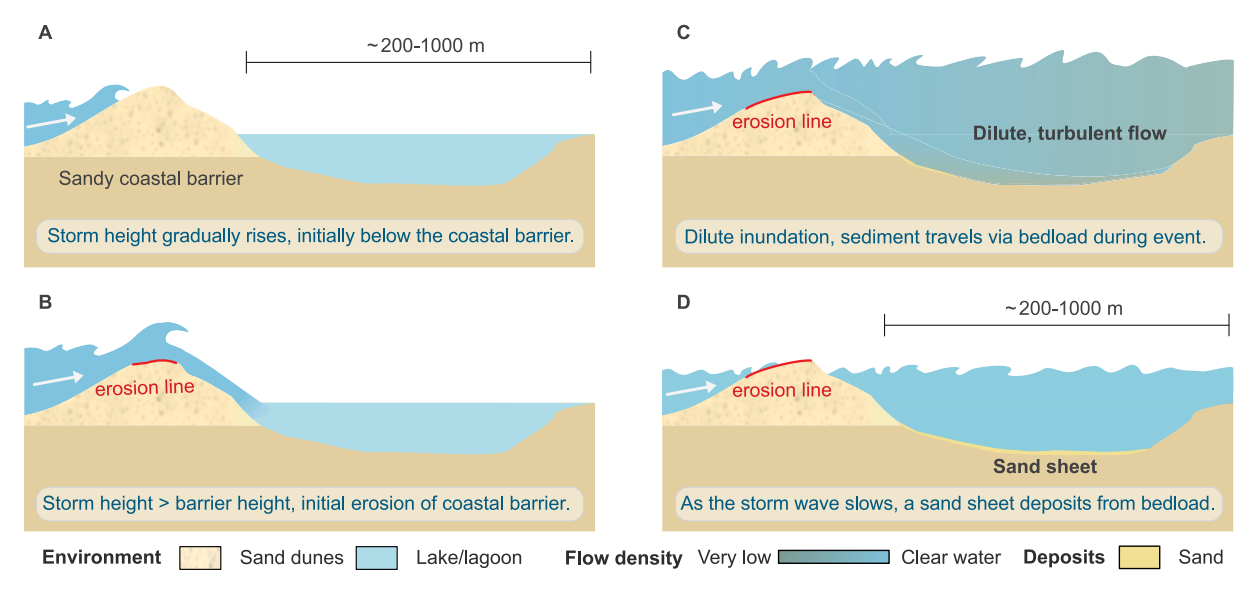


Fig. 12. Mechanism schematic for Group X deposits in shallow (<5 m depth) coastal lakes and lagoons. A: Set up phase of the storm as water level gradually rises. B: initial inundation of the coastal lake or lagoon by the storm induced flow after several hours. C-D: dilute flow during inundation (C) and as the flow wanes and sediment is deposited (D). The legend shows the environment, deposits and flow densities depicted.

#### 4.5.1. Processes of storm deposition in back-barrier settings

Overwash deposition in back-barrier settings results from the erosion and reworking of sediment (typically sand) from the littoral barrier by wave overtopping or breaching (Goslin and Clemmensen, 2017). The processes involved were first summarised by Sallenger (2000) and later described by Masselink and Van Heteren (2014) who proposed that during a storm flooding event, four regimes can occur that are defined as a function of the ratio between the wave and barrier heights for a given event. Each regime has a unique pattern and magnitude of net erosion and deposition, however, only the overwash and inundation regimes produce deposits in back-barrier settings. In the overwash regime, the barrier is overtopped but not fully submerged by the storm as only the maximum wave height is greater than the barrier (Masselink and Van Heteren, 2014). This regime induces the net transport of sediment (via bedload/traction transport) landward (Masselink and Van Heteren, 2014; Chaumillon et al., 2017) and produces thick (up to several metres thick) washover fan deposits (Hudock et al., 2014). A subset of this regime is barrier breaching events, where the storm waves breach the littoral barrier in discrete locations, causing inundation and deposition of washover deposits over a restricted spatial extent (Chaumillon et al., 2017). In contrast, in the inundation regime, the storm height is greater than the barrier and the storm can inundate and submerge the back barrier environment (Masselink and Van Heteren, 2014). This results in the net transport of sediment into the back-barrier environment over larger distances than the overwash (or barrier breaching) regime and deposition by suspension is thought to be more dominant (Goslin and Clemmensen, 2017). The deposits of Groups X and Y located in backbarrier lakes and lagoons will likely form under similar processes to one of these regimes.

#### 4.5.2. Group X processes

Group X deposits are typically thin sandy layers that are laterally extensive being located across the length and width of coastal lakes and lagoons over distances of up to around 1 km inland. Therefore, these deposits are likely formed under the inundation regime where the entire lake/lagoon may be submerged (Masselink and Van Heteren, 2014) and sediment transport distances are typically greater. Indeed, the modern events recorded as Group X deposits show that the maximum inundation depth far exceeded the barrier height (e.g. Woodruff et al., 2008; Bregy et al., 2018). The thin nature of the deposits (typically only 1-2 cm thick and often not visible to the naked eye), show similarities to the tsunami deposits of Group Cii shown in section 3, and indicates that the flow was dilute with a low sediment concentration. This is because each storm

wave breaks very close to shore and the wave only lasts for 10-25 s so each wave only transports a small amount of sediment (Goslin and Clemmensen, 2017). The primary erosion of sediment during a storm event occurs as the water overtops the barrier, where studies have suggested a supercritical flow can briefly form (Kuiry et al., 2014), inducing erosion of the coastal barrier. After this has occurred, sediment is moved within a highly turbulent flow which inundates the land for hours to days (Morton et al., 2007). The deposits in lakes and lagoons show these trends through the dominance of sediment eroded from the sandy barrier, with little to no erosion and deposition of finer, cohesive sediments from the lagoon bed or surrounding environment. Even in the relatively stable environment of coastal lakes and lagoons, some reworking of these deposits may still occur. In other less stable environments, such thin deposits may be rapidly reworked and lost as a record, especially >1 km inland (Watanabe et al., 2017).

Within the literature, the consensus appears that this storm inundation regime involves a greater proportion of suspension transport than the overwash regime (Sabatier et al., 2008; Goslin and Clemmensen, 2017). However, it is also acknowledged that during storms bedload transport is more prevalent (Morton et al., 2007) because of the lower velocity and depth of a storm compared to a tsunami wave. Theory dictates that a wave of lower energy (i.e. storms) will transport primarily through traction (bedload), only transitioning to suspension-dominated transport at very high velocities and depths (Chiodi et al., 2014). Here, the fining landward trend observed in several deposits coupled with their thin nature suggests deposition by longitudinal segregation under bedload transport even in an inundation regime. This results in the fining trend, with the smallest (and lowest density) grain sizes being transported farther into the lagoon. However, due to the limitations of bedload transport, this deposition generally does not reach near to the inundation limit on shallow gradient coastlines, except in localised topographic lows (Watanabe et al., 2017). Furthermore, in lakes of greater depths (> 5 m), the storm waves will be unable to penetrate to the base of the water column and thus sediment moving as bedload will disperse through the flow. This sediment will fall as suspension through the remainder of the inundated lake or lagoon but due to the lower energy of storm waves, such transport will be limited and laterally restricted cf. tsunami events.

Overall, we consider that during the Group X deposit storms an inundation flow regime occurs where the entire back-barrier, including the lake or lagoon, is submerged (Fig. 12a-d). During this storm flow, sediment is transported predominantly via bedload transport along the lakebed (Fig. 12b-d), except at depth, with finer particles travelling

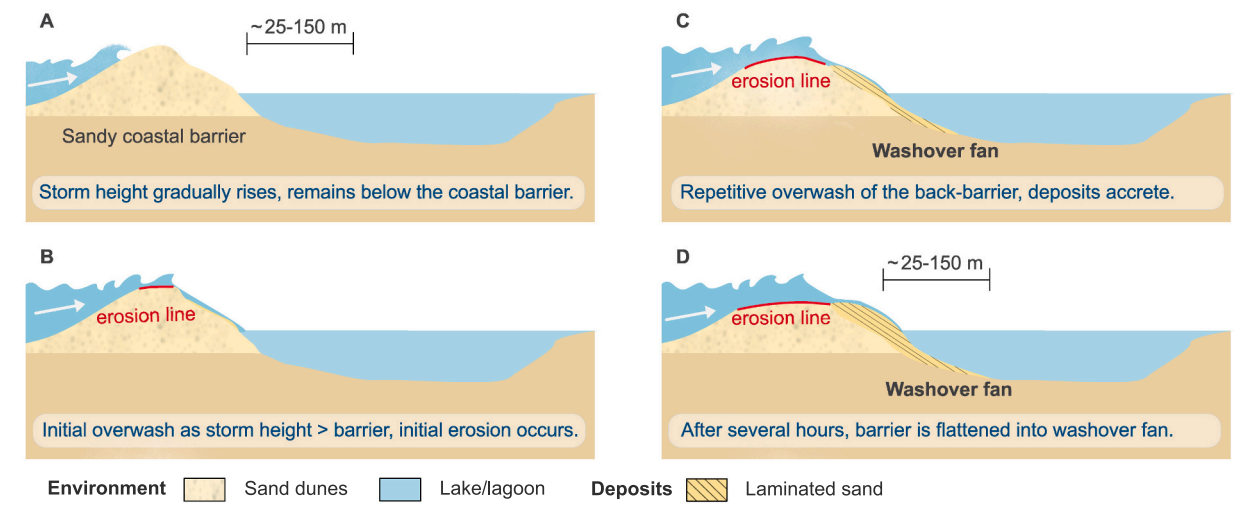
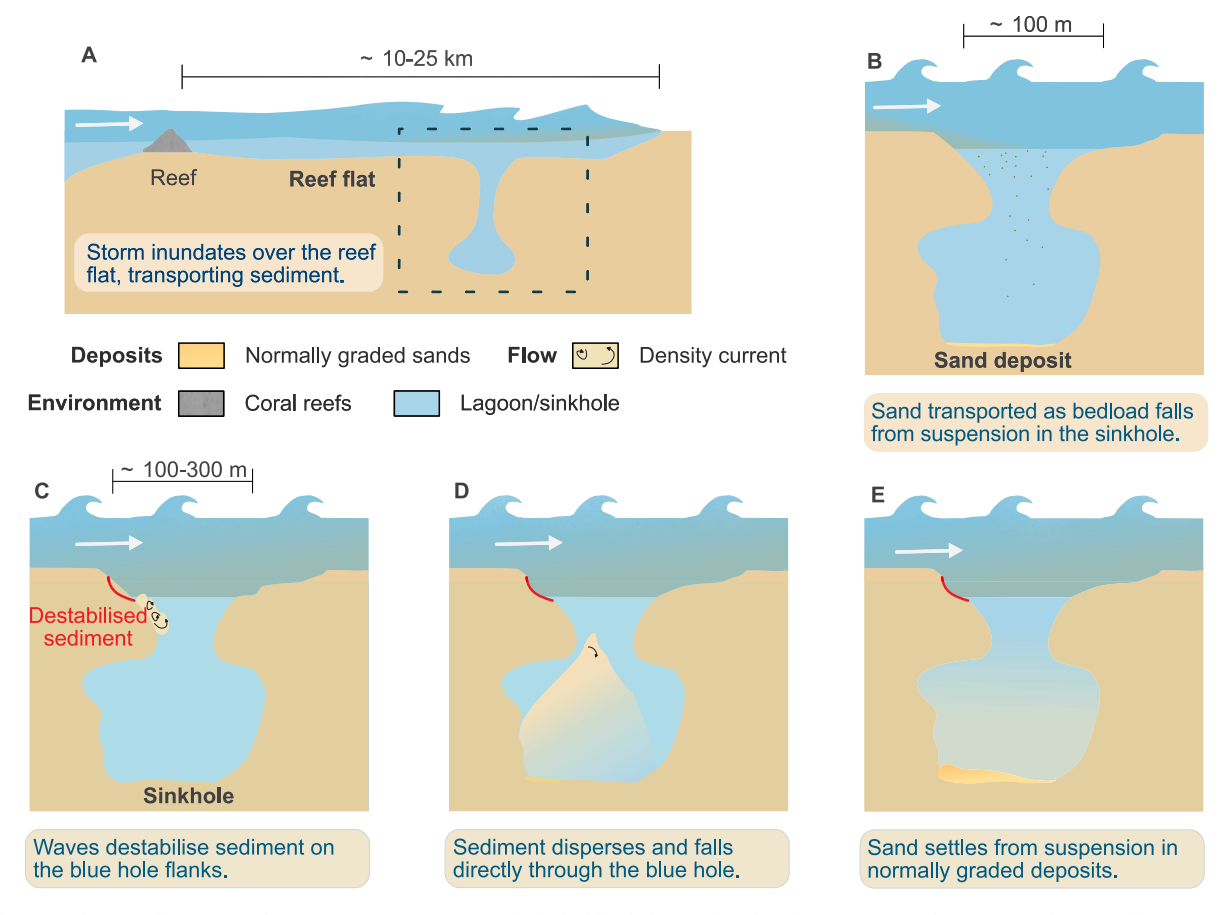


Fig. 13. Mechanism schematic for Group Y deposits. A: Set up phase of the storm as water level gradually rises. B: Initial overtopping by wind waves during the storm inundation. C-D: Repeated waves over several hours gradually transport sediment into a washover fan that smooths out the antecedent topography. The legend shows the environment and deposits depicted.



**Fig. 14.** Mechanism schematic for Group Z deposits. **A**: Environment in which the blue holes are found with a storm wave shown. **B**: Mechanism of formation of the thin sand layers. **C-E**: Processes involved in the formation of a normally graded sand deposit on the blue hole bed via the destabilisation of sediment on the edges of the sinkhole by storm waves. The legend shows the environment, deposits and flow depicted.

further through the lake resulting in a fining inland of the deposit. The low sediment volume transported results in only thin deposits throughout the lake environment (Fig. 12d).

#### 4.5.3. Group Y processes

Group Y deposits are laterally restricted, locally thick and extend only limited distances from the coastal barrier. Therefore, these events are correlated with an overwash regime where only a limited section of the coastal barrier is overtopped by storm-induced flooding. These deposits build up to thick deposits during storm inundation. In this regime, water overtops the barrier on each wave, but only in a short and shallow flow, failing to submerge the back-barrier environment (Masselink and Van Heteren, 2014). Each of these waves (low energy wind waves generated by strong winds) transports a small amount of sediment from the barrier crest downslope into the back-barrier environment (e.g. Ghionis et al., 2015). This can only occur via bedload transport in shallow and relatively low-energy waves that travel only a small distance inland. However, where the coastal lake or lagoon is close to the barrier, transport may extend into the existing water column (Goslin and Clemmensen, 2017). Throughout a storm event (several hours or even days), the continued wave action results in the sediment accumulating in the back-barrier environment, producing a thicker deposit over time that extends inland as a fan-like lobe (e.g. Fabbri et al., 2024). Gradually this process smooths out the antecedent landscape, filling in the edges of the lakes and lagoons (Goslin and Clemmensen, 2017). Within a lake or lagoon, this is observed through the deposits that thin and fine inland, abruptly pinching out over relatively short distances (~25-150 m; Table 6). Their thickness likely varies as a function of the amount of erodible sediment available on the coastal barrier and the duration of maximum inundation. Longer duration flows may facilitate more time for a thicker deposit to develop. Commonly, these deposits are termed "washover fans" in the literature (e.g. Goslin and Clemmensen, 2017).

During the overwash regime as the maximum wave height is greater than the coastal barrier, shallow flows overtop the barrier and begin to transport sediment into the back-barrier lake or lagoon (Fig. 13b). Over time, this sediment transport and deposition accretes over multiple waves to create a washover fan that extends into the lake or lagoon (Fig. 13c, d).

#### 4.5.4. Group Z processes

Blue holes/sinkholes are very stable environments where varved annual sedimentary sequences are formed and bioturbation, wind or wave movement of sediment is limited to non-existent (Wallace et al., 2021a). The base is below the pycnocline so is anoxic and very little life can survive, limiting bioturbation (Winkler et al., 2020). This makes these environments excellent at preserving past event deposits. The event deposits are visually identifiable due to the change in grain size (silts/clays to sands) and the break in lamination of the deposits. Previous studies have identified two different mechanisms for the deposition of these deposits (Brown et al., 2014). First, deposits can form through the settling of sediment that was suspended in the flow as the storm wave flowed over the blue hole. This sediment eventually settles through suspension as the wave energy dissipates. Second, during some events density flows may develop as the storm waves destabilise sediment on the steep, sub-vertical sides of the sinkhole and cause a density flow to develop which flows into the base of the sinkhole under the force of gravity (Brown et al., 2014). This mechanism has been reiterated in more recent studies (Wallace et al., 2021a; Schmitt et al., 2025).

The dataset presented here with two different deposit types (thick and thin) largely supports these two mechanisms with only subtle deviations. The thin deposits show similarities to those found during full inundation of coastal lakes and lagoons (Group X deposits), which form largely through bedload transport except at great depths where sediment settles from suspension (see section 4.5.1). Given the shallow nature of the lagoons (3-4 m depth) enclosing many blue holes, a similar process of bedload transport of sediment likely occurs as the storm waves pass over the lagoon. As this sediment moving as bedload reaches a blue hole, the large increase in depth of the water column prevents the shallow waves of the storm event from reaching the bed, causing sediment to disperse through the water column. This suspended sediment then settles over time into a uniform but relatively thin sand sheet on the base of the blue hole (Fig. 14b). Whether a storm transports sediment into the blue hole is dependent on the ability of the storm wave to move coarser grained sediment rather than whether it can overtop the barrier like in back-barrier lakes and lagoons. These thin, laterally extensive deposits appear as thicker layers than in lakes and lagoons (approximately 2-7 cm cf. 1-3 cm) likely due to the better preservation of the deposits whereas in the more active lakes and lagoons, the upper part of the sediment may be reworked both during and after the event.

The thicker deposits are likely formed by the second mechanism proposed by Brown et al. (2014) of a density flow. Unlike coastal lakes, blue holes are saline and thus a density contrast is not present between the marine inundation and the ambient water of the blue hole, hence a gravity current will only form with the addition of sediment to the flow. Instead, under storm conditions, the wave action may destabilise sediment that has built up on the margin or slopes of the sinkhole. This displacement transports the sediment from the shelf into the sinkhole, where it falls due to the density difference with the ambient water (Fig. 14c). However, the steep sides and high depth of blue holes may prevent the formation of a coherent density current. Instead, rapid mixing of the initial density current may lead to displaced sediment settling from suspension through the sinkhole, with coarse sediments depositing first into a normally graded deposit, as observed on the blue hole bed (Fig. 14d, e). The sediment accumulation on the bed would thus be thickest proximal to the failure on the seaward side of the lagoon, a trend observed in the group Z deposits. Only sufficiently large failures

generating a high-energy density current would enable sediment to be dispersed through the blue hole.

#### 4.6. Implications for storm sedimentation

The dataset and processes described highlight that the manner of sediment deposition in coastal lakes and lagoons will depend on the heights of the littoral barrier relative to the maximum elevation of the storm water level, as suggested previously for storms (Masselink and Van Heteren, 2014). When the barrier height is always less than the water depth of the storm surge then an inundation regime will occur where deposits are thin but laterally extensive and extend several hundred metres inland. However, where the storm water depth is only sufficient to overtop the barrier on the crest of the wind waves, a laterally restricted but relatively thick deposit forms. This is shown through the multiple lagoons and lakes where both deposit groups are present for events of differing magnitude (Liu and Fearn, 1993; Donnelly and Woodruff, 2007; Wallace and Anderson, 2010). Liu and Fearn (1993) inferred a relationship between the category (or intensity) of the hurricane for a given direction (path) and its inland extent, with only category 4 or 5 events that pass within 30 km of the site reaching the middle of the lake in an inundation regime. Here, category 3 events of a similar path only produced isolated washover lobes. A similar relationship between the intensity and deposit type would be expected in other stable coastlines. The dependence of the deposit type on the event characteristics is notably different from tsunamis where the environment and underlying substrate are more important in determining the resultant deposit (see section 3.6.1).

Previously in the storms vs tsunami literature, there has been a misconception that storms are thicker than tsunami deposits but are more laterally restricted (Morton et al., 2007; Switzer and Jones, 2008). However, this is only the case for the washover regime (Group Y deposits), where a washover lobe is deposited. Here, we have shown that storm deposits can extend further inland but remain thin and can be laterally extensive (Group X deposits). These two differing processes were acknowledged within the review of Goslin and Clemmensen (2017) but are largely absent within the storms versus tsunami debate (Morton et al., 2007; Kortekaas and Dawson, 2007; Brill et al., 2020). This may be

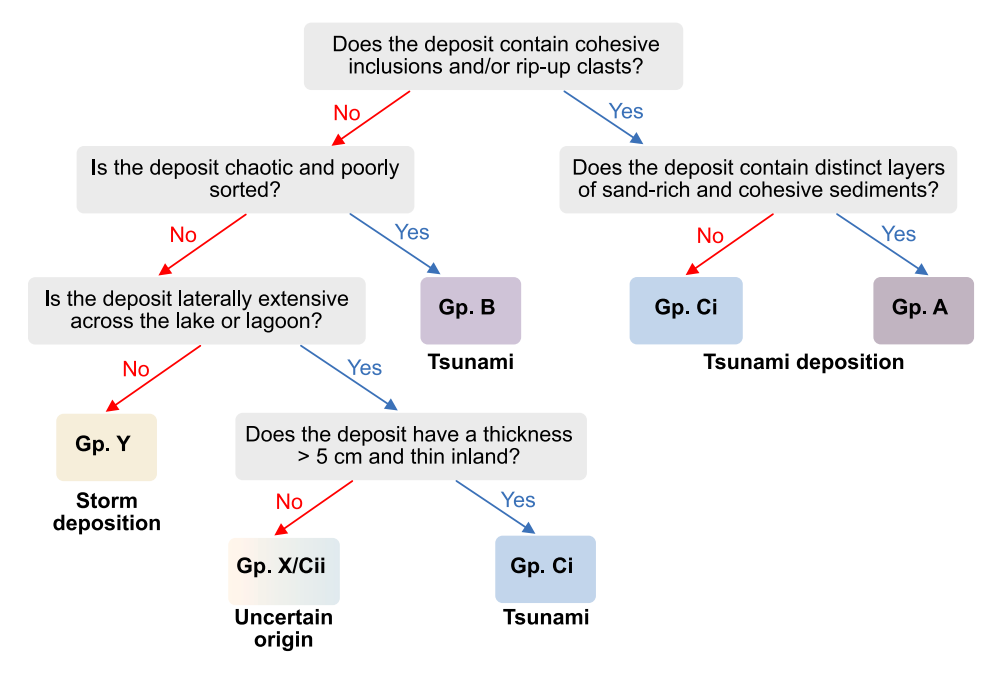
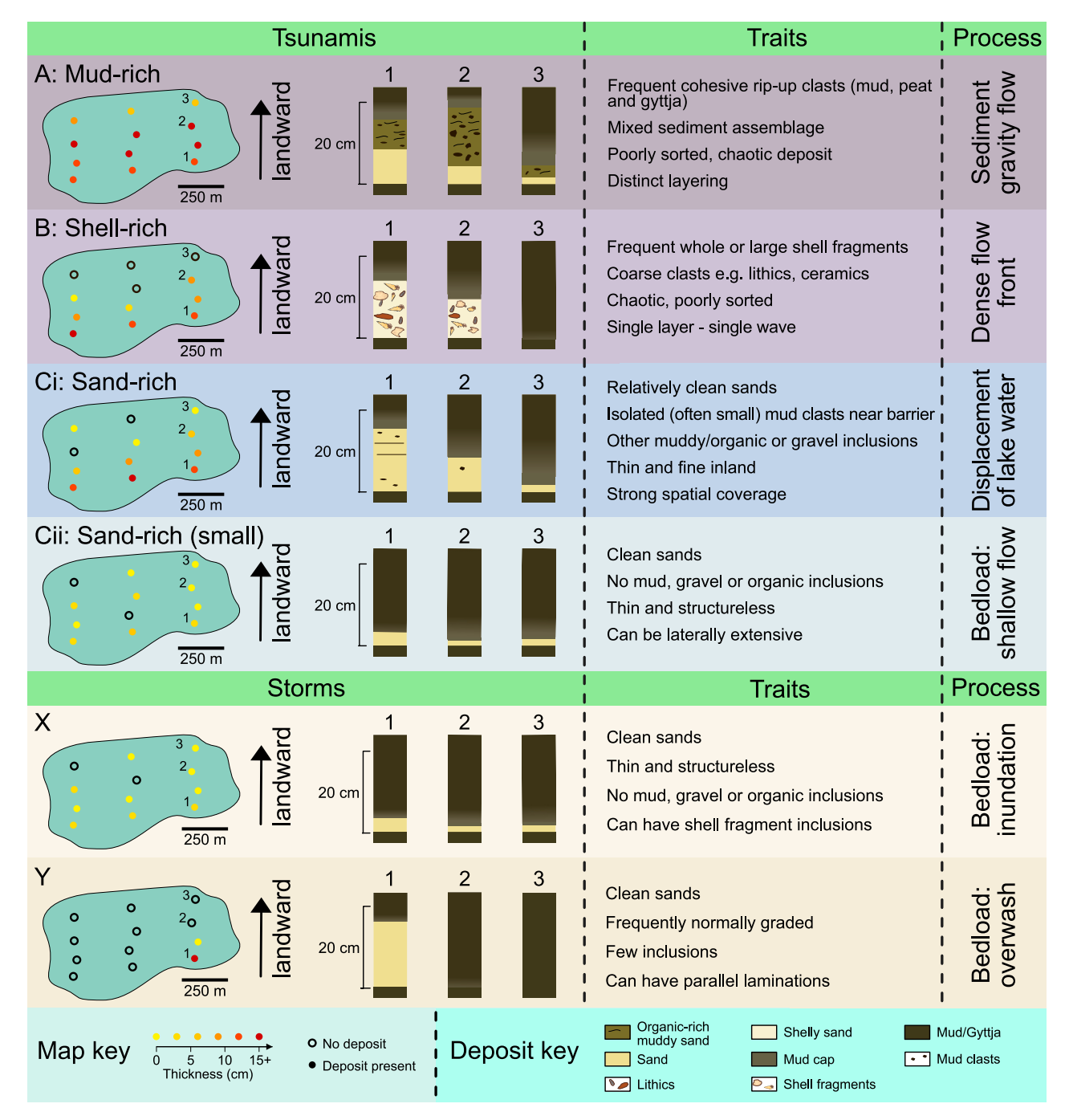


Fig. 15. Flow chart for identifying the deposit group for a candidate deposit in a coastal lake or lagoon using recognition criteria. The event origin is stated below each deposit group: either tsunami, storm or uncertain origin. For further information on each deposit group, the reader is referred to the text and summary schematic.



**Fig. 16.** Summary schematic for differentiating storms versus tsunamis in coastal lakes and lagoons. Each of 4 different scenarios for tsunamis and 2 for storms is shown through the typical spatial extent of the deposit and variation through the lake in its stratigraphy. Sediment type information is shown using colours – see key at base of figure; more detail on sediment type and associated structures and grain-size are provided in the main text. The typical features of each tsunami deposit type are also listed to enable comparison with a candidate deposit's features. The interpreted process of deposition is given on the right of each deposit group.

due to a lack of preservation of these thin deposits from palaeo events due to reworking of the deposits (Goto et al., 2011; Spiske et al., 2020). However, in blue holes, bioturbation is virtually absent (Wallace et al., 2021a) and so event layers (Group Z) appear distinct and readily identifiable within the background laminated sediment. Many lakes also show similar preservation but in others reworking appears to have taken place limiting their recognition to peaks in the grain size distribution (Donnelly et al., 2015). Overall, this means that in lakes and lagoons, the criteria for identifying storm deposits may differ from other environments. Here, the spatial dimensions of the deposit are crucial to identifying the deposit type (and differentiating with tsunamis) between a thin laterally extensive Group X deposit or a thicker spatially restricted

Group Y deposit.

# 5. Storms vs tsunami

# 5.1. Controls on deposit type

The controls on the event deposition are different for tsunamis and storms, with a dependence on the environmental conditions of the coastal lake and surrounding area in tsunamis, in contrast to the importance of the event characteristics in storms. However, these relationships only apply in coastlines where the environment is relatively stable and the sensitivity of the lake to coastal flooding has remained

consistent throughout the record. Minor changes in sea level or height of the coastal barrier can lead to environmental conditions where too few (or too many) events reach the lake to be recorded as distinct layers in the sedimentological record (Martin and Muller, 2021). Relative sea level changes, particularly in high latitudes, are the biggest driver of this change and are major for glacial regions such as Norway where sea level has varied by tens of metres over the last 8000 years (Bondevik et al., 1997b; Rasmussen et al., 2018). Therefore, we advocate that for a tsunami or storm deposit study, a sound understanding of the environmental history of a coastline is desirable. It is advantageous for reconstructing past events to determine the littoral barrier's variability in height and sensitivity to storms (and tsunamis) and the substrate of the environment surrounding the lake. However, in cases where this is uncertain, the deposits and their inferred processes may be used to determine likely aspects of the past environment.

#### 5.2. Environment-specific diagnostic criteria

The novel product to process approach applied in this study enables the deposits to be distinguished based on how the events fundamentally differ. The major deviation is in their mixing and dynamics, with a powerful bidirectional flow of a tsunami lasting several minutes contrasting with the high-frequency turbulent waves during a storm event that lasts for hours. This results in a poorly sorted, rapid deposition during tsunamis in marked contrast to well mixed layers during storms. These arguments can be applied in each of the three depositional environments identified for storms to observe why and how storm deposition differs from that of tsunamis. A flow diagram (Fig. 15) then outlines how these criteria can be applied to a candidate deposit, and a summary diagram (Fig. 16) adds further context for assigning a deposit to a particular deposit group.

#### 5.2.1. Blue holes

Blue holes offer excellent preservation of past coastal flooding events, providing a more complete record of past event chronologies, however, it is unclear how useful the records are to differentiate between storms and tsunamis. Unlike coastal lakes and lagoons, tsunami deposits have yet to be identified in blue holes. This absence has been attributed to a lack of seismically induced historical tsunamis impacting the areas in the Caribbean where blue hole deposits have been studied (e.g. Wallace et al., 2021a; Schmitt et al., 2025). However, caution must be taken when using such circular arguments that bias interpretation and fail to capture rare events, including landslide-generated tsunamis. Indeed, this line of reasoning has been extended to the only blue hole study outside of the Caribbean (Bramante et al., 2020), in the Marshall Islands, where 30 small far-field tsunamis have been recorded in the historical record (NCEI, 2024). Yet the study does not openly consider a tsunami origin. Furthermore, many unstudied blue holes are located in tsunami-prone regions such as the Maldives (Cutronea et al., 2023), which was impacted by the 2004 tsunami, and across parts of the Pacific (Montaggioni et al., 2023) and Western Australia (Backshall et al., 1979), where far-field tsunamis are common. These blue holes are vulnerable to inundation from both tsunamis and tropical cyclones, whose depositional mechanisms may be indistinguishable.

Storm deposition in Group Z deposits in blue holes is triggered by suspension fallout from initially bedload-transported sediment from the reef flat or margins, or flank failure triggered by bottom currents from the storm (Fig. 14). Both processes could also be the result of tsunamis. In both event types, as the lagoons where the blue holes are located are shallow (3-4 m), their wave bases would reach the bed, being able to transport a similar sedimentary assemblage from the reef flat and margins (Fig. 14a). As a sediment-laden tsunami wave reached a blue hole, the sudden increase in water depth would cause the denser tsunami flow to plunge. However, due to the steep sides and large depths of the blue holes, this sediment would likely disperse through the water column, rather than remain as a coherent density current. Therefore, sediment

would disperse through the water column, settling from suspension as a sheet on the blue hole surface. Deposits would likely be indistinguishable from the thinner storm deposits identified in Group Z. Furthermore, as tsunamis and storms' wave bases extend to the lagoon bed, both can trigger erosion of the blue hole margins, destabilising its flanks and producing the normally graded thicker subset of Group Z deposits (Fig. 14). Whilst the enhanced erosive power of a tsunami (Röbke and Vött, 2017) may trigger destabilisation more frequently than a storm, the event origin cannot be distinguished based on these thicker Group Z deposits. Therefore, in blue holes, the processes of deposition likely do not differ substantially enough so that event attribution based on sedimentology alone would be possible. Future work on modern tsunami deposits in blue holes should be conducted using a process to product approach to elucidate any additional mechanisms that occur during tsunamis in blue holes.

# 5.2.2. Coastal lakes and lagoons

The tsunami deposits of Groups A and B are interpreted to be deposited by flows (or flow fronts) of high density. Such flows are generated as the high-energy initially turbulent tsunami flow erodes and entrains large amounts of sediment from offshore, the coastal barrier, terrestrial environments and the lakebed (Atwater et al., 2012; Kempf et al., 2017). Where the underlying substrate is readily erodible and muddy, a cohesive flow state develops (Group A events). However, a storm wave (wind waves), even in the inundation regime has a lower velocity, depth and crucially a much shorter period (10-25 s) which prevents major erosion and entrainment during a single wave (Morton et al., 2007; Masselink and Van Heteren, 2014). Instead, small volumes of sediment are transported by each wave in a stepwise inundation process with typically only sand grains transported due to the higher energy needed to erode and transport gravels, clasts or cohesive elements (Komatsubara et al., 2008; Röbke and Vött, 2017). Therefore, storm waves exhibit a lower sediment concentration and density than tsunami flows, preventing the formation of either a sediment gravity flow or a dense, cohesionless head as the flow enters the lake even in environments which favour these transformations.

The tsunami deposits from the sandy coastlines of Group C share more characteristics with their storm counterparts, comprising a predominantly sandy matrix. However, the Group Ci subset shows important differences that enable differentiation between the events. First, many of the Group Ci deposits contain limited mud inclusions as rip-up clasts, mud laminae and/or mud caps. These features are absent in storm deposits in lacustrine environments because their flows have insufficient energy to erode and entrain cohesive muddy components from the lakebed or surrounding environment (Röbke and Vött, 2017). Therefore, where mud inclusions are found in a sandy deposit, a tsunami origin is likely in an enclosed coastal lake or lagoon. The spatial trends in the deposit can also distinguish between the events. In storms, the deposit will either be very laterally restricted and extend only ~100 m inland (Group Y) or be very thin <5 cm and more laterally extensive (Group X). However, tsunami deposits of Group Ci are laterally extensive across the entire, or most of, the, coastal lake or lagoon and thin (and often fine) inland up to an inundation limit, several hundred metres to kilometres inland. Therefore, given a strong spatial distribution of coring/sampling locations, the origin of the event can be determined.

The Group Cii, thin sand (< 5 cm) deposits can be readily discriminated from Group Y storm deposits using the spatial criteria outlined above. However, an issue arises when distinguishing from Group X deposits in storms. Their composition is very similar, they may both have similar lateral extents and are predominantly sandy. This is because the tsunami events are inferred to be small magnitude and/or shorter duration waves such as from distal tsunamis or localised events. Such waves would share the same characteristics as a storm event of high magnitude, which many Group X deposits represent (Liu and Fearn, 1993). Therefore, these deposits are fundamentally hard to differentiate as the waves that produce them are fundamentally similar, lying at

opposing extremes of event intensities. Currently, for these deposits, contextual evidence including correlating to dating within the wider record is the only method to attribute the event origin. However, more work in evaluating thin sand layers in tsunami-prone regions is required as many of the thin tsunami studies are based on single or dual cores so lack the spatial distribution that may enable the events to be distinguished.

Group Y deposits have often been termed "washover fans" in the literature, as they extend in a fan-like shape from a discrete low point in the coastal barrier (Goslin and Clemmensen, 2017). Whilst such deposits are common in storms, washover fans have been attributed to tsunamis in different back-barrier settings that are outside the scope of this study (Andrade, 1992; Goff et al., 2009), but also in lagoons on the Adriatic coasts of Italy (Gianfreda et al., 2001; Mastronuzzi and Sansò, 2012) and

Greece (May et al., 2012b). Such attribution hinges on the circular argument that tsunamis are more likely to impact the coastline than large storms in these regions (Mastronuzzi and Sansò, 2012). However, the distinct processes in either event generate fans that differ sedimentologically. A characteristic feature of Group Y deposits from storms is their limited lateral extent. Despite a similar morphology, tsunami washover fans are more laterally extensive, extending over 100,000–750,000 m² (Mastronuzzi and Sansò, 2012). Internally, the deposits also substantially differ. The example from Greece (May et al., 2012b) has four distinct layers, each a chaotic assemblage of coarsegrained material, hence, this deposit was assigned to Group B in this study. Storms are inherently incapable of generating these deposits that form under rapid capacity-driven sedimentation. Instead, Group Y deposits (washover fans) are formed under incremental bedload transport

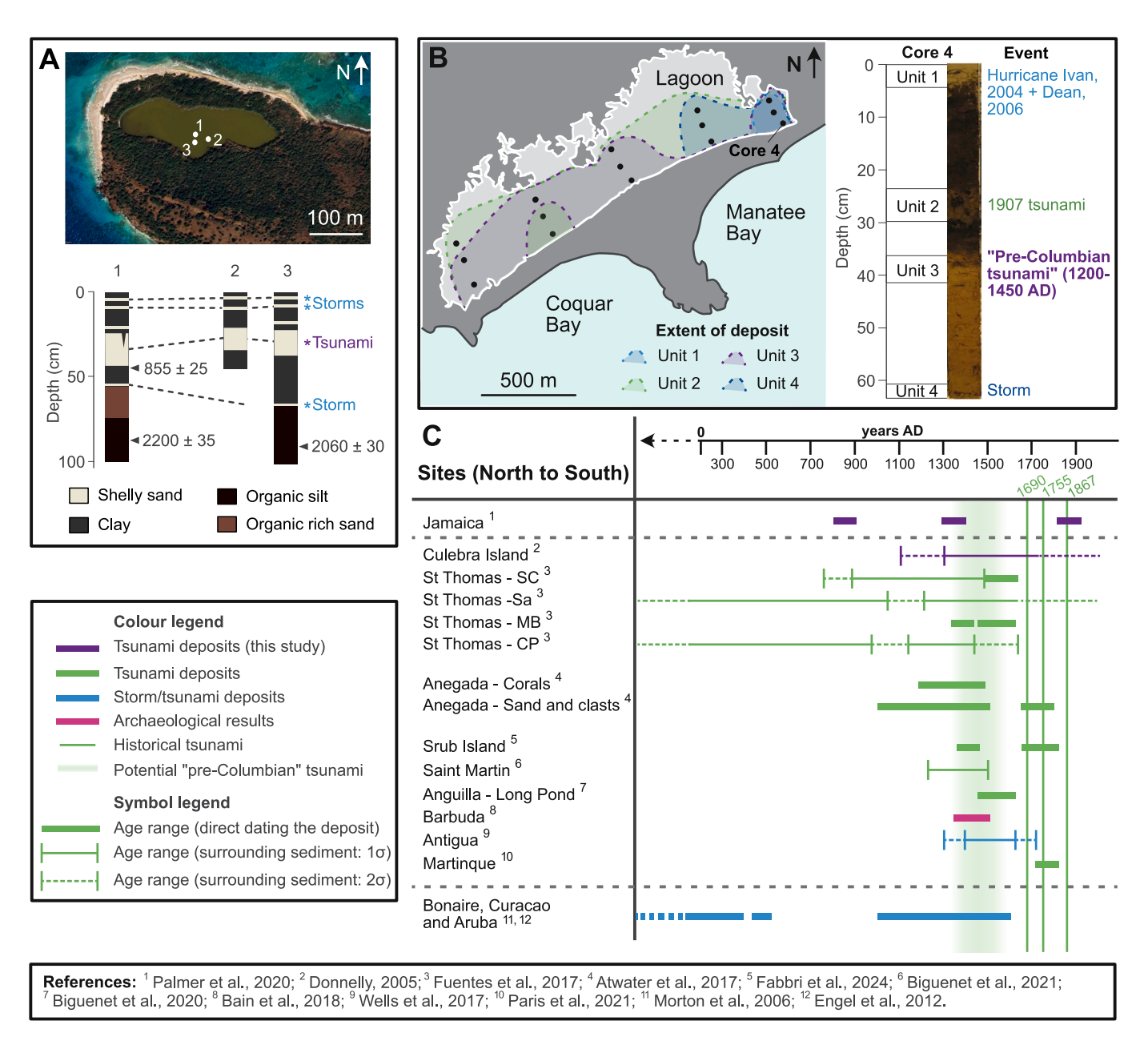


Fig. 17. Overview of the two reinterpreted sites and context of the surrounding region. A: Setting and stratigraphic record of three cores in Big Culberita salt pond (Puerto Rico); the 4 identified inundation events are highlighted by an asterisk. After Donnelly (2005). B: Distribution of deposits from four events in Manatee Bay lagoon, Jamaica; an image of core 4 is also shown with our interpretation of the events. After: Palmer et al. (2020), core image reprinted with permission from Springer Nature. C: Age ranges for sites in the Caribbean where deposits have been identified with a tsunami (or uncertain tsunami/storm origin). After Cordrie et al. (2022), references for C: Atwater et al., 2017; Bain et al., 2018; Biguenet et al., 2021; Biguenet et al., 2020; Engel et al., 2012; Fabbri et al., 2024; Fuentes et al., 2017; Morton et al., 2006; Paris et al., 2021; Wells et al., 2017.

(Fig. 13). Thus, the deposits of washover fans in coastal lakes and lagoons differ due to different processes of formation, enabling an attribution of event type where detailed sedimentological examination is undertaken.

Another criterion that is distinct to tsunamis is the formation of varves in deep (> 5 m depth) coastal lake environments. These varves are present immediately above the deposit in contrast to the unlaminated lake sediments below (Kelsey et al., 2005; Kempf et al., 2015). This feature is only observed during tsunamis, where the strong inflows (in all inferred processes) induce intense mixing and intrusion of saline water at depth within the lake, and it becomes trapped generating anoxic conditions that restrict bioturbation and permit varve formation (Minoura and Nakaya, 1991). However, during a storm event, the same process cannot occur in deep lakes as even in an inundation regime, the shallow wind waves do not penetrate to the base of the water column when depths exceed a few metres (Masselink and Van Heteren, 2014). This prevents the development of an anoxic layer, and the formation of varves, on the lakebed.

#### 5.3. Framework for event attribution

The previous section outlined where deposit types can be distinguished and the criteria that enable differentiation. Here, these criteria are condensed into a flow chart (Fig. 15) that enables a user to identify whether a set of deposits has a tsunamigenic (Groups A, B or C) or storm (Groups X and Y) origin. A summary diagram (Fig. 16) provides an easy visual comparison of the main traits, stratigraphy and spatial extents for each deposit group to validate the initial identification using the criteria and flow chart (Fig. 15). These figures assume that one or several candidate deposit(s) will have been identified in the sedimentary record of a coastal lake or lagoon with sufficient grain size, stratigraphic and spatial data evaluated.

For each candidate deposit, the grain size, stratigraphy and spatial extent should first be established, although a first-order assessment in the field is possible. This information can be used to answer the questions in the flow chart provided (Fig. 15) and to compare with the summaries in Fig. 16. Where Group A, B, Ci or Y deposition is inferred, the event origin can be determined. Indeed, where Group A or B deposition is confirmed, the surrounding environment was likely either mudrich (Group A) or shell-rich (Group B) (for more detail on the environments see section 3.6.1). This may provide a valuable insight for the palaeoenvironmental reconstruction of an area for a palaeo event. However, where the deposits are identified as Group X or Cii deposits, a differentiation between these events may often not be possible (see Section 5.2) and further information will be required. Overall, using Figs. 15 and 16, a candidate deposit can be assigned to a specific group except for some Group Cii/X deposits. By referring to the respective process diagrams (Figs. 6, 7, 8, 12, 13), the processes that occurred during the deposition of the candidate deposit can be reconstructed and the likely characteristics of the environment (for tsunamis) or relative event size (for storms) inferred.

# 5.4. Situations where event attribution is not possible

As observed in Fig. 16, event attribution is more difficult where the deposits and processes are fundamentally similar, either in an extremely intense storm inundation (Group X) or as a small (and/or distal) tsunami which forms a Group Cii deposit. Generally, storms inundate through a gradual rise in the water level superimposed by wind waves with a low height and high frequency (Goslin and Clemmensen, 2017). However, in 2013, typhoon Haiyan was observed to inundate parts of the Philippines with a series of 3-4 bore-like waves (strictly - infragravity surges) which each lasted 2-3 min and moved at up to 5 ms<sup>-1</sup> (Roeber and Bricker, 2015). Therefore, this event was perhaps more like a tsunami than a "typical" storm in its flow dynamics. Indeed, the deposits show a decrease in sorting inland, attributed to the erosion of multiple sediment

sources (Soria et al., 2018), which is a diagnostic signature of a tsunami wave (Richmond et al., 2012). This suggests that this event would be difficult to distinguish sedimentologically from the deposits of a tsunami wave due to the similar processes occurring. However, this phenomenon is rare and confined to specific conditions (Roeber and Bricker, 2015). The opposing situation is where a tsunami wave of low magnitude such as a localised event or the distal reflection of a larger event inundates a coastal lake. In this case, the event resembles more closely that of a storm being of lower velocity, depth and often shorter duration (for local events) and so comprises similar deposits as observed in Group Cii deposits. Therefore, at the opposing extremes event attribution is more difficult due to the similar processes in either event, but in their nature these extremes are comparatively rare occurrences.

#### 5.5. Requirements for successful differentiation

Outside of the environments and circumstances where an event attribution is impossible, as outlined above, a few requirements enable the criteria to be used to provide an unequivocal event identification. First, the spatial extent of the deposit data is required to evaluate certain criteria, especially in sandy coastlines. Here, where sedimentological criteria are less distinct, the spatial trends in the deposits can be vital to attributing the event origin as found in other depositional settings (Kortekaas and Dawson, 2007). This is shown in the compiled record as deposits identified from a single or dual cores have a higher uncertainty in their origin as the record is unlikely to be complete. Furthermore, the record shows that deposits studied without detailed grain size analysis (laser granulometry or dynamic imaging) have a higher uncertainty in their event attribution. This reinforces the need for such data to refine several of the key sedimentary criteria such as the sorting and grading of the deposit. Furthermore, detailed sedimentological descriptions of the inclusions and layers within a deposit are required for the criteria to be applied to the candidate deposit. Therefore, we suggest that future storm and tsunami studies incorporate multiple deposits over a transect, or another spatial scale, with detailed sedimentological descriptions and grain size analysis, if practicable. This is especially pertinent where both storms and tsunamis occur. This will enable more accurate identification of past events and aid in their reconstruction whilst improving predictions and models of future events.

#### 5.6. Application to other records

Whilst the deposits outlined in the database cover only the Holocene in date, given good preservation, the criteria and framework could be applied to deposits of older geological age. However, a deposit's provenance is likely to be more uncertain unless a sufficient spatial extent and knowledge of the depositional setting is available, as the presented criteria are formulated for, and apply best to, coastal lakes and lagoons. The process-orientated approach used here could be readily applied to determine the processes and thus the likely event type (storm or tsunami) from the deposits in other depositional locations (e.g. marshes and coastal plains), as recently shown by Majumdar and Bhattacharya (2025). Indeed, the inferred processes for Group C tsunami deposits in lakes and lagoons show that deposition occurs in a manner similar to on land, resulting in similar deposit signatures (e.g. Peters and Jaffe, 2010; Dura et al., 2015). Therefore, some of these criteria (Figs. 15 and 16) such as inclusions of rip-up clasts and/or organic or gravel inclusions that storm deposits do not show can be indicative of a tsunamigenic origin in these other environments. In these areas, a robust process sedimentological approach should be used to consider how the different environments would alter the processes of deposition. However, it is in coastal lakes and lagoons where the distinction between storms and tsunamis can be unequivocal due to the distinct inferred processes (formation of sediment gravity flows and dense, cohesionless flow fronts) that occur in tsunamis compared to storms. Therefore, notwithstanding practical constraints, coastal lakes and lagoons provide the

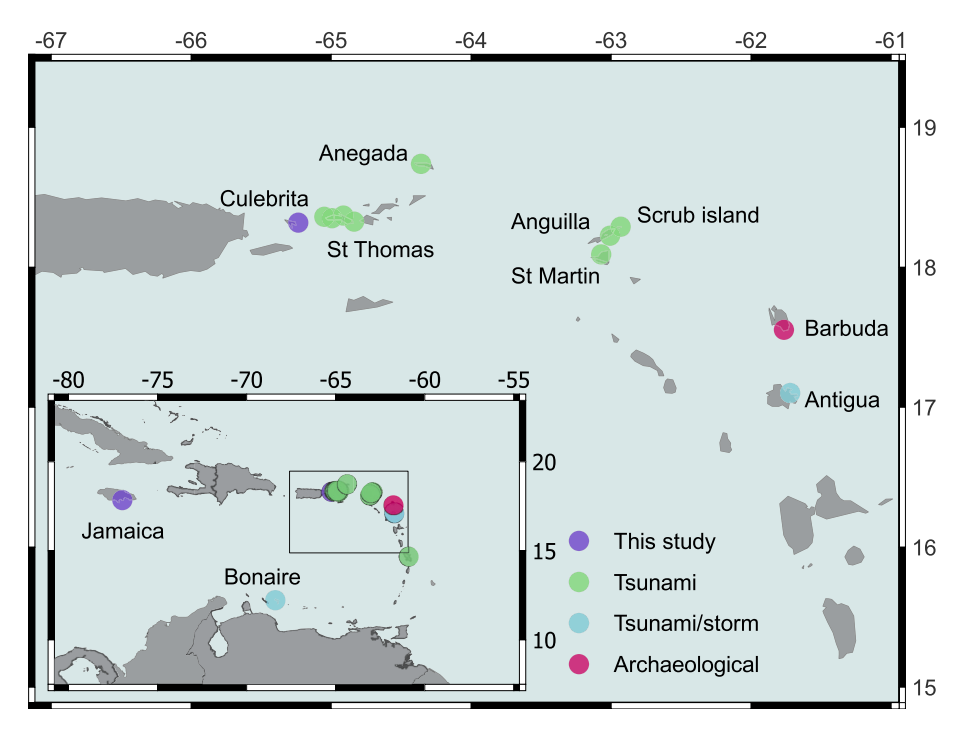


Fig. 18. Geographical position of the pre-Columbian tsunami deposits. Locations of the sites reinterpreted in text (purple) and previously identified sites (green) where tsunami deposits have been investigated, colours follow those of Fig. 17. Numbers indicate degrees latitude north and degrees longitude east respectively.

optimal location to distinguish between storms and tsunamis in the geological record.

# 6. Case study: Applying the framework to re-evaluate existing deposits

The confidence level of event attribution within the dataset showed that around a quarter of events had an uncertain origin, with a greater proportion of older events and Group C tsunami deposits. The interpreted processes in this study show that in some of these uncertain events, an event attribution based on sedimentology alone is impossible. However, in many studies with uncertain origin, given a sufficiently good spatial distribution of identified deposits, the event can be determined using the results of this study. This facilitates event attribution solely on the sedimentology, being independent of age, which will allow more certainty to be attributed to the origin of events outside the historical record. It is these events that are most important for updating hazard assessments, with the most famous example being that of the "orphan tsunami", identified using deposits as the Cascadia 1700 earthquake and tsunami (Atwater et al., 2005). Here, we consider two examples interpreted as storm events (Fig. 17) but with uncertain confidence and use the criteria in the flow chart (Fig. 15) and summary diagram (Fig. 16) presented to reinterpret four candidate deposits within two different studies.

#### 6.1. Case 1: Puerto Rico

On a small island to the east of Puerto Rico, a small and shallow (<1 m deep) pond, situated behind a barrier beach and mangroves, records several layers interpreted as storm deposits. These comprise three very thin layers (1-2 cm thick) together with a thicker layer that contains rare clay rip-up clasts, normal grading and some shell fragments (Fig. 17a; Donnelly, 2005). This thicker layer is consistent through 3 cores taken near the centre of the pond, varying between 15 and 21 cm thick. The layer has a sharp upper and lower contact with coarse shell fragments (clasts) >2 mm diameter at the base, similar to the coarse layer found at the base of tsunami deposits (Smith et al., 2004; Moore et al., 2011;

Richmond et al., 2012). Donnelly (2005) acknowledges the possibility of a tsunami origin but assigns the event to a storm origin using the criteria available (Goff et al., 2004; Tuttle et al., 2004).

To objectively consider the origin of these deposits, we follow the flow chart outlined in Fig. 15. Comparing the three thinner layers first, they lack cohesive inclusions and do not exhibit a chaotic or poorly sorted structure. The spatial extent of each deposit is consistent through the three cores, suggesting that Group Y deposition is unlikely. The thickness of these thinner layers is less than 5 cm, and thus they are inferred to represent either a Group X storm deposit or possibly a tsunami Group Cii deposition. In contrast, the thicker (15-21 cm thick) layer contains rare cohesive inclusions but lacks the distinct layers of cohesive and sand-rich sediments characteristic of Group A sedimentation; thus, Group Ci deposition is inferred. A comparison with Fig. 16 of the stratigraphy and traits of Group Cii deposits, sharing isolated mud clasts and a thicker overall deposit (15-21 cm), confirms this conclusion. The identification of a tsunami origin marks a departure from the initial interpretation of a storm event, highlighting the value of the applied framework in objectively determining depositional origins.

#### 6.2. Case 2: Jamaica

Another study in the Caribbean on the south coast of Jamaica records four sedimentary units (1-4), identified as the product of storms and tsunamis within a shallow (<1 m deep) lagoon sited behind a 5 m high sandy barrier (Fig. 17b; Palmer et al., 2020). The upper unit (unit 1; Fig. 17b) consists of fine, clean, moderately sorted sands (several cm thick) confined to the eastern edge of the lagoon (Fig. 17b), recognised as an amalgamation of deposits from two modern hurricanes, Ivan [2004] and Dean [2006] (Palmer et al., 2020). Unit 2, a sand (5-7 cm thick) with common marine bioclasts, organic debris and rip-up clasts was poorly sorted and found throughout every core in the lagoon (Fig. 17b). This was attributed to the 1907 Kingston tsunami. Unit 3, a sand (approximately 5 cm thick) with some marine bioclasts, occasional organic clasts and debris, again poorly sorted, was found within cores across the lagoon but in more sporadic locations (Fig. 17b). This unit was dated to 1290-1400 and attributed to a storm, although a tsunami

origin was considered (Palmer et al., 2020). The final unit (unit 4) was recorded as a thin (< 5 cm) relatively clean sandy layer with limited bioclasts and was confined to the east of the lagoon, this event was attributed to a storm older than 768-900 CE.

The same flow chart (Fig. 15) and criteria can also be applied to these deposits from an objective perspective. Units 2 and 3 contain cohesive inclusions, such as rip-up clasts, but in both deposits, the distinct layers of sand-rich and cohesive sediments of Group A deposits are missing, indicating Group Ci deposition. A comparison with Fig. 16 shows that the stratigraphy, extensive spatial coverage, and cohesive inclusions of the deposit are similar to those of Group Ci, although with thinner than average sequences. Therefore, it can be inferred that both layers resulted from Group Ci tsunami deposition. Units 1 and 4 are relatively clean sands lacking cohesive inclusions; they also exhibit moderate sorting, making Group B deposition unlikely. The lateral extent of both layers is limited to the north of the lagoon, suggesting Group Y deposition. The clean sands with few inclusions correspond to the characteristics of Group Y layers (Fig. 16), leading to the inference of Group Y deposition during a storm event. Consequently, based on the framework and criteria, the origins of units 1 and 4 are confirmed as storm layers, while unit 2 is attributed to a tsunami, and unit 3 is reinterpreted as a tsunami event. The significance of this identification, along with the other reinterpreted deposit, becomes clearer when considering the overlapping dates with other tsunami events recorded in the region.

#### 6.3. Implications for Caribbean tsunami hazard

The dating from both newly interpreted tsunami deposits in Puerto Rica and Jamaica overlaps with the window of a potential tsunami event termed the "pre-Columbian tsunami" of around 1350-1550 CE (Fig. 17c). This event was first identified in sedimentary deposits in the British Virgin Islands (Atwater et al., 2012, 2017) but deposits have since been found over a wide area (Figs. 17c and 18). Before the recognition of this event, large-scale tsunami events were considered rare in the Caribbean (Buckley et al., 2012) and thus the event's source (distal or local) is still uncertain, with the most likely possibility being a major megathrust earthquake (~8.7 Mw) on the Puerto Rico trench (Cordrie, 2021; Cordrie et al., 2022; Wei et al., 2024). The deposits reinterpreted here further constrain the spatial extent of this "orphan" tsunami through an extra data point in the Lesser Antilles arc and an outlier in Jamaica, far removed from the other deposits (Fig. 18). This suggests that the tsunami impacted the entire Caribbean Sea or that a different contemporary event occurred locally in Jamaica. In either case, this study strongly indicates that major tsunamis have reached Jamaica in the past and their future occurrence should be considered by the relevant stakeholders.

This case study has shown the issue with a persistent circular argument, where due to the prevalence of storms in the Caribbean region, a storm event is often assigned to a candidate deposit. Using new sedimentological criteria, we have been able to break this cycle by objectively characterising two 'storm' deposits as tsunami events. This reinterpretation has enabled a widening of the geological record for tsunami events in the Caribbean, which can be used to improve hazard assessments of future events. Future research should use these criteria to establish with greater confidence the origin of deposits from future and existing deposits to improve the accuracy and completeness of the records for both storms and tsunamis.

#### 7. Conclusions

This study has utilised a product to process approach to establish diagnostic criteria for identifying between storm and tsunami events in coastal lakes and lagoons. The existing sedimentary literature was grouped into three different subsets for tsunamis as well as three for storms. These comprised for tsunamis: A) thick clast- and mud-rich deposits, B) dense shell-rich layers, and C) relatively clean sands; and for

storms: X) thin but laterally extensive sands, Y) clean sands that were thick but laterally restricted and Z) variable sandy layers within sinkholes. From these deposits, differing processes were inferred, utilising knowledge from other fields such as sedimentary gravity flows. For tsunamis, these processes relate to common environments (mud-rich, clast and shell-rich, or sand-dominated) and lake characteristics and comprise:

- The formation of a sediment gravity flow that transforms rapidly (100 s of metres) into a hybrid flow as the tsunami inundates a coastal lake.
- The progression of a dense, cohesionless flow head similar in composition to recent observations in turbidity currents.
- The displacement of shallow lake water by a high energy and turbulent tsunami wave.

In contrast, the processes for storms were found to vary depending on the relationship between the barrier height and event size, with two regimes observed and a third for blue holes:

- An overwash regime where the coastal lake is not fully submerged, and deposition occurs incrementally via bedload transport.
- Inundation regime where full submersion of the coastal lake occurs and a dilute flow transports sediment throughout the lake via bedload, except at depths (>5 m) where suspension transport takes over.
- Whereas in blue holes, deposition occurred either from suspension in a dilute flow or via the displacement of sediment and subsequent fallout from the steep flanks of the blue hole.

The interpretation of processes has enabled the fundamental differences between storms and tsunamis (wave period, duration and energy) to be applied to distinguish between deposit types. Comparing the two events, storms are fundamentally incapable of producing a flow which exhibits the processes described for Group A, B and Ci deposits. Recognition that these deposits can only be produced by tsunamis enables an unequivocal differentiation between the events where these deposits are found. However, this differentiation is often only possible where a strong spatial distribution of deposits is constrained and detailed grain size analysis is undertaken. Even so, in some environments where sediment supply is low, within sinkholes or where the event is at two opposing extremes, identification is not possible as the processes involved would be virtually the same. This study has shown how the criteria outlined can be used to objectively determine the event origin of deposits based on sedimentology alone, breaking the reliance on contextual information. This has provided new insight into tsunami hazards in the Caribbean region, whilst showing that coastal lakes and lagoons are the optimal setting to distinguish between storm and tsunami deposits. The framework outlined here is envisaged to help settle the storm versus tsunami debate for deposits in many coastal lakes and lagoons and drive further research into how processes and deposits differ in other depositional settings.

# Declaration of competing interest

The authors declare that they have no known competing financial interests or personal relationships that could have influenced the work reported in this paper.

#### Acknowledgements

This work was supported by the Natural Environment Research Council [grant number NE/S007458/1]. We thank Dr. Romain Vaucher, an anonymous reviewer, and Editor Massimo Zecchin, for their comments, which have significantly improved the manuscript.

#### Appendix A. Supplementary data

Supplementary data to this article can be found online at https://doi.org/10.1016/j.earscirev.2025.105277.

#### Data availability

The dataset of tsunami and storm deposits in coastal lakes, lagoons and sinkholes compiled in this study is accessible via: https://doi.org/10.6084/m9.figshare.30002260.v1

#### References

- Abe, T., Goto, K., Sugawara, D., 2012. Relationship between the maximum extent of tsunami sand and the inundation limit of the 2011 Tohoku-oki tsunami on the Sendai Plain, Japan. Sediment. Geol. 282, 142–150.
- Adomat, F., Gischler, E., 2016. Assessing the suitability of Holocene environments along the central Belize coast, Central America, for the reconstruction of hurricane records. Int. J. Earth Sci. 106 (1), 283–309.
- Andrade, C., 1992. Tsunami generated forms in the Algarve Barrier Islands (South Portugal). Sci. Tsunami Hazards. 10 (1), 21–34.
- Arai, K., Naruse, H., Miura, R., Kawamura, K., Hino, R., Ito, Y., Inazu, D., Yokokawa, M., Izumi, N., Murayama, M., Kasaya, T., 2013. Tsunami-generated turbidity current of the 2011 Tohoku-Oki earthquake. Geology 41 (11), 1195–1198.
- Arcos, M., Macinnes, B.T., Arreaga, P., Rivera-Hernandez, F., Weiss, R., Lynett, P., 2013.
  An amalgamated meter-thick sedimentary package enabled by the 2011 Tohoku tsunami in El Garrapatero, Galapagos Islands. Quat. Res. 80, 9–19.
- Atwater, B.F., Satoko, M.-R., Satake, K., Yoshinobu, T., Kazue, U., Yamaguchi, D.K., 2005. The Orphan tsunami of 1700: Japanese clues to a parent earthquake in North America. In: U. S. Geological Survey Professional Paper, 1707, pp. 1–144.
- Atwater, B.F., Ten Brink, U.S., Buckley, M., Halley, R.S., Jaffe, B.E, López-Venegas, A.M., Reinhardt, E.G., Tuttle, M.P., Watt, S., Wei, Y., 2012. Geomorphic and stratigraphic evidence for an unusual tsunami or storm a few centuries ago at Anegada, British Virgin Islands. Nat. Hazards 63, 51–84. https://doi.org/10.1007/s11069-010-9622-6
- Atwater, B.F., ten Brink, U.S., Cescon, A.L., Feuillet, N., Fuentes, Z., Halley, R.B., Nuñez, C., Reinhardt, E.G., Roger, J.H., Sawai, Y., Spiske, M., Tuttle, M.P., Wei, Y., Weil-Accardo, J., 2017. Geologic evidence for catastrophic marine inundation in 1200–1480 C.E. near the Puerto Rico Trench at Anegada, British Virgin Islands. Geosphere 13 (2), 301–368.
- Baas, J.H., Best, J.L., Peakall, J., Wang, M., 2009. A phase diagram for turbulent, transitional, and laminar clay suspension flows. J. Sediment. Res. 79 (4), 162–183.
- Baas, J.H., Best, J.L., Peakall, J., 2011. Depositional processes, bedform development and hybrid bed formation in rapidly decelerated cohesive (mud-sand) sediment flows. Sedimentology 58 (7), 1953–1987.
- Baas, J.H., Tracey, N.D., Peakall, J., 2021. Sole marks reveal deep-marine depositional process and environment: Implications for flow transformation and hybrid-event-bed models. J. Sediment. Res. 91 (9), 986–1009.
- Backshall, D.G., Barnett, J., Davies, P.J., Duncan, D.C., Harvey, N., Hopley, D., Isdale, P., Jennings, J.N., Moss, R., 1979. Drowned dolines—the blue holes of the Pompey reefs, Great Barrier Reef. BMR J. Aust. Geol. Geophys. 4, 99–109.
- Bain, A., Faucher, A.M., Kennedy, L.M., LeBlanc, A.R., Burn, M.J., Boger, R., Perdikaris, S., 2018. Landscape transformation during the ceramic age and colonial occupations of Barbuda, West Indies. Environ. Archaeol. 23 (1), 36–46.
- Baranes, H.E., Woodruff, J.D., Wallace, D.J., Kanamaru, K., Cook, T.L., 2016. Sedimentological records of the C.E. 1707 H\u00f3ei Nankai Trough tsunami in the Bungo Channel, southwestern Japan. Nat. Hazards 84 (2), 1185–1205.
- Beck, H.E., McVicar, T.R., Vergopolan, N., Berg, A., Lutsko, N.J., Dufour, A., Zeng, Z., Jiang, X., van Dijk, A.I.J.M., Miralles, D.G., 2023. High-resolution (1 km) Köppen-Geiger maps for 1901–2099 based on constrained CMIP6 projections. Sci. Data. 10 (1), 1–16.
- Behrens, J., et al., 2021. Probabilistic tsunami hazard and risk analysis: a review of research gaps. Front. Earth Sci. 9, 628772.
- Bertran, P., Bonnissent, D., Imbert, D., Lozouet, P., Serrand, N., Stouvenot, C., 2004. Paléoclimat des Petites Antilles depuis 4000 ans BP: l'Enregistrement de la lagune de Grand-Case à Saint-Martin. Compt. Rendus Geosci. 336 (16), 1501–1510.
- Best, J.L., Kostaschuk, R.A., Peakall, J., Villard, P.V., Franklin, M., 2005. Whole flow field dynamics and velocity pulsing within natural sediment-laden underflows. Geology 33, 765–768.
- Biguenet, M., Sabatier, P., Chaumillon, E., Chagué, C., Arnaud, F., Feuillet, N., 2020. Sedimentary records of tsunamis and hurricanes in the Lesser Antilles. In: Abstract [NH004–05] Presented at 2020 AGU Fall Meeting, p. 1. 1–17 Dec.
- Biguenet, M., et al., 2021. A 1600 year-long sedimentary record of tsunamis and hurricanes in the Lesser Antilles (Scrub Island, Anguilla). Sediment. Geol. 412, 105806.
- Biguenet, M., Chaumillon, E., Sabatier, P., Paris, R., Vacher, P., Feuillet, N., 2022. Discriminating between tsunamis and tropical cyclones in the sedimentary record using X-ray tomography. Mar. Geol. 450, 106864.
- Biguenet, M., Chaumillon, E., Sabatier, P., Bastien, A., Geba, E., Arnaud, F., Coulombier, T., Feuillet, N., 2023. Hurricane Irma: an unprecedented event over the last 3700 years? Geomorphological changes and sedimentological record in Codrington Lagoon, Barbuda. *Hazards Earth Syst. Sci.* 23, 3761–3788.

- Blanco, C.L., Hawkes, A.D., Wallace, E.J., Donnelly, J.P., MacDonald, D., 2024. Tropical cyclone activity over the past 1200 years at the Pelican Cays, Belize. Mar. Geol. 475, 107365.
- Bondevik, S., Risebrobakken, B., Gibbons, S.J., Rasmussen, T.L., Løvholt, F., 2024. Contamination of 8.2 ka cold climate records by the Storegga tsunami in the Nordic Seas. Nat. Commun. 15, 1–7, 2904.
- Bondevik, S., Svendsen, J.I., Johnsen, G., Mangerud, J., Kaland, P.E., 1997a. The Storegga tsunami along the Norwegian coast, its age and runup. Boreas 26 (1), 29–53.
- Bondevik, S., Svendsen, J.I., Mangerud, J., 1997b. Tsunami sedimentary facies deposited by the Storegga tsunami in shallow marine basins and coastal lakes, western Norway. Sedimentology 44 (6), 1115–1131.
- Bondevik, S., Mangerud, J., Dawson, S., Dawson, A., Lohne, Ø., 2005. Evidence for three North Sea tsunamis at the Shetland Islands between 8000 and 1500 years ago. Quat. Sci. Rev. 24 (14–15), 1757–1775.
- Bony, G., Marriner, N., Morhange, C., Kaniewski, D., Perinçek, D., 2012. A high-energy deposit in the Byzantine harbour of Yenikapı, Istanbul (Turkey). Quat. Int. 266, 117–130.
- Bouma, A., 1962. Sedimentology of some Flysch Deposits: A Graphic Approach to Facies Interpretation. Elsevier, Amsterdam/New York, p. 168.
- Bramante, J.F., Ford, M.R., Kench, P.S., Ashton, A.D., Toomey, M.R., Sullivan, R.M., Karnauskas, K.B., Ummenhofer, C.C., Donnelly, J.P., 2020. Increased typhoon activity in the Pacific deep tropics driven by Little Ice Age circulation changes. Nat. Geosci. 13 (12), 806–811.
- Brandon, C.M., Woodruff, J.D., Lane, D.P., Donnelly, J.P., 2013. Tropical cyclone wind speed constraints from resultant storm surge deposition: A 2500 year reconstruction of hurricane activity from St. Marks, FL. Geochem. Geophys. Geosyst. 14 (8), 2993–3008.
- Brandon, C.M., Woodruff, J.D., Donnelly, J.P., Sullivan, R.M., 2014. How unique was Hurricane Sandy? Sedimentary reconstructions of extreme flooding from New York harbor. Sci. Rep. 4 (1), 1–9.
- Bregy, J.C., Wallace, D.J., Totten, R.L., Cruz, V.J., 2018. 2500-year paleotempestological record of intense storms for the northern Gulf of Mexico, United States. Mar. Geol. 396, 26–42.
- Brill, D., et al., 2020. Modern and historical tropical cyclone and tsunami deposits at the coast of Myanmar: Implications for their identification and preservation in the geological record. Sedimentology 67 (3), 1431–1459.
- Brown, A.L., Reinhardt, E.G., Van Hengstum, P.J., Pilarczyk, J.E., 2014. A coastal Yucatan sinkhole records intense hurricane events. J. Coast. Res. 30 (2), 418–428.
- Buckley, M.L., Wei, Y., Jaffe, B.E., Watt, S.G., 2012. Inverse modeling of velocities and inferred cause of overwash that emplaced inland fields of boulders at Anegada, British Virgin Islands. Nat. Hazards 63 (1), 133–149.
- Chaumillon, E., et al., 2017. Storm-induced marine flooding: Lessons from a multidisciplinary approach. Earth Sci. Rev. 165, 151–184.
- Chiodi, F., Claudin, P., Andreotti, B., 2014. A two-phase flow model of sediment transport: transition from bedload to suspended load. J. Fluid Mech. 755, 561–581.
- Cisternas, M., et al., 2005. Predecessors of the giant 1960 Chile earthquake. Nature 437 (7057) 404–407
- Clark, K., Cochran, U., Mazengarb, C., 2011. Holocene coastal evolution and evidence for paleotsunami from a tectonically stable region, Tasmania, Australia. Holocene 21 (6), 883–895.
- Clarke, J.E.H., et al., 2016. First wide-angle view of channelized turbidity currents links migrating cyclic steps to flow characteristics. Nat. Commun. 7 (1), 1–13. https://doi. org/10.1038/ncomms11896.
- Cochran, D.M., Reese, C.A., Liu, K.B., 2009. Tropical Storm Gamma and the Mosquitia of eastern Honduras: a little-known story from the 2005 hurricane season. Area 41 (4), 425–434.
- Cordrie, L., 2021. Identification and Characterization of the Lesser Antilles arc Past Earthquakes: Insight from Tsunami Modeling and Sediment Transport Simulation. PhD thesis,. Université Paris Cité, p. 241.
- Cordrie, L., Feuillet, N., Gailler, A., Biguenet, M., Chaumillon, E., Sabatier, P., 2022.

  A Megathrust earthquake as source of a Pre-Colombian tsunami in Lesser Antilles:
  Insight from sediment deposits and tsunami modeling. Earth Sci. Rev. 228, 104018.
- Costa, P.J.M., Andrade, C., 2020. Tsunami deposits: Present knowledge and future challenges. Sedimentology 67 (3), 1189–1206.
- Costa, P.J.M., Leroy, S.A.G., Dinis, J.L., Dawson, A.G., Kortekaas, S., 2012. Recent high-energy marine events in the sediments of Lagoa dédé Obidos and Martinhal (Portugal): recognition, age and likely causes. Nat. Hazards Earth Syst. Sci. 12, 1367–1380.
- Costa, P.J.M., Gelfenbaum, G., Dawson, S., La Selle, S., Milne, F., Cascalho, J., Lira, C.P., Andrade, C., Freitas, M.C., Jaffe, B., 2018. The application of microtextural and heavy mineral analysis to discriminate between storm and tsunami deposits. In: Tsunamis: Geology, Hazards and Risks (Eds: Scourse, E.M., Chapman, N.A., Tappin, D.R., Wallis, S.R.). Geol. Soc. Spec. Publ. 456 (1), 167–190.
- Costa, P.J.M., Dawson, S., Ramalho, R.S., Engel, M., Dourado, F., Bosnic, I., Andrade, C., 2021. A review on onshore tsunami deposits along the Atlantic coasts. Earth Sci. Rev. 212. 103441.
- Cutronea, L., Ahmed, H., Azzola, A., Fontana, H., Geneselli, I., Mancini, I., Montefalcone, M., Oprandi, A., Pancrazi, I., Vanin, S., Capello, M., 2023. First chemical-physical measurements by multi-parameter probe in the blue hole of Faanu Madugau (Ari Atoll, the Maldives). Environments 10, 180.
- Cuven, S., Paris, R., Audin, L., Mitra, S., Gielly, L., Aguirre, E., 2024. Tsunami deposits to reconstruct major earthquakes chronology in Southern Peru. Past Global Chang. Mag. 32 (1), 38–39.

- Das, O., Wang, Y., Donoghue, J., Xu, X., Coor, J., Elsner, J., Xu, Y., 2013. Reconstruction of paleostorms and paleoenvironment using geochemical proxies archived in the sediments of two coastal lakes in northwest Florida. Quat. Sci. Rev. 68, 142-153.
- De Martini, P.M., Barbano, M.S., Smedile, A., Gerardi, F., Pantosti, D., Del Carlo, P., Pirrotta, C., 2010. A unique 4000 year long geological record of multiple tsunami inundations in the Augusta Bay (eastern Sicily, Italy). Mar. Geol. 276 (1-4), 42-57.
- Dezileau, L., Sabatier, P., Blanchemanche, P., Joly, B., Swingedouw, D., Cassou, C. Castaings, J., Martinez, P., Von Grafenstein, U., 2011. Intense storm activity during the Little Ice Age on the French Mediterranean coast. Palaeogeogr. Palaeoclimatol. Palaeoecol. 299 (1-2), 289-297.
- Degeai, J.P., Devillers, B., Dezileau, L., Oueslati, H., Bony, G., 2015. Major storm periods and climate forcing in the Western Mediterranean during the Late Holocene. Quat. Sci. Rev. 129, 37-56.
- Dezileau, L., Pérez-Ruzafa, A., Blanchemanche, P., Degeai, J.-P., Raji, O., Martinez, P., Marcos, C., Von Grafenstein, U., 2016. Extreme storms during the last 6500 years from lagoonal sedimentary archives in the Mar Menor (SE Spain). Clim. Past 12,
- Dietz, M.E., Liu, K., Bianchette, T., Smith, D., 2021. Differentiating hurricane deposits in coastal sedimentary records: two storms, one layer, but different processes. Environ. Res. Commun. 3 (10), 101001.
- Donato, S.V., Reinhardt, E.G., Boyce, J.I., Pilarczyk, J.E., Jupp, B.P., 2009. Particle-size distribution of inferred tsunami deposits in Sur Lagoon, Sultanate of Oman. Mar. Geol. 257 (1-4), 54-64.
- Donnelly, J.P., 2005. Evidence of past intense tropical cyclones from backbarrier salt pond sediments: a case study from isla de Culebrita, Puerto Rico, USA. J. Coast. Res.
- Donnelly, J.P., Woodruff, J.D., 2007. Intense hurricane activity over the past 5,000 years controlled by El Niño and the West African monsoon. Nature 447 (7143), 465-468.
- Donnelly, J.P., Hawkes, A.D., Lane, P., Macdonald, D., Shuman, B.N., Toomey, M.R., Van Hengstum, P.J., Woodruff, J.D., 2015. Climate forcing of unprecedented intensehurricane activity in the last 2000 years. Earth's Future 3 (2), 49-65.
- Dorrell, R.M., Peakall, J., Darby, S.E., Parsons, D.R., Johnson, J., Sumner, E.J., Wynn, R. B., Özsoy, E., Tezcan, D., 2019. Self-sharpening induces jet-like structure in seafloor gravity currents. Nat. Commun. 10 (1), 1381, pp.1–10.
- Dura, T., Cisternas, M., Horton, B.P., Ely, L.L., Nelson, A.R., Wesson, R.L., Pilarczyk, J.E., 2015. Coastal evidence for Holocene subduction-zone earthquakes and tsunamis in central Chile. Quat. Sci. Rev. 113, 93-111.
- Earland, J.L., Scourse, J.D., Ehmen, T., Kender, S., Ascough, P., 2024. Identification of the Storegga event offshore Shetland. Mar. Geol. 474, 107334.
- Engel, M., Brückner, H., Messenzehl, K., Frenzel, P., May, S.M., Scheffers, A., Scheffers, S., Wennrich, V., Kelletat, D., 2012. Shoreline changes and high-energy wave impacts at the leeward coast of Bonaire (Netherlands Antilles), Earth Planets Space 64 (10), 905–921.
- Engel, M., Oetjen, J., May, S.M., Brückner, H., 2016. Tsunami deposits of the Caribbean -Towards an improved coastal hazard assessment, Earth Sci. Rev. 163, 260-296.
- Engel, M., Hess, K., Dawson, S., Patel, T., Koutsodendris, A., Vakhrameeva, P., Klemt, E., Kempf, P., Schön, I., Heyvaert, V.M.A., 2023. Sedimentary evidence of the Late Holocene tsunami in the Shetland Islands (UK) at Loch Flugarth, northern Mainland. Boreas 53, 27-41.
- Ercolani, C., Muller, J., Collins, J., Savarese, M., Squiccimara, L., 2015. Intense Southwest Florida hurricane landfalls over the past 1000 years. Quat. Sci. Rev. 126,
- Fabbri, S.C., et al., 2024. Deciphering the sedimentary imprint of tsunamis and storms in the Lesser Antilles (Saint Martin): A 3500-year record in a coastal lagoon, Mar. Geol. 471, 107284.
- Feist, L., et al., 2023. Holocene offshore tsunami archive Tsunami deposits on the Algarve shelf (Portugal). Sediment. Geol. 448, 106369.
- Felix, M., Peakall, J., McCaffrey, W.D., 2006. Relative importance of processes that govern the generation of particulate hyperpycnal flows. J. Sediment. Res. 76, 382\_387
- Finkler, C., Fischer, P., Baika, K., Rigakou, D., Metallinou, G., Hadler, H., Vött, A., 2018. Tracing the Alkinoos Harbor of ancient Kerkyra, Greece, and reconstructing its paleotsunami history. Geoarchaeology 33 (1), 24-42.
- Fischer, P., Finkler, C., Röbke, B.R., Baika, K., Hadler, H., Willershäuser, T., Rigakou, D., Metallinou, G., Vött, A., 2016. Impact of Holocene tsunamis detected in lagoonal environments on Corfu (Ionian Islands, Greece): Geomorphological, sedimentary and microfaunal evidence. Quat. Int. 401, 4-16.
- Fonnesu, M., Haughton, P., Felletti, F., McCaffrey, W., 2015. Short length-scale variability of hybrid event beds and its applied significance. Mar. Pet. Geol. 67,
- Fonnesu, M., Felletti, F., Haughton, P.D.W., Patacci, M., McCaffrey, W.D., 2018. Hybrid event bed character and distribution linked to turbidite system sub-environments: The North Apennine Gottero Sandstone (north-west Italy). Sedimentology 65 (1), 151-190.
- Fritz, H.M., Borrero, J.C., Synolakis, C.E., Yoo, J., 2006. 2004 Indian Ocean tsunami flow velocity measurements from survivor videos. Geophys. Res. Lett. 33 (24), L24605.
- Fruergaard, M., Piasecki, S., Johannessen, P.N., Noe-Nygaard, N., Andersen, T.J., Pejrup, M., Nielsen, L.H., 2015. Tsunami propagation over a wide, shallow continental shelf caused by the Storegga slide, southeastern North Sea, Denmark. Geology 43 (12), 1047-1050.
- Fuentes, Z., Tuttle, M.P., Schmidt, W.E., 2017. Sand scripts of past tsunamis in coastal ponds of St. Thomas, U.S. Virgin Islands. Seismol. Res. Lett. 88 (6), 1516-1526.
- Garrison-Laney, C.E., 1998. Diatom Evidence for Tsunami Inundation from Lagoon Creek, a Coastal Freshwater Pond, Del Norte County, California. MSc thesis, Humboldt State University, California, p. 97.

- Ghionis, G., Poulos, S.E., Verykiou, E., Karditsa, A., Alexandrakis, G., Andris, P., 2015. The impact of an extreme storm event on the barrier beach of the Lefkada Lagoon, NE Ionian Sea (Greece). Mediterr. Mar. Sci. 16 (3), 562-572.
- Gianfreda, F., Mastronuzzi, G., Sansò, P., 2001. Impact of historical tsunamis on a sandy coastal barrier: an example from the northern Gargano coast, southern Italy. Nat. Hazards Earth Syst. Sci. 1, 213-219.
- Girardclos, S., Schmidt, O.T., Sturm, M., Ariztegui, D., Pugin, A., Anselmetti, F.S., 2007. The 1996 AD delta collapse and large turbidite in Lake Brienz. Mar. Geol. 241 (1-4),
- Gischler, E., Shinn, E.A., Oschmann, W., Fiebig, J., Buster, N.A., 2008. A 1500-year Holocene Caribbean climate archive from the Blue Hole, Lighthouse Reef, Belize. J. Coast. Res. 24 (6), 1495–1505.
- Gischler, E., Schmitt, D., Wiegand, A., Behling, H., Shumilovskikh, L., Melles, M., Wennrich, V., Nolte, E., Grego, J., Anselmetti, F.S., Vogel, H., Birgel, D., Peckmann, J., 2025. Late Pleistocene to Holocene sedimentation in the Great Blue Hole (Lighthouse Reef, Belize): Results from a 30 m long core. Depositional Rec.
- Goff, J.R., Rouse, H.L., Jones, S.L., Hayward, B.W., Cochran, U., McLea, W., Dickinson, W.W., Morley, M.S., 2000. Evidence for an earthquake and tsunami about 3100-3400 yr ago, and other catastrophic saltwater inundations recorded in a coastal lagoon, New Zealand. Mar. Geol. 170 (1-2), 231-249.
- Goff, J., McFadgen, B.G., Chagué-Goff, C., 2004. Sedimentary differences between the 2002 Easter storm and the 15th-century Okoropunga tsunami, southeastern North Island, New Zealand. Mar. Geol. 204 (1-2), 235-250.
- Goff, J.R., Lane, E., Arnold, J., 2009. The tsunami geomorphology of coastal dunes. Nat. Hazards Earth Syst. Sci. 9 (3), 847-854.
- Goslin, J., Clemmensen, L.B., 2017. Proxy records of Holocene storm events in coastal barrier systems: Storm-wave induced markers. Quat. Sci. Rev. 174, 80-119.
- Goto, K., et al., 2011. New insights of tsunami hazard from the 2011 Tohoku-oki event. Mar. Geol. 290 (1-4), 46-50.
- Grauert, M., Björck, S., Bondevik, S., 2001. Storegga tsunami deposits in a coastal lake on Suouroy, the Faroe Islands. Boreas 30 (4), 263–271.
- Gwiazda, R., et al., 2022. Near-bed structure of sediment gravity flows measured by motion-sensing "boulder-like" benthic event detectors (BEDs) in Monterey Canyon. J. Geophys. Res. Earth Surf. 127 (2) (e2021JF006437).
- Hadler, H., Vött, A., Koster, B., Mathes-Schmidt, M., Mattern, T., Ntageretzis, A.K., Reicherter, K., Willershäuser, T., 2013. Multiple late-Holocene tsunami landfall in the eastern Gulf of Corinth recorded in the palaeotsunami geo-archive at Lechaion, harbour of ancient Corinth (Peloponnese, Greece). Zeitschrift für Geomorphologie, Supplementary Issues. 57 (4), 139–180.
- Haffidason, H., Lien, R., Sejrup, H.P., Forsberg, C.F., Bryn, P., 2005. The dating and morphometry of the Storegga Slide. Mar. Pet. Geol. 22 (1–2), 123–136.
   Haughton, P.D.W., Barker, S.P., McCaffrey, W.D., 2003. 'Linked' debrites in sand-rich
- turbidite systems origin and significance. Sedimentology 50 (3), 459–482.
- Haughton, P., Davis, C., McCaffrey, W., Barker, S., 2009. Hybrid sediment gravity flow deposits - Classification, origin and significance. Mar. Pet. Geol. 26 (10), 1900-1918.
- Hayashi, S., Koshimura, S., 2013. The 2011 Tohoku tsunami flow velocity estimation by the aerial video analysis and numerical modeling. J. Disast. Res. 8 (4), 561-572.
- Hess K et al. 2024. A 1500-year record of North Atlantic storm flooding from lacustrine sediments, Shetland Islands (UK). J. Quat. Sci. 39 (1), 37-53.
- Hill, J., Rush, G., Peakall, J., Johnson, M., Hodson, L., Barlow, N.L.M., Bowman, E.T., Gehrels, W.R., Hodgson, D.M., Kesserwani, G., 2023. Resolving tsunami wave dynamics: Integrating sedimentology and numerical modelling. Depositional Rec. 9 (4) 1046-1065
- Hiscott, R.N., 1994. Loss of capacity, not competence, as the fundamental process governing deposition from turbidity currents. J. Sediment. Res. 64 (2a), 209-214.
- Hocking, E.P., Garrett, E., Aedo, D., Carvajal, M., Melnick, D., 2021. Geological evidence of an unreported historical Chilean tsunami reveals more frequent inundation. Commun. Earth Environ. 2 (1), 1-10. https://doi.org/10.1038/s43247-021-00319-z.
- Hudock, J.W., Flaig, P.P., Wood, L.J., 2014. Washover Fans: A modern geomorphologic analysis and proposed classification scheme to improve reservoir models. J. Sediment. Res. 84 (10), 854-865.
- Hutchinson, I., Clague, J., 2017. Were they all giants? Perspectives on late Holocene plate-boundary earthquakes at the northern end of the Cascadia subduction zone. Quat. Sci. Rev. 169, 29-49.
- Hutchinson, I., Guilbault, J.P., Clague, J.J., Bobrowsky, P.T., 2000. Tsunamis and tectonic deformation at the northern Cascadia margin: a 3000-year record from Deserted Lake, Vancouver Island, British Columbia, Canada. The Holocene 10 (4), 429\_439
- IPCC, 2019. Summary for policymakers. In: IPCC Special Report on the Ocean and Cryosphere in a Changing Climate, pp. 3-35.
- Jackson, K.L., Eberli, G.P., Amelung, F., McFadden, M.A., Moore, A.L., Rankey, E.C., Jayasena, H.A.H., 2014. Holocene Indian Ocean tsunami history in Sri Lanka. Geology 42 (10), 859-862.
- Jaffe, B.E., Gelfenbuam, G., 2007. A simple model for calculating tsunami flow speed from tsunami deposits. Sediment. Geol. 200 (3-4), 347-361.
- Jaffe, B., Goto, K., Sugawara, D., Gelfenbaum, G., La Selle, S.P., 2016. Uncertainty in tsunami sediment transport modeling. J. Disast. Res. 11 (4), 647–661.
- Kane, I.A., Pontén, A.S.M., Vangdal, B., Eggenhuisen, J.T., Hodgson, D.M., Spychala, Y. T., 2017. The stratigraphic record and processes of turbidity current transformation across deep-marine lobes. Sedimentology 64 (5), 1236-1273.
- Kelsey, H.M., Nelson, A.R., Hemphill-Haley, E., Witter, R.C., 2005. Tsunami history of an Oregon coastal lake reveals a 4600 yr record of great earthquakes on the Cascadia subduction zone. GSA Bull. 117 (7-8), 1009-1032.

- Kempf, P., Moernaut, J., Van Daele, M., Vermassen, F., Vandoorne, W., Pino, M., Urrutía, R., Schmidt, S., Garrett, E., De Batist, M., 2015. The sedimentary record of the 1960 tsunami in two coastal lakes on Isla de Chiloé, south central Chile. Sediment. Geol. 328, 73–86.
- Kempf, P., Moernaut, J., Van Daele, M., Vandoorne, W., Pino, M., Urrutia, R., De Batist, M., 2017. Coastal lake sediments reveal 5500 years of tsunami history in south central Chile. Ouat. Sci. Rev. 161. 99–116.
- Kempf, P., Moernaut, J., Van Daele, M., Pino, M., Urrutia, R., De Batist, M., 2020. Paleotsunami record of the past 4300 years in the complex coastal lake system of Lake Cucao, Chiloé Island, south central Chile. Sediment. Geol. 401, 105644.
- King, D.N., et al., 2023. Tsunami or storm deposit? A late Holocene sedimentary record from Swamp Bay, Rangitoto ki te Tonga/D'Urville Island, Aotearoa – New Zealand. N. Z. J. Geol. Geophys. 66 (4), 629–645.
- Kohila, B.S., Dezileau, L., Boussetta, S., Melki, T., Kallel, N., 2021. Review article: Extreme marine events revealed by lagoonal sedimentary records in Ghar El Melh during the last 2500 years in the northeast of Tunisia. Nat. Hazards Earth Syst. Sci. 21 (12), 3645–3661.
- Koiwa, N., Kasai, M., Kataoka, S., Isono, T., 2014. Examination of relation with tsunami behavior reconstructed from on-site sequence photographs, topography, and sedimentary deposits from the 2011 Tohoku-oki tsunami on the Kamikita Plain, Japan. Mar. Geol. 358, 107–119.
- Komatsubara, J., Fujiwara, O., Takada, K., Sawai, Y., Aung, T.T., Kamataki, T., 2008. Historical tsunamis and storms recorded in a coastal lowland, Shizuoka Prefecture, along the Pacific Coast of Japan. Sedimentology 55 (6), 1703–1716.
- Konsoer, K., Zinger, J., Parker, G., 2013. Bankfull hydraulic geometry of submarine channels created by turbidity currents: Relations between bankfull channel characteristics and formative flow discharge. J. Geophys. Res. Earth Surf. 118, 216–228.
- Korsgaard, N.J., Svennevig, K., Søndergaard, A.S., Luetzenburg, G., Oksman, M., Larsen, N.K., 2024. Evidence of Middle Holocene landslide-generated tsunamis recorded in lake sediments from Saqqaq, West Greenland. Nat. Hazards Earth Syst. Sci. 24 (3), 757–772.
- Kortekaas, S., Dawson, A.G., 2007. Distinguishing tsunami and storm deposits: An example from Martinhal, SW Portugal. Sediment. Geol. 200 (3-4), 208-221.
- Koster, B., Vött, A., Mathes-Schmidt, M., Reicherter, K., 2015. Geoscientific investigations in search of tsunami deposits in the environs of the Agoulinitsa peatland, Kaiafas Lagoon and Kakovatos (Gulf of Kyparissia, western Peloponnese, Greece). Zeitschrift für Geomorphologie 59 (4), 125–156.
- Kremer, K., Hilbe, M., Simpson, G., Decrouy, L., Wildi, W., Girardclos, S., 2015.
  Reconstructing 4000 years of mass movement and tsunami history in a deep periAlpine lake (Lake Geneva, France-Switzerland). Sedimentology 62, 1305–1327.
- Kremer, K., Anselmetti, F.S., Evers, F.M., Goff, J., Nigg, V., 2021. Freshwater (paleo) tsunamis a review. Earth Sci. Rev. 212, 103447.
- Kuiry, S.N., Ding, Y., Wang, S.S.Y., 2014. Numerical simulations of morphological changes in barrier islands induced by storm surges and waves using a supercritical flow model. Front. Struct. Civ. Eng. 8 (1), 57–68.
- La Selle, S.M., Lunghino, B.D., Jaffe, B.E., Gelfenbaum, G., Costa, P.J.M., 2017.
  Hurricane Sandy Washover Deposits on Fire Island, New York. U.S. Geological Survey
  Open-File Report 2017-1014.
- Lane, P., Donnelly, J.P., Woodruff, J.D., Hawkes, A.D., 2011. A decadally-resolved paleohurricane record archived in the late Holocene sediments of a Florida sinkhole. Mar. Geol. 287 (1–4), 14–30.
- Łapcik, P., Baas, J.H., 2024. Integrating transitional-flow signatures into hybrid event beds: implications for hybrid-flow evolution on a submarine lobe fringe. J. Sediment. Res. 94 (6) 799–821
- Lawrence, T., 2016. Reconstructing Abrupt, High-Magnitude Sea-Level Changes from Near-Field Coastal Environments - Durham e-Theses. *Doctoral thesis, Durham University*. [Online] [Accessed 9 December 2024]. Available from: https://etheses.dur.ac.uk/11655/.
- Leal, K., Scremin, L., Audemard, F., Carrillo, E., 2014. Paleotsunamis en el Geologico de Cumana, estado sucre, Venezuela oriental. Boletín de Geología. 36 (2), 45–70.
- León, T., Lau, A.Y.A., Easton, G., Goff, J., 2023. A comprehensive review of tsunami and palaeotsunami research in Chile. Earth Sci. Rev. 236, 104273.
- Liu, K., Fearn, M.L., 1993. Lake-sediment record of late Holocene hurricane activities from coastal Alabama. Geology 21 (9), 793–800.
- Liu, K.B., Fearn, M.L., 2000. Reconstruction of prehistoric landfall frequencies of catastrophic hurricanes in northwestern Florida from lake sediment records. Quat. Res. 54 (2), 238–245.
- Liu, K.-B., Lu, H., Shen, C., 2008. A 1200-year proxy record of hurricanes and fires from the Gulf of Mexico coast: Testing the hypothesis of hurricane–fire interactions. Quat. Res. 69 (1), 29–41.
- Liu, K.-B., Li, C., Bianchette, T.A., Mccloskey, T.A., Yao, Q., Weeks, E., 2011. Storm deposition in a coastal backbarrier lake in Louisiana caused by Hurricanes Gustav. J. Coast. Res. 64, 1866–1870.
- López, G.I., 2012. Evidence for mid- to late-Holocene palaeotsunami deposits, Kakawis Lake, Vancouver Island, British Columbia. Nat. Hazards 60 (1), 43–68.
- Macabuag, J., Rossetto, T., Ioannou, I., Eames, I., 2018. Investigation of the effect of debris-induced damage for constructing tsunami fragility curves for buildings. Geosciences 8 (4), 117–132.
- Majumdar, D., Bhattacharya, H.N., 2025. Event beds in Andaman beach sediments records of 2004 Tsunami. Mar. Geol. 480, 107470.
- Malaizé, B., 2012. Hurricanes and climate in the Caribbean during the past 3700 years B. P. Quat. Int. 279–280, 302.
- Marras, S., Mandli, K.T., 2020. Modeling and simulation of tsunami impact: a short review of recent advances and future challenges. Geosciences 11 (1), 5–23.

- Martin, T., Muller, J., 2021. The geologic record of Hurricane Irma in a Southwest Florida back-barrier lagoon. Mar. Geol. 441, 106635.
- Masselink, G., Van Heteren, S., 2014. Response of wave-dominated and mixed-energy barriers to storms. Mar. Geol. 352, 321–347.
- Mastronuzzi, G., Sansò, P., 2012. The role of strong earthquakes and tsunami in the Late Holocene evolution of the Fortore River coastal plain (Apulia, Italy): A synthesis. Geomorphology 138 (1), 89–99.
- Matsumoto, D., Shimamoto, T., Hirose, T., Gunatilake, J., Wickramasooriya, A.,
   DeLile, J., Young, S., Rathnayake, C., Ranasooriya, J., Murayama, M., 2010.
   Thickness and grain-size distribution of the 2004 Indian Ocean tsunami deposits in Periya Kalapuwa Lagoon, eastern Sri Lanka. Sediment. Geol. 230 (3–4), 95–104.
- Mattheus, C.R., Fowler, J.K., 2015. Paleotempestite distribution across an isolated carbonate platform, San Salvador Island, Bahamas. J. Coast. Res. 31 (4), 842–858.
- May, S.M., Vött, A., Brückner, H., Grapmayer, R., Handl, M., Wennrich, V., 2012a. The Lefkada barrier and beachrock system (NW Greece) — Controls on coastal evolution and the significance of extreme wave events. Geomorphology 139–140, 330–347.
- May, S.M., Vött, A., Brückner, H., Smedile, A., 2012b. The Gyra washover fan in the Lefkada Lagoon, NW Greece Possible evidence of the 365 AD Crete earthquake and tsunami. Earth Planets Space 64 (10), 859–874.
- McCloskey, T.A., Liu, K.-B., 2013. A 7000 year record of paleohurricane activity from a coastal wetland in Belize. Holocene 23 (2), 278–291.
- Middleton, G.V., Hampton, M.A., 1973. Sediment gravity flows: mechanics of flow and deposition. In: Middleton, G.V., Bouma, A.H. (Eds.), Turbidites and Deep-water Sedimentation. SEPM Pacific Section short course, pp. 1–38.
- Minoura, K., Nakaya, S., 1991. Traces of tsunami preserved in inter-tidal lacustrine and marsh deposits: Some examples from northeast Japan. J. Geol. 99 (2), 265–287.
- Minoura, K., Nakaya, S., Uchida, M., 1994. Tsunami deposits in a lacustrine sequence of the Sanriku coast, northeast Japan. Sediment. Geol. 89 (1–2), 25–31.
- Misra, P., Tandon, S.K., Sinha, R., 2019. Holocene climate records from lake sediments in India: Assessment of coherence across climate zones. Earth Sci. Rev. 190, 370–397.
- Montaggioni, L.F., Salvat, B., Pons-Branchu, E., Dapoigny, A., Martin-Garin, B., Poli, G., Zanini, J.M., Wan, R., 2023. Mid-late Holocene accretional history of low-lying, coral reef rim islets, South Marutea Atoll, Tuamotu, south central Pacific: the key role of marine hazard events. Nat. Hazards Res. 3, 219–239.
- Moore, A., Goff, J., McAdoo, B.G., Fritz, H.M., Gusman, A., Kalligeris, N., Kalsum, K., Susanto, A., Suteja, D., Synolakis, C.E., 2011. Sedimentary deposits from the 17 July 2006 western Java tsunami, Indonesia: use of grain size analyses to assess tsunami flow depth, speed, and traction carpet characteristics. Pure Appl. Geophys. 168 (11), 1951–1961.
- Moreira, S., Costa, P.J.M., Andrade, C., Ponte Lira, C., Freitas, M.C., Oliveira, M.A., Reichart, G.J., 2017. High resolution geochemical and grain-size analysis of the AD 1755 tsunami deposit: Insights into the inland extent and inundation phases. Mar. Geol. 390, 94–105.
- Mörner, N.-A., Ambrosiani, B., Ambrosiani, P.A., 2020. A mega-tsunami in the Baltic Sea 1171 BC: Geological records with special reference to the Lake Malaren area in Sweden. Int. J. Geosci. 11 (10), 667–707.
- Morton, R.A., Sallenger, A.H., 2003. Morphological impacts of extreme storms on sandy beaches and barriers. J. Coast. Res. 19 (3), 560–573.
- Morton, R.A., Richmond, B.M., Jaffe, B.E., Gelfenbaum, G., 2006. Reconnaissance investigation of Caribbean extreme wave deposits – preliminary observations, interpretations, and research directions. In: USGS Open-File Report 2006-1293, pp. 1–46.
- Morton, R.A., Gelfenbaum, G., Jaffe, B.E., 2007. Physical criteria for distinguishing sandy tsunami and storm deposits using modern examples. Sediment. Geol. 200 (3–4), 184–207
- Mountjoy, J.J., Wang, X., Woelz, S., Fitzsimons, S., Howarth, J.D., Orpin, A.R., Power, W., 2019. Tsunami hazard from lacustrine mass wasting in Lake Tekapo, New Zealand. Geol. Soc. Lond., Spec. Publ. 477 (1), 413–426.
- Mulder, T., Alexander, J., 2001. The physical character of subaqueous sedimentary density flows and their deposits. Sedimentology 48 (2), 269–299.
- Nanayama, F., Shigeno, K., Satake, K., Shimokawa, K., Koitabashi, S., Miyasaka, S., Ishii, M., 2000. Sedimentary differences between the 1993 Hokkaido-nansei-oki tsunami and the 1959 Miyakojima typhoon at Taisei, southwestern Hokkaido, northern Japan. Sediment. Geol. 135 (1–4), 255–264.
- Naruse, H., Abe, T., 2017. Inverse tsunami flow modeling including nonequilibrium sediment transport, with application to deposits from the 2011 Tohoku-Oki tsunami. J. Geophys. Res. Earth Surf. 122 (11), 2159–2182.
- NCEI, 2024. NCEI/WDS Global Historical Tsunami Database. NOAA National Centres for Environmental Information. [Online] [Accessed 29 January 2024]. Available from: https://doi.org/10.7289/V5PN93H7.
- Nichol, S.L., Goff, J.R., Devoy, R.J.N., Chagué-Goff, C., Hayward, B., James, I., 2007. Lagoon subsidence and tsunami on the West Coast of New Zealand. Sediment. Geol. 200 (3–4), 248–262.
- Obrocki, L., Vött, A., Wilken, D., Fischer, P., Willershäuser, T., Koster, B., Lang, F., Papanikolaou, I., Rabbel, W., Reicherter, K., 2020. Tracing tsunami signatures of the AD 551 and AD 1303 tsunamis at the Gulf of Kyparissia (Peloponnese, Greece) using direct push in situ sensing techniques combined with geophysical studies. Sedimentology 67 (3), 1274–1308.
- Oliva, F., Peros, M.C., Viau, A.E., Reinhardt, E.G., Nixon, F.C., Morin, A., 2018a. A multiproxy reconstruction of tropical cyclone variability during the past 800 years from Robinson Lake, Nova Scotia, Canada. Mar. Geol. 406, 84–97.
- Oliva, F., Viau, A.E., Peros, M.C., Bouchard, M., 2018b. Paleotempestology database for the western North Atlantic basin. The Holocene 28 (10), 1664–1671.
- Oppenheimer, M., Glavovic, B.C., Hinkel, J., van de Wal, R., Magnan, A.K., Abd-Elgawad, A., Cai, R., Cifuentes-Jara, R.M., DeConto, R.M., Ghosh, T., Hay, J., Isla, F., Marzeion, B., Meyssignac, B., Sebesvari, Z., 2019. Sea Level Rise and Implications for

- Low-lying Islands, Coasts and Communities. In: IPCC Special Report on the Ocean and Cryosphere in a Changing Climate. Cambridge University Press, Cambridge, UK and New York, NY, USA., pp. 321–445
- Oropeza, J., Audemard, F., Beck, C., Vallée, M., 2015. New potential sedimentary evidences of paleotsunamis on coastal lagoons of Chacopata, State of Sucre, Venezuela. Int. J. Literary Stud. 27, 329–331.
- Palmer, S.E., Burn, M.J., Holmes, J., 2020. A multiproxy analysis of extreme wave deposits in a tropical coastal lagoon in Jamaica, West Indies. Nat. Hazards 104 (3), 2531–2560.
- Paris, R., Sabatier, P., Biguenet, M., Bougouin, A., André, G., Roger, J., 2021. A tsunami deposit at Anse Meunier, Martinique Island: evidence of the 1755 CE Lisbon tsunami and implication for hazard assessment. Mar. Geol. 439, 106561.
- Paull, C.K., et al., 2018. Powerful turbidity currents driven by dense basal layers. Nat. Commun. 9 (4114), 1–9. https://doi.org/10.1038/s41467-018-06254-6.
- Peakall, J., Best, J., Baas, J.H., Hodgson, D.M., Clare, M.A., Talling, P.J., Dorrell, R.M., Lee, D.R., 2020. An integrated process-based model of flutes and tool marks in deepwater environments: Implications for palaeohydraulics, the Bouma sequence and hybrid event beds. Sedimentology 67 (4), 1601–1666.
- Peakall, J., Best, J., Baas, J.H., Wignall, P.B., Hodgson, D.M., Łapcik, P., 2024. Flow-induced Interfacial Deformation Structures (FIDS): Implications for the interpretation of palaeocurrents, flow dynamics and substrate rheology. Sedimentology 71, 1709–1743.
- Peros, M., Gregory, B., Matos, F., Reinhardt, E., Desloges, J., 2015. Late-Holocene record of lagoon evolution, climate change, and hurricane activity from southeastern Cuba. Holocene 25 (9), 1483–1497.
- Peters, R., Jaffe, B., 2010. Identification of Tsunami Deposits in the Geologic Record: Developing Criteria Using Recent Tsunami Deposits. U.S. Geological Survey Open-File Report 2010-1239, pp. 1–39.
- Pilarczyk, J.E., Reinhardt, E.G., 2012. Testing foraminiferal taphonomy as a tsunami indicator in a shallow arid system lagoon: Sur, Sultanate of Oman. Mar. Geol. 295–298, 128–136.
- Pilarczyk, J.E., Dura, T., Horton, B.P., Engelhart, S.E., Kemp, A.C., Sawai, Y., 2014. Microfossils from coastal environments as indicators of paleo-earthquakes, tsunamis and storms. Palaeogeogr. Palaeoclimatol. Palaeoecol. 413, 144–157.
- Pilarczyk, J.E., Sawai, Y., Matsumoto, D., Namegaya, Y., Nishida, N., Ikehara, K., Fujiwara, O., Gouramanis, C., Dura, T., Horton, B.P., 2020. Constraining sediment provenance for tsunami deposits using distributions of grain size and foraminifera from the Kujukuri coastline and shelf, Japan. Sedimentology 67, 1373–1392.
- Pinegina, T.K., Bazanova, L.I., Zelenin, E.A., Bourgeois, J., Kozhurin, A.I., Medvedev, I. P., Vydrin, D.S., 2018. Holocene tsunamis in Avachinsky Bay, Kamchatka, Russia. Pure Appl. Geophys. 175 (4), 1485–1506.
- Pizer, C., Clark, K., Howarth, J., Garrett, E., Wang, X., Rhoades, D., Woodroffe, S., 2021.

  Paleotsunamis on the Southern Hikurangi subduction zone. Seismic Record 1, 75–84.
- Pleskot, K., Cwynar, L.C., Kowalczyk, C., Kokociński, M., Szczuciński, W., 2023. Refining the history of extreme coastal events in southern Newfoundland, NW Atlantic, with lake sediment archives. Ouat. Sci. Rev. 322, 108401.
- Pope, E.L., et al., 2022. First source-to-sink monitoring shows dense head controls sediment flux and runout in turbidity currents. Sci. Adv. 8 (20), eabj3220.
- Privat, A.M.-L.J., Peakall, J., Hodgson, D.M., Schwarz, E., Jackson, C.A.L., Arnol, J.A., 2024. Evolving fill-and-spill patterns across linked early post-rift depocentres control lobe characteristics: Los Molles Formation, Argentina. Sedimentology 71 (5), 1639–1685.
- Prizomwala, S.P., Gandhi, D., Bhatt, N., Winkler, W., Kumar, M.R., Makwana, N., Bhatt, N., 2018. Geological evidence for AD 1008 tsunami along the Kachchh coast, Western India: Implications for hazard along the Makran Subduction Zone. Sci. Rep. 8 (1), 1–8 article 16816.
- Punyawardena, B.V.R., 2009. Climate of Sri Lanka. In: Proceedings of the First National Conference on Global Climate Change and its Impacts on Agriculture, Forestry and Water in the Tropics, pp. 7–20.
- Qi, H.S., Chen, M., Shen, L.N., Cai, F., Zhang, A.M., Fang, Q., 2021. Sedimentological and microfossil records of modern typhoons in a coastal sandy lagoon off southern China coast. J. Palaeogeogr. 10 (4), 529–549.
- Qi, H., Chen, M., Cai, F., Shen, L., Li, J., 2024. Characteristics of storm deposits in Wangcun Lagoon on the southern China coast during Typhoon Rammasun. Mar. Geol. 469, 107244.
- Raji, O., Dezileau, L., Von Grafenstein, U., Niazi, S., Snoussi, M., Martinez, P., 2015. Extreme sea events during the last millennium in the northeast of Morocco. *Hazards Earth Syst. Sci.* 15, 203–211.
- Ramírez-Herrera, M.T., Coca, O., 2024. A global database of tsunami deposits. Geosci. Data J. 11 (4), 974–994.
- Ranasinghage, P.N., Ortiz, J.D., Moore, A.L., Siriwardana, C., McAdoo, B.G., 2010. Signatures of paleo-coastal hazards in back-barrier environments of eastern and southeastern Sri Lanka. AGUFM 2010 (3) pp.NH21A-1397.
- Rasmussen, H., Bondevik, S., Corner, G.D., 2018. Holocene relative sea level history and Storegga tsunami run-up in Lyngen, northern Norway. J. Quat. Sci. 33 (4), 393–408.
- Reicherter, K., Becker-Heidmann, P., 2009. Tsunami deposits in the western Mediterranean: Remains of the 1522 Almería earthquake? In: Reicherter, K., Michetti, A.M., Silva, P.G. (Eds.), Palaeoseismology: Historical and Prehistorical Records of Earthquake Ground Effects for Seismic Hazard Assessment, 316. Geological Society Special Publication, pp. 217–235.
- Reinhardt, E.G., Pilarczyk, J., Brown, A., 2012. Probable tsunami origin for a Shell and Sand Sheet from marine ponds on Anegada, British Virgin Islands. Nat. Hazards 63 (1), 101–117.
- Richmond, B., et al., 2012. Erosion, deposition and landscape change on the Sendai coastal plain, Japan, resulting from the March 11, 2011 Tohoku-oki tsunami. Sediment. Geol. 282, 27–39.

- Riou, B., Chaumillon, E., Schneider, J.L., Corrège, T., Chagué, C., 2020. The sediment-fill of Pago Pago Bay (Tutuila Island, American Samoa): New insights on the sediment record of past tsunamis. Sedimentology 67 (3), 1577–1600.
- Röbke, B.R., Vött, A., 2017. The tsunami phenomenon. Prog. Oceanogr. 159, 296–322.
   Rodysill, J.R., et al., 2020. Historically Unprecedented Northern Gulf of Mexico
   Hurricane Activity from 650 to 1250 CE. Sci. Rep. 10 (1), 1–17.
- Roeber, V., Bricker, J.D., 2015. Destructive tsunami-like wave generated by surf beat over a coral reef during Typhoon Haiyan. Nat. Commun. 6 (1), 1–9 article 7854.
- Roger, J., Baptista, M.A., Sahal, A., Accary, F., Allgeyer, S., Hébert, H., 2011. The transoceanic 1755 Lisbon Tsunami in Martinique. Pure Appl. Geophys. 168 (6–7), 1015–1031.
- Romundset, A., Bondevik, S., 2011. Propagation of the Storegga tsunami into ice-free lakes along the southern shores of the Barents Sea. J. Quat. Sci. 26 (5), 457–462.
- Rydgren, K., Bondevik, S., 2015. Moss growth patterns and timing of human exposure to a Mesolithic tsunami in the North Atlantic. Geology 43 (2), 111–114.
- Sabatier, P., Dezileau, L., Condomines, M., Briqueu, L., Colin, C., Bouchette, F., Le Duff, M., Blanchemanche, P., 2008. Reconstruction of paleostorm events in a coastal lagoon (Hérault, South of France). Mar. Geol. 251 (3–4), 224–232.
- Sabatier, P., Dezileau, L., Colin, C., Briqueu, L., Bouchette, F., Martinez, P., Siani, G., Raynal, O., Von Grafenstein, U., 2012. 7000 years of paleostorm activity in the NW Mediterranean Sea in response to Holocene climate events. Quat. Res. 77 (1), 1–11.
- Sabatier, P., Moernaut, J., Bertrand, S., Van Daele, M., Kremer, K., Chaumillon, E., Arnaud, F., 2022. A review of event deposits in lake sediments. Quaternary 5 (3), 34.
- Sallenger, A.H., 2000. Storm impact scale for barrier islands. J. Coast. Res. 16 (3), 890–895.
- Satake, K., Heidarzadeh, M., Quiroz, M., Cienfuegos, R., 2020. History and features of trans-oceanic tsunamis and implications for paleo-tsunami studies. Earth Sci. Rev. 202, 103112
- Sawai, Y., Fujii, Y., Fujiwara, O., Kamataki, T., Komatsubara, J., Okamura, Y., Satake, K., Shishikura, M., 2008. Marine incursions of the past 1500 years and evidence of tsunamis at Suijin-numa, a coastal lake facing the Japan Trench. The Holocene 18 (4), 517–528.
- Schmitt, D., Gischler, E., Anselmetti, F.S., Vogel, H., 2020. Caribbean cyclone activity: an annually-resolved Common Era record. Sci. Rep. 10 (1), 1–17 article 11780.
- Schmitt, D., Gischler, E., Melles, M., Wennrich, V., Behling, H., Shumilovskikh, L., Anselmetti, F.S., Vogel, H., Peckmann, J., Birgel, D., 2025. An annually resolved 5700-year storm archive reveals drivers of Caribbean cyclone frequency. Sci. Adv. 11. eads5624.
- Schwartz, R.K., 1982. Bedform and stratification characteristics of some modern small-scale washover sand bodies. Sedimentology 29 (6), 835–849.
- Shanmugam, G., 2011. Process-sedimentological challenges in distinguishing paleotsunami deposits. Nat. Hazards 63 (1), 5–30.
- Shimada, Y., Sawai, Y., Matsumoto, D., Tanigawa, K., Ito, K., Tamura, T., Namegaya, Y., Shishikura, M., Fujino, S., 2023. Marine inundation history during the last 3000 years at Lake Kogare-ike, a coastal lake on the Pacific coast of central Japan. Progr. Earth Planet. Sci. 10 (1), 1–28.
- Shinozaki, T., Goto, K., Fujino, S., Sugawara, D., Chiba, T., 2015. Erosion of a paleotsunami record by the 2011 Tohoku-oki tsunami along the southern Sendai Plain. Mar. Geol. 369, 127–136.
- Shinozaki, T., Yamaguchi, N., Sekiguchi, T., 2020. Flume experiments test grain-size distribution of onshore tsunami deposits. Sediment. Geol. 407, 105750.
- Simmons, S.M., Azpiroz-Zabala, M., Cartigny, M.J.B., Clare, M.A., Cooper, C., Parsons, D. R., Pope, E.L., Sumner, E.J., Talling, P.J., 2020. Novel acoustic method provides first detailed measurements of sediment concentration structure within submarine turbidity currents. J. Geophys. Res. Oceans 125 (e2019)C0159041.
- Siwek, P., Waskowska, A., Wendorff, M., 2023. Mud-rich low-density turbidites in structurally-controlled intraslope mini-basin: The influence of flow containment on depositional processes and sedimentation patterns (Szczawa, Oligocene, Polish Outer Carpathians). Sedimentology 70 (6), 1741–1784.
- Smit, J., Roep, B., Alvarez, W., Montanari, A., Claeys, P., Grajales-Nishimura, J.M., Bermudez, J., 1996. Coarse-grained, clastic sandstone complex at the K/T boundary around the Gulf of Mexico: Deposition by tsunami waves induced by the Chicxulub impact. Geol. Soc. Am. Spec. Pap. 307, 151–182.
- Smith, D.E., Shi, S., Cullingford, R.A., Dawson, A.G., Dawson, S., Firth, C.R., Foster, I.D. L., Fretwell, P.T., Haggart, B.A., Holloway, L.K., Long, D., 2004. The Holocene Storegga Slide tsunami in the United Kingdom. Quat. Sci. Rev. 23 (23–24), 2291–2321.
- Soria, J.L.A., et al., 2018. Surf beat-induced overwash during Typhoon Haiyan deposited two distinct sediment assemblages on the carbonate coast of Hernani, Samar, central Philippines. Mar. Geol. 396, 215–230.
- Spence, R., Palmer, J., Petal, M., Kelman, I., Saito, K., 2007. Analysing eyewitness reports of the 2004 Asian tsunami. Proceed. Inst. Civil Engin. 160 (2), 75–85.
- Spiske, M., Tang, H., Bahlburg, H., 2020. Post-depositional alteration of onshore tsunami deposits – Implications for the reconstruction of past events. Earth Sci. Rev. 202, 103068.
- Steidtmann, J.R., 1982. Size-density sorting of sand-size spheres during deposition from bedload transport and implications concerning hydraulic equivalence. Sedimentology 29 (6), 877–883.
- Stevenson, C.J., Peakall, J., Hodgson, D.M., Bell, D., Privat, A., 2020.  $T_B$  or not  $T_B$ : banding in turbidite sandstones. J. Sediment. Res. 90 (8), 821–842.
- Sullivan, T., Broszeit, S., O'Sullivan, K.P.A., McAllen, R., Davenport, J., Regan, F., 2013. High resolution monitoring of episodic stratification events in an enclosed marine system. Estuar. Coast. Shelf Sci. 123, 26–33.
- Svennevig, K., et al., 2024. A rockslide-generated tsunami in a Greenland fjord rang Earth for 9 days. Science 385, 1196–1205.

- Switzer, A.D., Jones, B.G., 2008. Large-scale washover sedimentation in a freshwater lagoon from the southeast Australian coast: sea-level change, tsunami or exceptionally large storm? The Holocene 18 (5), 787–803.
- Szczuciński, W., Kokociński, M., Rzeszewski, M., Chagué-Goff, C., Cachão, M., Goto, K., Sugawara, D., 2012. Sediment sources and sedimentation processes of 2011 Tohokuoki tsunami deposits on the Sendai Plain, Japan — Insights from diatoms, nannoliths and grain size distribution. Sediment. Geol. 282, 40–56.
- Takashimizu, Y., Urabe, A., Suzuki, K., Sato, Y., 2012. Deposition by the 2011 Tohokuoki tsunami on coastal lowland controlled by beach ridges near Sendai, Japan. Sediment. Geol. 282. 124–141.
- Talling, P.J., Amy, L.A., Wynn, R.B., Peakall, J., Robinson, M., 2004. Beds comprising debrite sandwiched within co-genetic turbidite: origin and widespread occurrence in distal depositional environments. Sedimentology 51 (1), 163–194.
- Talling, P.J., Amy, L.A., Wynn, R.B., 2007. New insights into the evolution of large volume turbidity currents; comparison of turbidite shape and previous modelling results. Sedimentology 54, 737–769.
- Talling, P.J., Masson, D.G., Sumner, E.J., Malgesini, G., 2012. Subaqueous sediment density flows: Depositional processes and deposit types. Sedimentology 59 (7), 1937–2003.
- Tanigawa, K., Shishikura, M., Fujiwara, O., Namegaya, Y., Matsumoto, D., 2018. Mid- to late-Holocene marine inundations inferred from coastal deposits facing the Nankai Trough in Nankoku, Kochi Prefecture, southern Japan. Holocene 28 (6), 867–878.
- Thouret, J.C., Antoine, S., Magill, C., Ollier, C., 2020. Lahars and debris flows: Characteristics and impacts. Earth Sci. Rev. 201, 103003.
- Toomey, M.R., Donnelly, J.P., Woodruff, J.D., 2013. Reconstructing mid-late Holocene cyclone variability in the Central Pacific using sedimentary records from Tahaa, French Polynesia. Quat. Sci. Rev. 77, 181–189.
- Tuttle, M., Fuentes, Z., 2021. Learning from hurricane Irma, differentiating tsunami from hurricane deposits and reevaluating possible tsunami deposits on St Thomas, US Virgin Islands. In: Final Technical Report to US Geological Survey, EHP Award No. G19AP00101, pp. 1–59.
- Tuttle, M.P., Ruffman, A., Anderson, T., Jeter, H., 2004. Distinguishing tsunami from storm deposits in eastern North America: The 1929 Grand Banks tsunami versus the 1991 Halloween Storm. Seismol. Res. Lett. 75 (1), 117–131.
- Vallance, J.W., Iverson, R.M., 2015. Chapter 37 Lahars and their deposits. In: Sigurdsson, H. (Ed.), The encyclopedia of volcanoes, Second edition. Academic Press, Amsterdam, pp. 649–664.
- Van Daele, M., Haeussler, P.J., Witter, R.C., Praet, N., De Batist, M., 2020. The Sedimentary record of the 2018 Anchorage earthquake in Eklutna Lake, Alaska: Calibrating the lacustrine seismograph. Seismol. Res. Lett. 91 (1), 126–141.
- Van Hengstum, P.J., Donnelly, J.P., Fall, P.L., Toomey, M.R., Albury, N.A., Kakuk, B., 2016. The intertropical convergence zone modulates intense hurricane strikes on the western North Atlantic margin. Sci. Rep. 6, 21728.
- Vasskog, K., Waldmann, N., Bondevik, S., Nesje, A., Chapron, E., Ariztegui, D., 2013. Evidence for Storegga tsunami run-up at the head of Nordfjord, western Norway. J. Onat. Sci. 28 (4), 391–402.
- Vött, A., Hadler, H., Willershäuser, T., Ntageretzis, K., Brückner, H., Warnecke, H., Grootes, P.M., Lang, F., Nelle, O., Sakellariou, D., 2014. Ancient harbours used as tsunami sediment traps-the case study of Krane (Cefalonia Island, Greece). BYZAS 19, 743–771
- Wallace, D.J., Anderson, J.B., 2010. Evidence of similar probablility of intense hurricane strikes for the Gulf of Mexico over the late Holocene. Geology 38 (6), 511–514.

- Wallace, E.J., Donnelly, J.P., van Hengstum, P.J., Wiman, C., Sullivan, R.M., Winkler, T. S., d'Entremont, N.E., Toomey, M., Albury, N., 2019. Intense hurricane activity over the past 1500 years at South Andros Island, The Bahamas. Paleoceanogr. Paleoclimatol. 34 (11), 1761–1783.
- Wallace, E., et al., 2021a. Regional shifts in paleohurricane activity over the last 1500 years derived from blue hole sediments offshore of Middle Caicos Island. Quat. Sci. Rev. 268, 107126.
- Wallace, E.J., et al., 2021b. 1,050 years of Hurricane Strikes on Long Island in The Bahamas. Paleoceanogr. Paleoclimatol. 36 (3) (e2020PA004156).
- Wang, Y., Van Beynen, P., Wang, P., Brooks, G., Herbert, G., Tykot, R., 2021. Investigation of sedimentary records of Hurricane Irma in sinkholes, Big Pine Key, Florida. Progr. Phys. Geogr. 45 (6), 885–906.
- Watanabe, M., Bricker, J.D., Goto, K., Imamura, F., 2017. Factors responsible for the limited inland extent of sand deposits on Leyte Island during 2013 Typhoon Haiyan. JGR Oceans 122, 2795–2812.
- Wei, Y., ten Brink, U.S., Atwater, B.F., 2024. Modeled flooding by tsunamis and a storm versus observed extent of coral erratics on Anegada, British Virgin Islands—Further evidence for a great Caribbean earthquake six centuries ago. J. Geophys. Res. Solid Earth 129 (3), e2023JB028387.
- Wells, E.C., Pratt, S.M., Fox, G.L., Siegel, P.E., Dunning, N.P., Murphy, A.R., 2017.Plantation soilscapes: initial and cumulative impacts of colonial agriculture in Antigua, West Indies. Environ. Archaeol. 23 (1), 23–35.
- Wilson, R., et al., 2013. The Search for Geologic Evidence of Distant-Source Tsunamis Using New Field Data in California. The SAFRR (Science Application for Risk Reduction) tsunami scenario: U.S. Geological Survey Open-File Report 2013–1170–C 1–122. https://doi.org/10.3133/ofr20131170c.
- Winkler, T.S., van Hengstum, P.J., Donnelly, J.P., Wallace, E.J., Sullivan, R.M., MacDonald, D., Albury, N.A., 2020. Revising evidence of hurricane strikes on Abaco Island (The Bahamas) over the last 700 years. Sci. Rep. 10 (1), 1–17 article 16556.
- Woodroffe, S.A., Hill, J., Bustamante-Fernandez, E., Lloyd, J.M., Luff, J., Richards, S., Shennan, I., 2023. On the varied impact of the Storegga tsunami in northwest Scotland. J. Quat. Sci. 38 (8), 1219–1232.
- Woodruff, J.D., Donnelly, J.P., Mohrig, D., Geyer, W.R., 2008. Reconstructing relative flooding intensities responsible for hurricane-induced deposits from Laguna Playa Grande, Vieques, Puerto Rico. Geology 36 (5), 391–394.
- Woodruff, J.D., Donnelly, J.P., Okusu, A., 2009. Exploring typhoon variability over the mid-to-late Holocene: evidence of extreme coastal flooding from Kamikoshiki, Japan. Ouat. Sci. Rev. 28 (17–18), 1774–1785.
- Xian, H., Dong, X., Li, Y., Zhan, N., Jeppesen, E., 2022. High-resolution reconstruction of typhoon events since ~1850 CE based on multi-proxy sediment records in a coastal lagoon. South China. Sci. Total Environ. 803, 150063.
- Yoshii, T., Tanaka, S., Matsuyama, M., 2018. Tsunami inundation, sediment transport, and deposition process of tsunami deposits on coastal lowland inferred from the Tsunami Sand Transport Laboratory Experiment (TSTLE). Mar. Geol. 400, 107–118.
- Zhou, L., Gao, S., Yang, Y., Zhao, Y., Han, Z., Li, G., Jia, P., Yin, Y., 2017. Typhoon events recorded in coastal lagoon deposits, southeastern Hainan Island. Acta Oceanol. Sin. 36 (4), 37–45.
- Zhou, L., et al., 2021. Tracking historical storm records from high-barrier lagoon deposits on the southeastern coast of Hainan Island, China. Acta Oceanol. Sin. 40 (11), 162–175.